2005

# Resource Allocation Schemes And Performance Evaluation Models For Wavelength Division Multiplexed Optical Networks

Mounire El Houmaidi
*University of Central Florida*

# RESOURCE ALLOCATION SCHEMES AND PERFORMANCE EVALUATION MODELS FOR WAVELENGTH DIVISION MULTIPLEXED OPTICAL NETWORKS

by

MOUNIRE EL HOUMAIDI
M.S. University of Central Florida, 2000

A dissertation submitted in partial fulfillment of the requirements
for the degree of Doctor of Philosophy
in the School of Computer Science
in the College of Engineering and Computer Science
at the University of Central Florida
Orlando, Florida

Spring Term
2005

# ABSTRACT

Wavelength division multiplexed (WDM) optical networks are rapidly becoming the technology of choice in network infrastructure and next-generation Internet architectures. WDM networks have the potential to provide unprecedented bandwidth, reduce processing cost, achieve protocol transparency, and enable efficient failure handling. This dissertation addresses the important issues of improving the performance and enhancing the reliability of WDM networks as well as modeling and evaluating the performance of these networks.

Optical wavelength conversion is one of the emerging WDM enabling technologies that can significantly improve bandwidth utilization in optical networks. A new approach for the sparse placement of full wavelength converters based on the concept of the k-Dominating Set (k-DS) of a graph is presented. The k-DS approach is also extended to the case of limited conversion capability using three scalable and cost-effective switch designs: flexible node-sharing, strict node-sharing and static mapping. Compared to full search algorithms previously proposed in the literature, the K-DS approach has better blocking performance, has better time complexity and avoids the local minimum problem. The performance benefit of the K-DS approach is demonstrated by extensive simulation.

Fiber delay line (FDL) is another emerging WDM technology that can be used to obtain limited optical buffering capability. A placement algorithm, k-WDS, for the sparse placement of FDLs at a set of selected nodes in Optical Burst Switching (OBS) networks is proposed. The algorithm can handle both uniform and non-uniform traffic patterns. Extensive performance tests have

shown that k-WDS provides more efficient placement of optical fiber delay lines than the well-known approach of placing the resources at nodes with the highest experienced burst loss. Performance results that compare the benefit of using FDLs versus using optical wavelength converters (OWCs) are presented. A new algorithm, A-WDS, for the placement of an arbitrary numbers of FDLs and OWCs is introduced and is evaluated under different non-uniform traffic loads. This dissertation also introduces a new cost-effective optical switch design using FDL and a QoS-enhanced JET (just enough time) protocol suitable for optical burst switched WDM networks. The enhanced JET protocol allows classes of traffic to benefit from FDLs and OWCs while minimizing the end-to-end delay for high priority bursts.

Performance evaluation models of WDM networks represent an important research area that has received increased attention. A new analytical model that captures link dependencies in all-optical WDM networks under uniform traffic is presented. The model enables the estimation of connection blocking probabilities more accurately than previously possible. The basic formula of the dependency between two links in this model reflects their degree of adjacency, the degree of connectivity of the nodes composing them and their carried traffic. The usefulness of the model is illustrated by applying it to the sparse wavelength converters placement problem in WDM networks. A lightpath containing converters is divided into smaller sub-paths such that each sub-path is a wavelength continuous path and the nodes shared between these sub-paths are full wavelength conversion capable. The blocking probability of the entire path is obtained by computing the blocking probabilities of the individual sub-paths. The analytical-based sparse placement algorithm is validated by comparing it with its simulation-based counterpart using a number of network topologies.

Rapid recovery from failure and high levels of reliability are extremely important in WDM networks. A new Fault Tolerant Path Protection scheme, FTPP, for WDM mesh networks based on the alarming state of network nodes and links is introduced. The results of extensive simulation tests show that FTPP outperforms known path protection schemes in terms of loss of service ratio and network throughput. The simulation tests used a wide range of values for the load intensity, the failure arrival rate and the failure holding time. The FTPP scheme is next extended to the differentiated services model and its connection blocking performance is evaluated. Finally, a QoS-enhanced FTPP (QEFTPP) routing and path protection scheme in WDM networks is presented. QEFTPP uses preemption to minimize the connection blocking percentage for high priority traffic. Extensive simulation results have shown that QEFTPP achieves a clear QoS differentiation among the traffic classes and provides a good overall network performance.

*To my mother, sister and brothers who have supported me all the way since the beginning of my studies.*

*To all my friends. You keep my spirit alive!*

# ACKNOWLEDGMENTS

My deepest gratitude is directed to my advisors, Professor Mostafa Bassiouni and Professor Guifang Li, who have guided me throughout my research and challenged me to expand my dissertation. This work would not have been possible without their constant support over the past three years.

I would like to thank my committee members, Professor Ratan Guha, Professor Charles Hughes and Professor Joohan Lee for their comments, suggestions and timely advice.

# TABLE OF CONTENTS

# LIST OF FIGURES

# LIST OF TABLES

# LIST OF ACRONYMS/ABBREVIATIONS

| | |
|---|---|
| AR | Adaptive Routing |
| BP | Blocking Probability |
| CAP | Candidate Active Path |
| CBDP | Connection Blocking-Disconnection Percentage |
| CBP | Connection Blocking Percentage |
| CFARR | Connection and Failure Arrival Rate Ratio |
| CPP | Candidate Protection Path |
| DS | Dominating Set |
| DPP | Dedicated Path Protection |
| DR | Delay Ratio |
| DSPP | Disjoint Shared Path Protection |
| EED | End to End Delay |
| FAR | Fixed Alternate Routing |
| FCHTR | Failure and Connection Holding Time Ratio |
| F-SEARCH | Full Search |
| FDL | Fiber Delay Lines |
| FF | First Fit |
| FTTP | Fault Tolerant Path Protection |
| ILP | Integer Linear Program |
| JET | Just Enough Time |
| JIT | Just In Time |

| | |
|---|---|
| JSPP | Joint Shared Path Protection |
| LSR | Loss of Service Ratio |
| LU | Least Used |
| MU | Most Used |
| OBS | Optical Burst Switching |
| OCS | Optical Circuit Switching |
| OPS | Optical Packet Switching |
| OXC | Optical Cross Connect |
| OWC | Optical Wavelength Converter |
| NPSP | Non Preempted with Shared Protection |
| NPGP | Non Preempted with Guaranteed Protection |
| NSFNET | National Science Foundation NETwork topology |
| PNP | Preempted with No Protection |
| PSP | Preempted with Shared Protection |
| QEJET | Quality of Service for Enhanced Just Enough Time signaling |
| QoS | Quality of Service |
| RWA | Routing and Wavelength Assignment |
| SR | Static Routing |
| SRLG | Shared Risk Link Group |
| TAG | Tell And Go |
| TAW | Tell And Wait |
| USLH | United States of America's Long Haul topology |
| WDM | Wavelength Division Multiplexed optical networks |

| | |
|---|---|
| WDS | Weighted Dominating Set |
| WF | Weighting Factor |
| WRON | Wavelength Routed Optical Networks |

# 1. INTRODUCTION

In an optical network, the routing and wavelength assignment (RWA) of incoming connection requests should be efficient, scalable, fast and fault tolerant. When a connection request is initiated at the source node, the RWA protocol should set up a light-path to the destination node by finding a path between the source and destination nodes and using the same wavelength in each link traversed by the connection.

This restriction is referred to in the literature as the wavelength continuity constraint. The advantage of this constraint is the fact that no wavelength conversion is required at any intermediate node. If there is no path from the source to destination with the same wavelength available in every link of the path, the call is blocked.

There are techniques for static routing where the connections are known in advance and stay for an infinite period of time in the network. The problem is usually to find the optimal number of wavelengths needed to serve all the connections. A review of approaches for solving the static light path establishment problem is given in [ZJM00].

We focus on dynamic routing which deals with sequences of connection requests that arrive to the optical network in a random fashion. After the path is established to serve the incoming connection, the network resources are used for a finite amount of time. We also adopt the forward reservation for light path establishment and apply the random wavelength assignment since it is widely used in the literature and is more amenable to analytical modeling.

In this dissertation, we investigate four important issues that affect the performance and the reliability of wavelength division multiplexed (WDM) optical networks as well as our ability to model and evaluate the performance of these networks. Below, we introduce each of these four issues, survey the related previous results and motivate the new approach that we adopted for each issue.

## 1.1 Placement of wavelength converters in optical networks

The performance of a Wavelength Routed Optical Network (WRON) is directly dependent on the capability of its Optical Cross-Connects (OXC) to allow wavelength conversion. A wavelength converter can transfer an optical signal on one wavelength at an input port to another wavelength at an output port. Not only has the cost of these devices and OXC complexity made it expensive to have full wavelength conversion capability at every node, but also wavelength conversion does not always minimize the network's connection blocking. For instance, with a fully connected network, any connection request requires a 1-hop path from source to destination. Wavelength converters are not needed at all to improve the blocking percentage of such dense network. Wavelength conversion must therefore be used judiciously and should be placed in nodes that maximize the overall network performance taking into consideration the network topology and the traffic flowing through its nodes.

The placement of wavelength converters in All-optical WDM networks has been an active research topic in the recent years. This is due to the fact that the optimal placement of converters

in WRON of a general topology is NP-hard [RKR72, CLY94]. Most known algorithms apply to special topologies or are based on placement heuristics.

The author in [ABR96] showed analytically that having all nodes capable of full wavelength conversion improves the blocking probability. Also, when no wavelength conversion is available in the network (wavelength continuity constraint), the blocking probabilities grow faster with the number of hops. For realistic networks with large number of wavelengths and high number of hops (diameter), the analytical model's time complexity of order $O(W^{(H+1)})$ represents a challenge; where W is the number of wavelengths per link and H is the number of hops.

In [SAS96], the authors assumed that each node is capable of full wavelength conversion with a probability q independently of the other nodes (q is the conversion density of the network). A 3-D Markov model is introduced to take into account the correlation of wavelength usage between adjacent links. On three network topologies (ring, mesh-torus, hypercube), the study shows that uniformly placing wavelength converters is more efficient than randomly placing them. The uniform placement technique works well for topologies with low connectivity such as rings but is not applicable for general topologies.

The study in [VRK98] showed via simulation that wavelength conversion at nodes with high nodal degree is cost effective compared to having all nodes capable of full conversion. For dynamic light path establishment, an auxiliary graph with M nodes is constructed based on the physical topology of the network. M is the product of N, the number of nodes in the network and W, the number of wavelengths. The arcs are labeled with channel costs and conversion costs.

Dijkstra's algorithm is applied for each connection request. The used arcs are removed to reflect the wavelength usage in the network requiring O(M) time complexity. The algorithm complexity is O ($C \cdot N^4 \cdot W^2$), where C is the total number of connections requests received during the simulation.

The authors in [JIM99] explored optical switch designs with limited number of wavelength converter units at each node. We will refer to this design as the limited wavelength conversion with shared-nodal switch design using tunable optical multiplexers. A converter bank is used in an optical router to provide per-demand conversion shared among the outbound links of this node [KLM93, KLJ93, CCB96]. The router can contain share-per-node wavelength converter units, or share-per-link wavelength converter units that are shared by the incoming circuits. This type of limited conversion switch has the potential of achieving most of the benefits of a full conversion-capable switch at a much lower cost. A heuristic of complexity $O(N^3)$ was introduced in [JIM99] for placement of individual limited wavelength converter units in the nodes of the optical network.

The study in [KLM93, KLJ93] shows that routing and wavelength assignment with wavelength conversion capability is an NP-complete problem and introduces a routing algorithm, similar to [VRK98], with a reported time complexity of order $O(N^4 \cdot W^2)$ without including the number of incoming connection requests to the network in the analysis.

In [CCB96], the authors introduced an interconnected–layered–graph model of the network with limited number of wavelength converters at each node. The simulation results show that the performance of the proposed algorithm is comparable to the one presented in [KLJ93].

We will approach the design of WDM networks from a different perspective; we will introduce various techniques to improve the overall performance by judiciously placing wavelength conversion at key nodes dominating the entire topology. Our motivation is based on the fact that equipping all nodes of a large optical network with full conversion capability is prohibitively costly. To improve performance at reduced cost, sparse converter placement algorithms are used to select a subset of nodes for full-conversion deployment. Further cost reduction can be obtained by deploying only limited conversion capability in the selected nodes. In this dissertation, we present wavelength converters placement algorithms based on the k-Dominating Set (k-DS) concept described in Chapter 2.

We propose three different cost effective optical switch designs using the technologically feasible non-tunable optical multiplexers. These three switch designs are Flexible Node-Sharing, Strict Node-Sharing and Static Mapping. Compared to the full search heuristic of $O(N^3)$ complexity based on ranking nodes by blocking percentages, our algorithm not only has a better time complexity $O(\mathfrak{R}.N^2)$, where $\mathfrak{R}$ is the number of disjoint sets provided by k-DS, but also avoids the local minimum problem.

The performance benefit of our algorithm is demonstrated by network simulation with the U.S Long Haul topology having 28 nodes ($\mathfrak{R}$ is 5) and the NSF network having 16 nodes ($\mathfrak{R}$ is 4).

Our simulation considers the case when the traffic is not uniformly distributed between node pairs in the network using a weighted placement approach, referred to as k-WDS. From the optical network management point of view, our results also show that the limited conversion capability can achieve performance very close to that of the full conversion capability; while not only decreasing the optical switch cost but also enhancing its fault tolerance.

## 1.2 Contention resolution in optical burst switched networks

One of the candidates for next generation high speed network infrastructures will be based on optical burst switching that is envisioned to be able to combine the best of optical circuit/flow switching and optical packet switching. However it's been proven that under highly variable burst sizes, Optical Burst Switching suffers from excessive burst loss due to contention. This issue is due to the fact that the core nodes have very limited or no buffering capability and contending bursts for the same output link will suffer from losses. To reduce the burst loss in Optical Burst Switching, contention resolution is the main challenge to overcome in any Optical Burst Switching architecture.

Several studies propose feasible solutions based on burst segmentation [VJS02], QoS based on burstification [YST02] or classes of traffic isolation by extra offset-time [YQD00], wavelength reservation [OAM01] and burst assembly [SOK02] schemes.

Another approach for solving contention is based on deflection:

1. In the time domain using FDLs [PPP03, CQY99, YQD00, JCP02, YQD01, JLA02].
2. In the space domain with deflection routing [HLH02, XPR01, VJS02];
3. In the wavelength domain using OWCs [JRT02, NLR03, BLJ03, JIM99, MSS02].

The authors in [CQY99, YQD00, YQD01, KKK02] propose two optical burst switching protocols, classless OBS and prioritized OBS based on the offset-time. The use of an extra offset time to separate high priority class from lower priority class increases the overall end-to-end delay but the end-to-end delay for high priority classes is low and predictable. In [XPR01, JWM00], the authors survey signaling protocols for optical burst switching; in the Tell-And-Go (TAG) scheme, a source transmits its burst without receiving a confirmation from the network. With Tell-And-Wait (TAW), the burst is transmitted when all switches on the path accept the burst. An intermediate scheme is proposed in [CQY99], just-enough-time (JET). It eliminates the need for burst buffering and reserves the resources at the optical switch just for the duration of the burst. Full wavelength conversion is assumed to be available in all switches using OWCs. The study in [JWM00] introduces the just-in-time signaling protocol (JIT). The out-of-band control eliminates burst buffering at the intermediate nodes. JIT does not guarantee better resource utilization than JET but supports optical flow switching (when connection duration is longer than the cut through time) and does not require additional synchronization and scheduling [BRP02].

The studies in [HLH02, XPR01, VJS02] introduce deflection routing for optical burst switching as an alternative to resolve contentions for the same output link instead of using delay lines for buffering. Several studies [JRT02, MDB02, PPP03, LNR03, DMB02, KDZ02] suggest the use of fiber delay lines and wavelength conversion at the core nodes as a feasible solution to the contention limitation of OBS. Not only it is cost effective and scalable; but also provides a better statistical multiplexing performance.

Our work focuses on the sparse placement of Fiber Delay Lines at the core nodes of an Optical Burst Switched Network as a solution to burst contention. Our proposed scheme places the Fiber Delay Line capabilities at key nodes, i.e., nodes that have good connectivity and are well placed within the network. We will show that when the nodes selected by our scheme are equipped with Fiber Delay Lines, they significantly reduce the burst loss rate and improve network throughput.

In this dissertation, we propose efficient and highly scalable algorithms for the sparse placement of Fiber Delay Lines in optical WDM networks. The algorithms use the k-weighted dominating set concept and are particularly suitable for solving the contention resolution problem in Optical Burst Switching under Just Enough Time signaling. To our knowledge, our work is the first attempt to apply the weighted dominating set approach for solving a design and engineering problem in Optical Burst Switched networks in general and to the sparse Fiber Delay Lines placement in particular.

Under heavy tail traffic and high burst contention, we introduce a Quality of Service capable Just Enough Time Signaling using a simple scheduling scheme and allowing controlled burst loss and

end-to-end delay for all classes of traffic. We also introduce a cost effective optical switch design with variable Fiber Delay Line capability and show its benefits via simulation under different classes of traffic.

## 1.3 Dependency based analytical model for blocking rates computation

Another important area of WRON research is the performance evaluation for lightpath establishment. A number of approximate analytical models [ABR96, MKA96, HMH99, RRM02, CLC03] for evaluating the performance of WRON made the assumption that link blocking events are independent. Several recent models [ZRP00, ASS00, LXC03, ASS04], however, have considered the correlation of blocking events. Below, we briefly review relevant existing analytical models with no wavelength conversion and with sparse conversion.

The study in [LLS00] explores multifiber WDM networks as an alternative solution to wavelength conversion. A 3-D Markov model for two-hop paths is applied for blocking probability computation and a path decomposition scheme is used to estimate the conditional blocking probabilities. The authors in [RBM95] introduced an analytical model for optical networks without wavelength converters and tested it for a variety of network topologies.

In [ABR96, MKA96], a single-link blocking model is introduced and is used to compute the blocking probabilities for paths of one, two and three links. The random variables, $X_i$, reflecting the number of available wavelengths on link i, are assumed independent. The authors in [RRM02] derived an analytical model that incorporates alternate routing and wavelength

conversion and the authors in [CLC03] presented a model for the sparse placement of full wavelength conversion under various RWA schemes.

The study in [SAS96, SAS99] focused on the placement of K full wavelength converters on a path with H hops. The key assumption of the model is that the load on link i of a path given the loads on links 1, 2… i-1, depends only on the load on link i-1. The model proposed in [ZRP00] calculates the blocking probability of a path using a multi-dimensional Markov chain formulation.

The model in [ASS00, ASS04] first provides a simple solution to calculate the blocking probability of multi-hop paths. A wavelength correlation model is then applied to take into account the correlation of the same wavelength on two adjacent links. The authors in [LXC03] further extended this model to evaluate the blocking performance of networks with sparse conversion in distributed conditions.

Existing analytical models for WRON's performance evaluation suffer from accuracy and scalability problems (e.g., the complexity of the model in [LLS00] is intractable for general network topologies, the model in [RBM95] tends to over-predict the blocking probabilities under high loads or with a large number of wavelengths, the tractability of the model in [ABR96, MKA96] is guaranteed only for networks with a small diameter). Models that take the correlation between links into consideration are more accurate than models that assume link independence but are also more computationally intensive.

In this dissertation, we develop a link dependency model that improves our ability to capture the correlation of wavelength availability among different network links. To analytically handle the presence of wavelength converters, a light path containing converters is divided into smaller sub-paths such that each sub-path is a wavelength continuous path and the nodes shared between these sub-paths are full wavelength conversion capable. The blocking probability of the entire path is easily obtained by computing the probabilities in the individual sub-paths.

Our analytical model captures link dependencies in all-optical WDM networks under uniform traffic and enables the estimation of connection blocking probabilities more accurately than previously possible. The basic formula of the dependency between two links in this model reflects their degree of adjacency, the degree of connectivity of the nodes composing them and their carried traffic.

We extensively validate the analytical model using the NSFNET backbone, the U.S. Long Haul network, the ring topology and randomly generated graphs.

## 1.4 Path protection in survivable wavelength routed all-optical

In wavelength routed all optical networks, there is a need for fault tolerant routing mechanisms to protect network performance against link failures and optical cross-connect failures. A wide range of protection and restoration schemes for WDM networks have been investigated in the literature. Some researchers in the area of protection have mainly considered the static model (i.e. offline routing). Those models are reasonable only when connection demands are known in

advance. We consider the dynamic routing scenario with random connection arrivals to the network. When a new connection request arrives to the network, our scheme establishes the active and the protection resources according to the traffic already present in the network.

Path protection schemes previously reported in the literature have primarily addressed the computation of protection paths that are link disjoint with active paths under the assumption of a single link failure at a time. These path protection schemes use standard routing cost functions for the selection of active and protection paths. In this dissertation, we present a path protection approach that uses the alarms/alerts gathered by network surveillance modules in selecting the active and protection paths. Below, we briefly discuss the motivation of our alarm-based scheme.

Network service providers have made significant investments in building operational surveillance and trouble management tools. It is expected that next-generation network surveillance tools, alarm-analysis engines and network operations centers will have extensive capabilities not only for early problem detection and the prompt repair of failures but also for building up an overall picture of the operational condition and health of the various network components. The alarm-analysis engines of next-generation networks will have the capability to process unprecedented numbers of alarms, alerts, and warning messages from multitechnology/multivendor software and hardware components and precisely pinpoint the root-cause problems of failures (e.g., fiber cuts, laser failure, high levels of signal cross-talk).

Equally important, these alarm-analysis engines will also be able to proactively analyze impending network issues and identify network elements that can be the source of future

problems. Existing network technology, for example, has already produced alarm interface controller modules (e.g., Cisco NM-AIC-64 card) that help in the remote monitoring of network elements & interfaces, thereby permitting the detection and reporting of alarms on building security (e.g., door and window open and close), fire and smoke indication, building environmental state (e.g., temperature and humidity) and utility power readings.

The alarm-based path protection approach presented in this dissertation is based on the idea of modifying the routing and path selection process by taking into consideration the alarms posted for the various links/nodes of the network in order to improve the reliability of the network and reduce service outage.

## 1.5 Dissertation organization

The remainder of this dissertation is organized as follows:

In Chapter 2, we present the k-DS algorithm for the sparse placement of full wavelength converters. We also introduce the HYBRID algorithm for placing an arbitrary number of full wavelength converters and compare its performance to k-BLK.

Chapter 3 describes our extension of k-DS for the limited wavelength conversion case and introduces three different cost effective optical switch designs. We also investigate the network performance under uniform and non uniform traffic.

In Chapter 4, we study the contention resolution problem in optical burst switching using sparse fiber delay lines and their class-based allocation. We combine fiber delay lines and optical wavelength conversion as the solution for the burst contention problem in Optical Burst Switching. We present a placement algorithm, *k-WDS*, for the sparse placement of Fiber Delay Lines at a set of selected nodes.

Chapter 5 defines our dependency and correlation based analytical model for computing the blocking rates in WDM networks. We validate the analytical-based sparse placement algorithm by comparing it with its simulation-based counterpart using a number of network topologies.

In Chapter 6, we extensively validate a novel alarm based routing and path protection in survivable wavelength routed all-optical mesh networks. The simulation tests used a wide range of values for the load intensity, the failure arrival rate and the failure holding time. The effectiveness of our method has been demonstrated by using the US Long Haul and the NSFNET topologies.

We make concluding remarks and describe our proposed future research in Chapter 7.

# 2. k-DS ALGORITHM FOR SPARSE PLACEMENT OF FULL CONVERTERS

In this chapter, we discuss the problem of full and limited wavelength converters placement in optical networks and present our new placement approach based on the dominating set concept.

## 2.1 Background

In WRON (Wavelength Routed Optical Networks), when a connection request is initiated at the source node, the RWA (Routing and Wavelength Assignment) protocol should set up a light-path between the source and destination nodes using the same wavelength in each link traversed by the connection. This restriction is referred to as the wavelength continuity constraint. This constraint implies that no wavelength conversion is required at any intermediate node. However, if there is no path from the source to destination with the same wavelength available in every link of the path, the call is blocked. Different RWA approaches [ZJM00, RRS00, ZJS01, JPX01] have been investigated for static routing, fixed-alternate routing and adaptive routing. These approaches use numerous wavelength assignment heuristics including First-Fit, Random, Least-Used, and Most-Used.

When the continuity constraint is removed by using wavelength converters, the network blocking performance is reduced, the wavelength reuse is increased, higher loads are supported and the network throughput is enhanced [ABR96, SAS96, VRK98, JIM99]. The introduction of converters in WDM (Wavelength Division Multiplexed networks) increases the cost and complexity of the optical cross-connects (OXCs). Converters must therefore be used judiciously

and must be placed in nodes that maximize performance improvement. Hence, there have been a number of studies to investigate sparse and limited wavelength converter placement in optical networks [KLM93, KLJ93, CCB96, SAS96, ABR96, VRK98, JIM99].

In the next sections, we present new, efficient and highly scalable algorithms for the sparse placement of full and limited wavelength converters in an optical network based on the concept of k-Dominating Sets (k-DS). The idea is to have wavelength conversion capability at the nodes receiving higher traffic to decrease the overall network blocking percentage. These nodes, as dominating nodes, have to be closer to the nodes without wavelength conversion to increase the throughput. A dominating set, D, is one in which each vertex is either in D or adjacent to some vertex in D. Our algorithm uses the network topology as input to provide a sub-optimal wavelength converters placement. The k-DS scheme solves this minimization problem by finding a solution taking into consideration the traffic flowing through the nodes and doesn't build the solution incrementally but via a voting mechanism based on the connectivity of each node. We will show via simulation that putting full wavelength conversion at the members of D is cost effective and improves the utilization of the network. To our knowledge, our work is the first attempt to apply the Dominating Set approach to the design and engineering of optical networks.

In the k-DS algorithm for sparse placement of conversion, we assume that we can equip some nodes with the capability of full wavelength conversion from any wavelength to any other wavelength if available. We formulate the placement problem as a k-DS problem: given a graph G(V,E), determine a set $D \subset V$ such that every vertex in the graph is either in D or is at distance k

or less from at least one member in D. The members of the set D represent special nodes that act as wavelength conversion sites within the network.

## 2.2 k-DS: Application and Examples

The Minimum Dominating Set problem is NP-complete [RKR72, CLY94] and it is related to the traveling salesperson problem [SGK96] requiring approximating heuristics. This concept was applied to Wormhole-Routing in massively parallel computers [TTM97] by finding dominating nodes that can deliver and receive messages to and from a larger set of nodes (not in the dominating set) while avoiding channel contention.

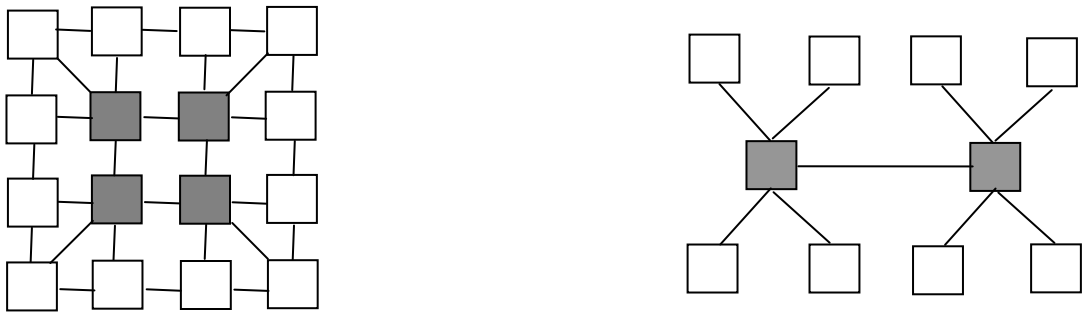

Figure 1: Topology 1 with 1-DS has 4 nodes and Topology 2 with 1-DS has 2 nodes

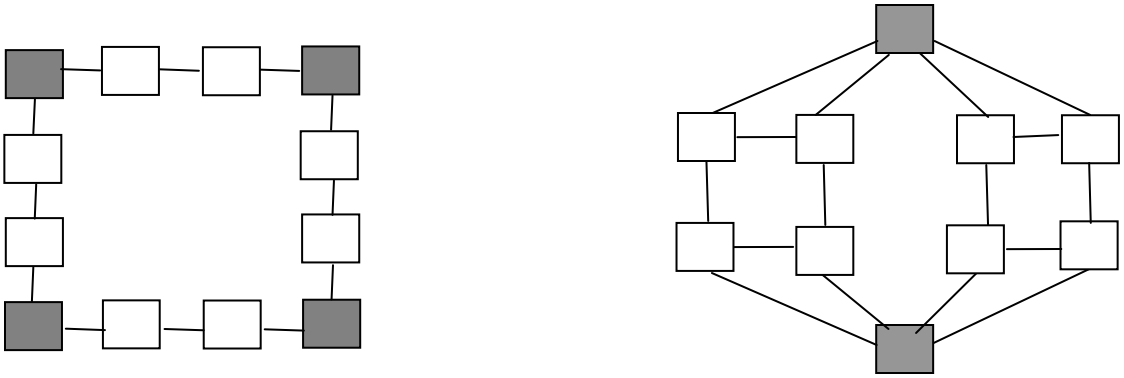

Figure 2: Topology 3 with 1-DS has 6 nodes and Topology 4 with1-DS has 2 nodes

In the above examples, the 1-DS set is shown for four different topologies. In the 4x4 mesh topology 1, the size of the 1-DS set is 4. We can see that every node is either a master node (member of the dominating set) or is at one hop away of a master node. Topology 2 with 10 nodes has a 1-DS set of size 2. However the 12 nodes ring topology has 4 nodes in its 1-DS set. In topology 4 with 10 nodes, the 1-DS set has 2 nodes in it.

In [SSZ02], Dominating sets are used for broadcasting in wireless networks to determine gateway nodes where reliability and fault tolerance are desired. If position information is available to every node, each node can determine, without any message exchange with the neighbors, if it is a gateway node in $O(\Delta^3)$ computation time; $\Delta$ is the number of neighbors which can be of order O(N) in the worst case.

## 2.3 k-DS: Algorithm

We developed an approximation algorithm for the k-DS problem that computes the set of master nodes to be equipped with full conversion capability. The algorithm provides a sub-optimal placement of wavelength converters in an optical network using the topology of the network as input and independently of the number of wavelengths per link. The k-DS approach assumes a uniform traffic pattern between each node pair (source s and destination d). The algorithm ensures that the resulting set D has the following property: every node $v \in V$ is either in D or is at most k hops away from a node in D.

We first give the definitions and notations that are used in the k-DS algorithm:

1. Cardinality (S): is the number of members in the set S.

2. Neighbor (v): is the set of nodes sharing a link with a node v.

3. $\text{Neighbor}_k$ (v): is the set of nodes that are at most within k hops away from a node v. For k equals 0, $\text{Neighbor}_0$(v) contains the node v only.

4. $Connect_k(v)$, called the k-connectivity of a node v, represents a connectivity index based on nodes within k hops of the node v. It's defined as:

$$Connect_0(v) = Degree(v) = Cardinality(Neighbor(v))$$

$$Connect_1(v) = Connect_0(v) + \sum_{m \in Neighbor(v)} Connect_0(m)$$

Recursively we define $Connect_k(v)$ as:

$$Connect_k(v) = Connect_{k-1}(v) + \sum_{m \in Neighbor(v)} Connect_{k-1}(m)$$

With a uniform traffic assumption, higher values of the k-connectivity of node v correspond to higher volumes of traffic passing through node v. Note that, a node m can contribute more than once to the k-connectivity of a node v, since traffic can arrive from the same node through different paths.

5. $Master_k(v)$, called the k-Master of a node v, represents the node p, member of $Neighbor_k(v)$, with the highest $Connect_k$ value over all nodes m that are at most k hops away from node v (i.e., all nodes $m \in Neighbor_k(v)$). For k equals 0, $Master_k(v)$ is the node v itself.

Our k-DS algorithm initializes the k-DS set to the empty set. Each node computes its connectivity index k-Connect by adding the $Connect_{k-1}$ values of its neighbors including itself. A

voting stage allows each node to select its $Master_k$ from its neighbors within k hops based on their connectivity index.

The algorithm also implements a priority voting scheme for cases with ties and also to keep a master node from voting for a node outside the k-DS set. The k-DS heuristic for a graph G uses k iterations to compute the sets 1-DS, 2-DS,…, k-DS. In iteration # j, the connectivity values $Connect_{j-1}$ of iteration j-1 are used to compute the connectivity values $Connect_j$ of the current iteration (as explained earlier). Below is the pseudo code of iteration # k of the heuristic algorithm.

The k-DS algorithm is described below, for $k > 0$:

1. Initialize the working set S to the empty set $\phi$.

2. For all nodes v in G, compute $Connect_k$ (v).

3. For all nodes v do

   If $S \cap Neighbor_k$ (v) is empty do

   { find the node m that is $Master_k$ (v);

   add node m to the set S }

4. Set k-DS to S; Return( k-DS )

Lemma: k-DS is a k-Dominating Set for the graph G(V,E).

To prove this, we can look at the simple case when k equals 1: a node v will vote for the node m in 1-Neighbor (v), which is $Neighbor(v) \cup \{v\}$ and m has the highest 1-Connect value. The node m is in the set 1-DS, so v will either be in the set 1-DS (for the case m=v) or v is directly connected to m which is a node in 1-DS.

For the general case for k, the same type of argument applies; a node will be a member of the k-DS set or will have a selected master, member of k-DS, that is within k hops from it.

## 2.4 k-DS: Results and comparison

For illustration, we show the execution of k-DS through $Connect_k$ computations and the voting phase. The following describes the execution of k-DS, for k equals 1, using topology 1. The labels inside the nodes represent the $Connect_k$ values and the directed arrows represent voting for the $Master_k$ node. The 1-DS set has 4 nodes in it.

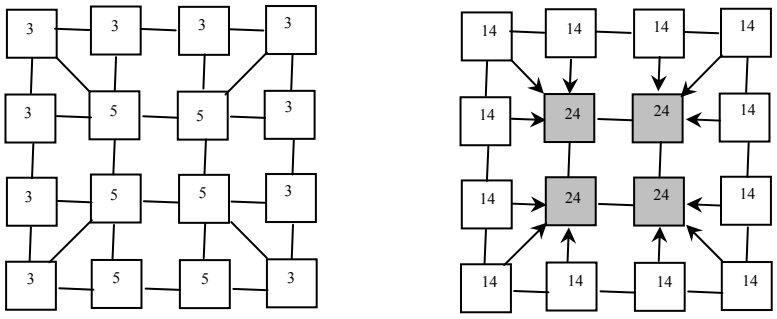


Figure 3: Topology 1, Compute $Connect_1$ and vote

For topology 2, the following describes the execution of k-DS for k equals 1. We have 2 nodes in the computed 1-DS set.

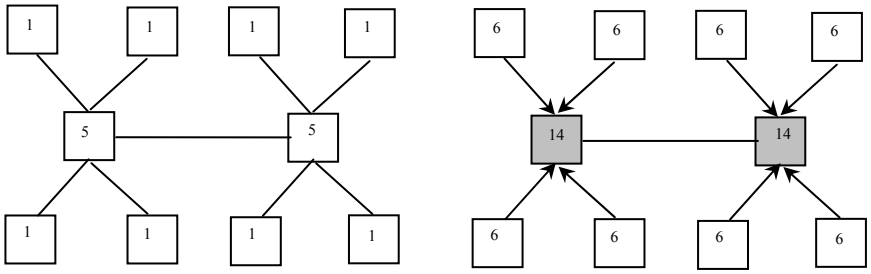


Figure 4: Topology 2, Compute $Connect_1$ and vote

The order of processing nodes in step 3 of the k-DS algorithm may produce different results; we have often used increasing order of $Connect_k$ values in step 3. The following four examples show the 1-DS results returned by the above simple heuristic. Notice that the 1-DS sets for topologies 1, 2 and 4 are optimal sets (i.e., have minimum size). The 1-DS set of size 6 for the ring network of topology 3 is not optimal (since the four nodes at the four corners of the topology represent an optimal set). However, this later 1-DS is non-redundant in the sense that if any of its six nodes is dropped, the set is no longer 1-DS set (which is similar to the concept of local minimum).

In general, the set returned by the heuristic algorithm may have some redundant nodes. A polynomial time procedure can be used to remove this redundancy. For example if S is the 1-DS returned by the heuristic algorithm, then the following code is used to remove the redundancy in the set S:

For each node v in S do

Flag = True;

For each node u $\in$ {v} $\cup$ Neighbor (v) do

If the set difference S-{v} does not contain u or a direct neighbor of u then

{Flag = False};

If (Flag) remove v from S

Our extensive simulation tests with randomly generated topologies have shown that the k-DS algorithm provides excellent placement for nodes with full wavelength conversion. We now apply our algorithm to a realistic topology: the U.S Long haul.

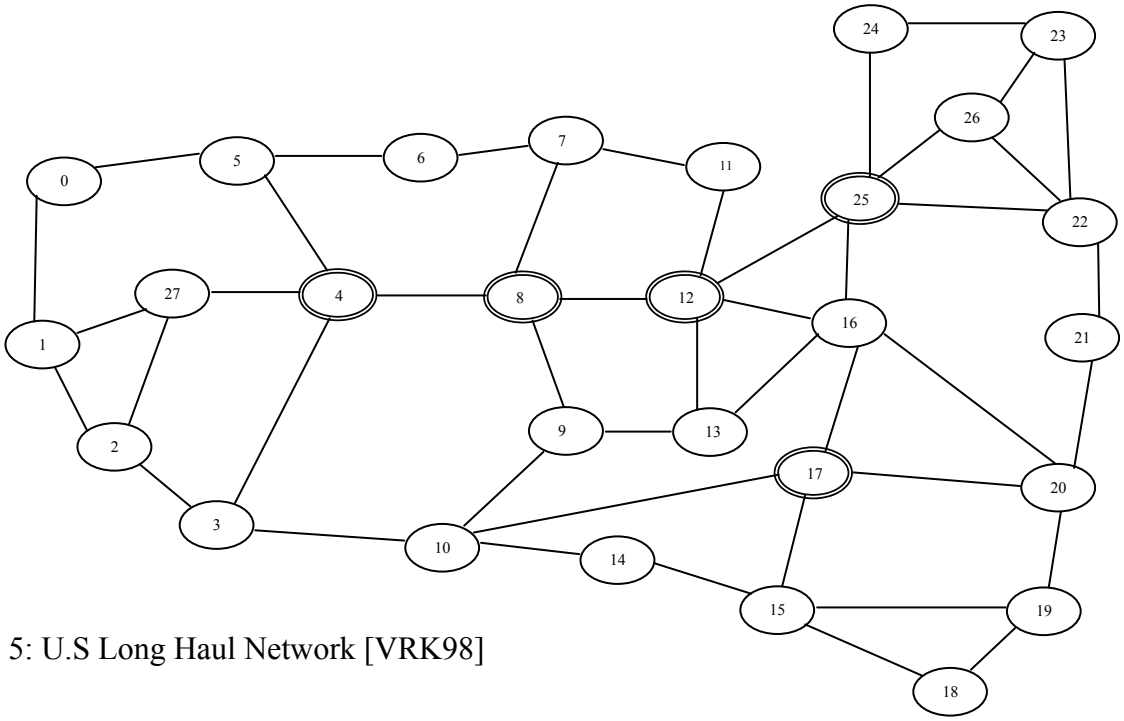


Figure 5: U.S Long Haul Network [VRK98]

Figure 5 shows the U.S long haul network [VRK98] with 28 nodes and 45 links. This is a popular topology used in the literature for the simulation and analysis of optical networks. Note that the marked (double circled) nodes are the members of the 2-DS set and every node is either in 2-DS or at most 2 hops away from a member of 2-DS.

For example, the $Connect_k$ indices of node 0 in U.S. Long Haul Network shown in Figure 5 have the following values:

$Connect_0$(node 0) = 2

$Connect_1$(node 0) = 8

$Connect_2$(node 0) = 30

For node 0 in the U.S. Long Haul Network of Figure 5, the $Master_k$ selection is:

$Master_0$(node 0) = {node 0}

$Master_1$(node 0) = {node 1}

$Master_2$(node 0) = {node 4}

$Master_3$(node 0) = {node 8}

$Master_4$(node 0) = {node 12}

Our k-DS algorithm produces the following results for the U.S long Haul network:

1-DS(U.S Long Haul)={1,3,4,5,8,10,12,15,17,20,22,25,27}

2-DS(U.S Long Haul)={4, 8, 12, 17, 25}

3-DS (U.S Long Haul) = {8, 12, 17}

4-DS (U.S Long Haul) = {12}

We evaluated our algorithm by a simulation model. The simulation uses hop-based shortest path routing with forward reservation and random wavelength assignment. Each link is a bidirectional fiber and the number of wavelengths on each link is 8. The traffic is uniformly distributed over all node pairs and the connection holding time is exponentially distributed.

The load, in Erlangs, is the product of the connection arrival rate and the average connection holding time. All of our results are based on simulating a total, connection requests arriving to the network, of $10^6$ times the considered load ($C = 10^6$. load). All simulation results are given with 95% confidence intervals using the batch means method with 50 batches or more.

We compared our k-DS placement algorithm against the well-known approach of placing converters in nodes having the highest blocking probabilities [JIM99, MSS02]. We denote this latter approach by k-BLK algorithm. The use of "k" in k-BLK is introduced to indicate that the number of full converters used in this approach is equal to the same number of full converters used by our k-DS algorithm. For example, 3-BLK uses the same number of full converters as 3-DS but it may place them in a different set of nodes. k-BLK algorithm solves the sparse wavelength placement problem by adding the node that experienced the highest blocking at each simulation step to the final solution.

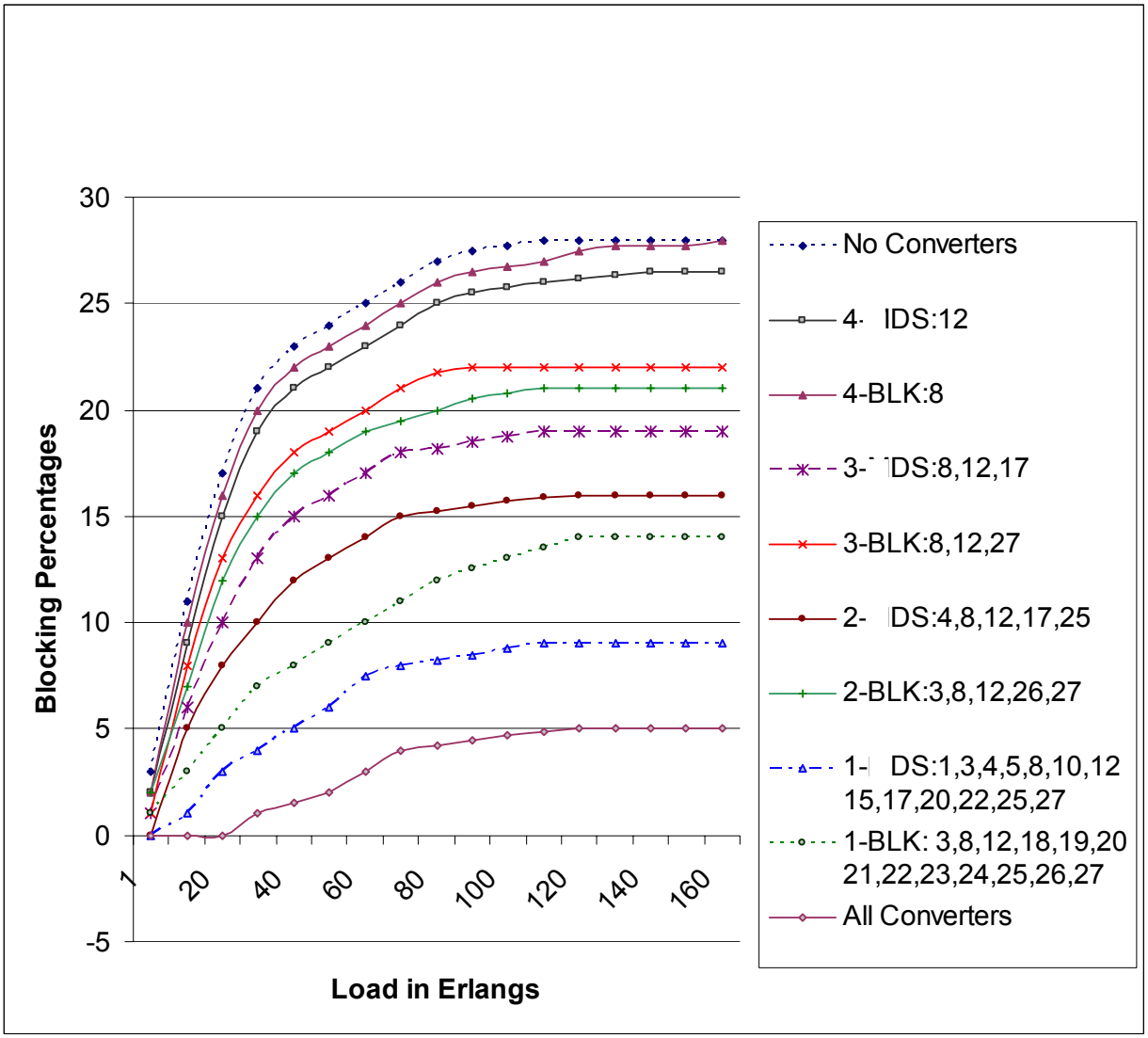


Figure 6: U.S. Long Haul Topology: k-BLK versus k-DS

To evaluate our k-DS algorithm, we adopted a comparison method similar to that described in [JIM99]. Specifically, we do the following steps for a given network: We initially, run the RWA simulation assuming that full conversion is not available in any node (this is the case of no converters).

Starting with k at 1, we next run RWA simulations using the placement suggested by k-DS and k-BLK (the latter simulation is made to have the same number of converters as the former). We then increase k and repeat the same process until k-DS returns only one master node. After each simulation, we measure the blocking percentage experienced in the network.

As shown in Figure 6, better results are obtained when we put full conversion in the nodes selected by the k-DS algorithm instead of putting them in the nodes with the highest blocking percentages based on k-BLK. For instance, under a typical load of 60, without any wavelength conversion the blocking percentage is around 25%. When we have full wavelength conversion at node 12, member of the singleton 4-DS, the blocking percentage is improved by 2% to 23%. However when we put full wavelength conversion in node 8 designated by k-BLK heuristic, the measured blocking percentage is 24%. The placement suggested by 4-DS improves the performance by 8% and 4-BLK only by 4%.

At load 60, 3-DS with 3 nodes decreases the blocking to 17% (32 % improvement) while 3-BLK achieves 20% blocking (i.e., 20% improvement). 2-DS with 5 nodes achieves 13% blocking at load 60 (equivalent to 48% improvement) while 2-BLK achieves 19% blocking (equivalent to 24% improvement). Thus we can achieve almost 50% improvement from the no wavelength conversion case with only 5 nodes selected by 2-DS. Finally, 1-DS, with 13 nodes, reduces the blocking at load 60 to 7% (72% improvement) while 1-BLK reduces blocking only to 10% (60% improvement).

From the above results, we can see that the k-DS selection based only on the network topology as input provides better improvements than the simulation based k-BLK heuristic introduced in [JIM99]. k-DS is able to provide a better placement of full wavelength conversion since its solution is a global minimum based on the connectivity of each node and the traffic that will go through each one of them.

These results are due to the fact that the k-DS algorithm selects a set of vertices that have good connectivity (strongly connoted to the other nodes) and that are well placed within the network. When the selected vertices are equipped with full wavelength conversion, they significantly improves performance since these nodes dominate the entire topology, i.e, each other node is within closer distance from a selected node in the dominating set.

The algorithm solves this minimization problem using a global approach that avoids local (false) minimums. The k-BLK approach is using an incremental minimization approach that doesn't always lead to the global minimum by using the union of local minimums found at each iteration. As shown earlier, k-DS algorithm time complexity is order O (N . $\Delta$ . k) and k-BLK is order O(N . C . NUMCONV) + O($N^3$) since each connection request requires processing at each node in its path and shortest paths between all pairs have to be computed before the simulation starts. C is the total number of connection requests arriving to the network during the RWA simulation and NUMCONV is the number of converters to be placed.

An obvious limitation of the k-DS algorithm is that it cannot answer the question about where an arbitrary number X of full wavelength converters should be placed given the topology of the

network. For example if X is 6 in the US. Long Haul network, 2-DS tells us that five converters should be placed in nodes: 4, 8, 12, 17 and 25. However, our 1-DS returns 13 nodes and cannot give a direct answer to the case X=6.

## 2.5 k-DS: HYBRID Algorithm for Placement of Arbitrary Number of Converters

To overcome this limitation, we extended the k-DS algorithm to be able to provide solutions to the problem of a number of full wavelength converters that does not exactly match the cardinality of any k-Master set. The extension, denoted as HYBRID, takes advantage of both k-DS and k-BLK.

Given X as the arbitrary number of full wavelength converters to be placed in the network, we start with the largest k-DS set of size smaller than X and add a new node at each step. In each step we run the RWA simulation and measure the blocking percentage. The node with the highest experienced blocking is added to the final solution. Our HYBRID algorithm stops when we have X nodes selected. The HYBRID algorithm takes advantage of k-DS by building the initial set and uses k-BLK to extend it.

Our HYBRID algorithm is described as follows:

1. Repeat starting at k =1

   Compute k-DS

   Increment k by 1

   Until NumberNodes = cardinality(k-DS)≤ X.

   We denote the largest k, such that the size of $\Im$-DS ≤ X, as $\Im$.

2. If NumberNodes = X, return $\Im$-DS as the list of nodes that should have full wavelength converters and exit the algorithm.

   Otherwise, put full wavelength conversion in each of the nodes in $\Im$-DS (the largest k-DS set of size smaller than X)

3. Repeat starting at j = NumberNodes

   3.1 Run RWA simulation with j nodes having full wavelength conversion as selected in the pervious step.

   3.2 Select the next $(j+1)^{th}$ node to be the node with the highest blocking percentage.

   Add a full wavelength converter to this node.

   3.3 Increment j by 1

   Until j =X

The first step in which we build the initial $\mathfrak{I}$-DS set has a time complexity of O(N. $\Delta$. $\mathfrak{I}$). $\mathfrak{I}$-DS is the largest k-DS set of size smaller than X. The iterative step where we use RWA simulation to find the next node to add has a time complexity of order O(N . RWA). RWA is the simulation time complexity which is order O(N . C) since each connection request will require updating the statistics at every node on its path.

We fixed the load at 100 Erlangs and run HYBRID(X) for X varying from 1 to the maximum number of nodes in the network (28 for the U.S Long Haul). Figure 7 shows the blocking percentages for the U.S Long Haul when the load is fixed at 100 Erlangs. k-DS coincides with HYBRID for 1 node (k=4), 3 nodes (k=3), 5 nodes (k=2) and 13 nodes (k=1). This is due to the fact that HYBRID returns the nodes computed by k-DS when X is equal to the cardinality of any k-DS master set. Notice that the points of the k-DS curve exist only at values of X equal to the cardinality of the k-Master set for k=1, 2, 3 and 4.

The HYBRID algorithm performs better than pure k-BLK which is based on ranking the nodes based on the blocking percentages. With higher number of nodes having full conversion (around X=22), HYBRID and k-BLK start to have similar results. Notice that the set of nodes selected by HYBRID always includes the k-DS master nodes. Our approach with HYBRID to the minimization problem is based on starting with the largest k-DS set possible. And iteratively adding the node experiencing the highest blocking.

As stated earlier, the time complexity of HYBRID is of order $O(N . \Delta . \Im) + O (N . C . (X- \text{sizeof} (\Im\text{-DS})))$.

k-BLK has a complexity of $O(N. C. X) + O(N^3)$. Where N is the number of nodes in the network, C is the total number of connection requests simulated, X is the number of nodes to be equipped with full wavelength conversion and K is the size of largest k-DS set less than X.

In terms of time complexity, HYBRID is similar to k-BLK but its performance is better since it takes advantage of k-DS and k-BLK simultaneously (i.e., it starts with the largest K-DS and iteratively adds a node at each step).

This is confirmed by the simulation results shown in Figure 7.

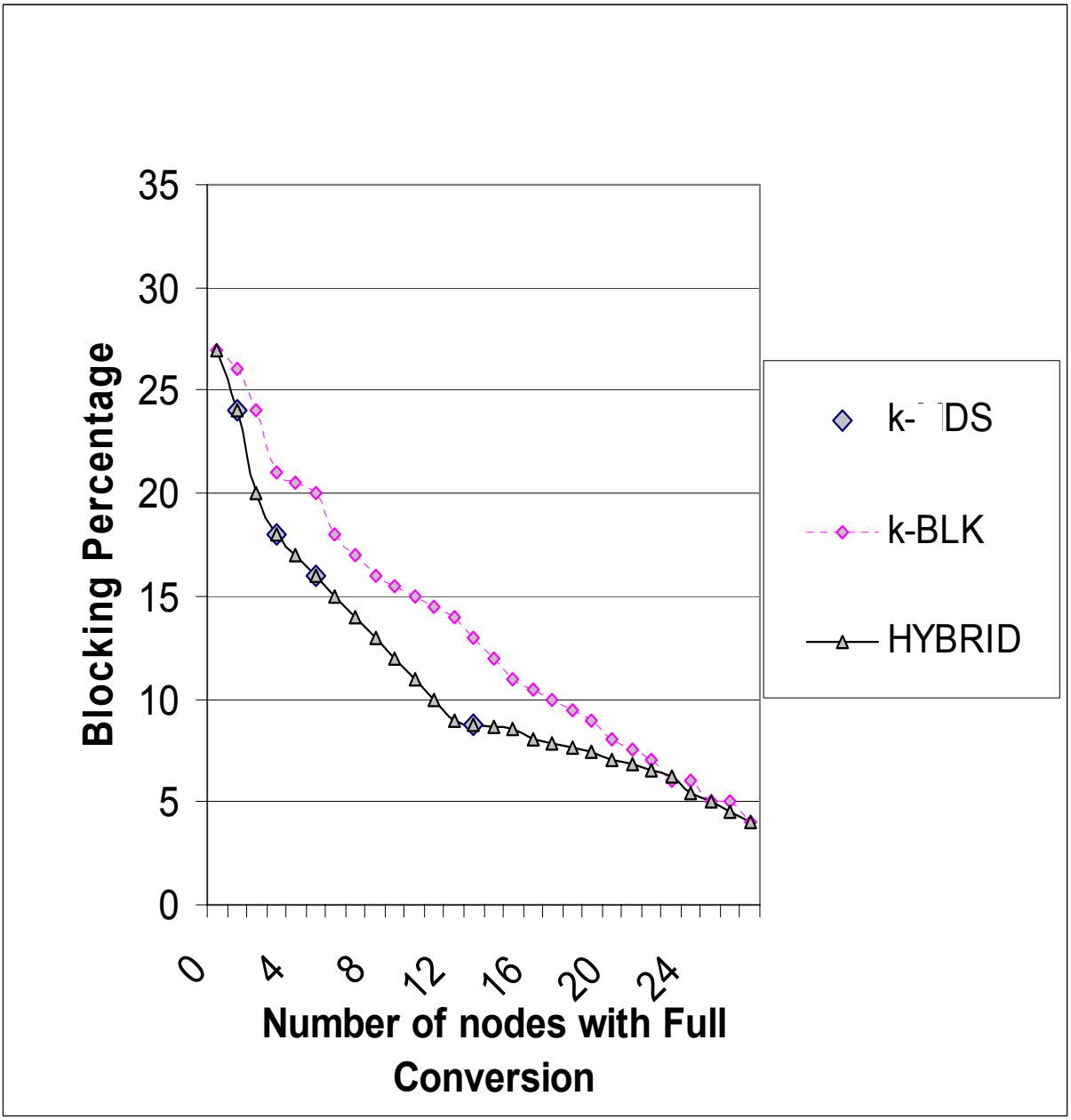


Figure 7: U.S. Long Haul, HYBRID with 100 Erlangs

# 3. ALGORITHM FOR PLACEMENT OF LIMITED WAVELENGTH CONVERTERS

In this chapter, we extend our k-DS algorithm [BLJ03] to the case of Limited wavelength conversion using three OXC designs. Our extension of k-DS to the case of limited wavelength conversion is based on dividing the nodes of the network into $\Re+1$ disjoint sets based on the domination factor. To place a wavelength converter given that Z wavelength converters are already sub-optimally placed, one node is selected from each set based on the experienced blocking performance. We simulate the network with the wavelength converter placed in each of the selected ($\Re+1$) nodes separately; the $(Z+1)^{th}$ wavelength converter will be placed at the node that gives the lowest overall network blocking performance. Our simulation considers also the case when the traffic is non-uniformly distributed between node pairs as in [BLO03].

Our approach minimizes the search space and allows better results than the full search algorithm previously proposed in the literature [JIM99, MSS02]. The local minimum problem reported in [JIM99] is eliminated since the k-DS scheme solves this minimization problem by finding a solution taking into consideration the traffic flowing through the nodes. We will show via simulation that our placement algorithm for limited wavelength conversion is cost effective and improves the utilization of the network. To our knowledge, our work is the first attempt to apply the Dominating Set approach to the design and engineering of optical networks in general and to the limited wavelength conversion placement in particular.

## 3.1 Background

The introduction of optical wavelength conversion (OWC) into wavelength routed optical networks allows a significant reduction of the blocking probabilities and an increase of the overall throughput. The conversion capability also increases the cost and complexity of the optical cross connects (OXCs). Converters must therefore be used judiciously and must be placed in nodes that maximize performance improvement. Hence there have been a number of studies to investigate sparse and limited wavelength converter placement in optical networks.

In [SAS96], the authors introduced the conversion density factor, q, of the network and an analytical model taking into consideration the correlation of wavelength usage between adjacent links. On three network topologies (ring, mesh-torus, hypercube), the reported results show that the uniform placement of sparse wavelength conversion (only selected nodes equipped with full conversion capability) is cost effective and can achieve most of the benefits of full conversion at every node of the network. The authors reported that the uniform placement technique works well for topologies with low connectivity such as rings but is not suitable for general topologies. This is due to the fact that the scheme doesn't take into consideration the topology of the network, the connectivity of each node and the expected traffic load.

The study in [VRK98] explores the heuristic of placing full wavelength conversion at nodes with high nodal degree. A network simulation is used to show the benefits of this placement heuristic. The simulation model uses an auxiliary graph, with M nodes, constructed based on the physical topology of the network. M is the product of N, the number of nodes in the network and W, the

number of wavelengths. The arcs are labeled with channel costs and conversion costs. Dijkstra's algorithm is applied for each connection request. The model considers a dynamic light path establishment. The used arcs are removed to reflect the wavelength usage in the network. When the connection is terminated, the graph is updated to reflect the newly released resources. The simulation results show that it is cost effective to place full wavelength conversion at high degree nodes; and that wavelength converters provide a significant gain in sparse networks but very little improvement in highly dense networks.

The authors in [JIM99] explored optical switch designs with limited number of wavelength converter units at each node. The designs implement the limited wavelength conversion with shared-nodal switch design using tunable optical multiplexers. The OXC can contain share-per-node wavelength converter units, or share-per-link wavelength converter units that are shared by the incoming circuits. This type of limited conversion switch has the potential of achieving most of the benefits of a full conversion-capable switch at a much lower cost. A heuristic of complexity $O(N^3)$ was introduced in [JIM99] for placement of individual limited wavelength converter units in the nodes of the optical network.

In [MSS02], the authors introduced a ranking based heuristic for limited converter placement. Via simulation, each node is ranked given the experienced blocking performance. Iteratively, the heuristic reshuffles the wavelength converters between nodes with low blocking to nodes with high blocking until there is no improvement in the overall blocking performance. The results indicate that shared-per-link architecture is cost effective and provide a good tradeoff for

performance compared to the shared-per-node architecture. The disadvantage of such heuristic is its complexity when considering large networks.

The study in [KLM93, KLJ93] shows that routing and wavelength assignment with wavelength conversion capability is an NP-complete problem. The optical cross-connect allows wavelength converters to be shared at the node level or between links. It also requires tunable optical multiplexers that make the design more expensive. A routing algorithm is introduced, similar to [VRK98], with a reported time complexity of order $O(N^4 . W^2)$ without including the number of incoming connection requests to the network in the analysis.

The authors in [AAS02], instead of using time-consuming simulations, presented an analytical model for arbitrary topologies and traffic loads. It is assumed that each node has a converter with a probability q. An analytical model is introduced to take into consideration the dependence and correlation of wavelength usage between adjacent links. It is assumed that the wavelength usage on a link is dependent only on the usage on an adjacent link. The authors reported that the model provides accurate blocking probabilities compared to simulation results but it is not tractable for networks with high diameter.

In [DLJ02], the authors focused on shared-per-link design; where each outgoing link has a dedicated converter bank that is only used by the connection passing through this particular link. The complexity of such design, based on tunable multiplexers, is cost effective compared to the shared-per-node OXC design. The placement problem is modeled as an Integer Linear Program (ILP) in which the objective function is to maximize the total amount of traffic passing through

the network. An acyclic auxiliary graph is built in the same way as in [VRK98] and the Bellman-Ford algorithm is used to find the shortest path between a source and destination to establish a connection request. The time complexity of the approach is dependable on the size of the network, N, the number of wavelength per link, W, and the total number of simulated connection requests, C. The time complexity of the approach is order $O(C. N^4. W^2)$.

The study in [XJD02] introduces a novel placement for full OWC for minimal wavelength usage. This is achieved by making the number of wavelength needed to be equal to the maximal link load. The scheme achieves load-wavelength assignability and it is based on splitting a general topology network into simpler sub-graphs such as paths and spiders as in [GWW98]. The reported results show that the approach combines the problem of finding the minimum number of wavelengths needed and the problem of full OWC placement.

The authors in [WLW01] focus on survivability, load balancing and capacity constraints as criteria for OWC placement for the static RWA problem. The scheme places a full OWC at the node with the highest transit load. To avoid that the network traffic becomes unevenly distributed, a conversion cost function is used to allow backtracking so that the proposed heuristic can remove a full OWC if it is not needed in the final placement. The proposed algorithm reduce the number of used wavelength by 21% than the approach in [OCB98] which uses higher objective functions for states where capacity constraints are violated.

In [BSR02], a path-metric based algorithm is used for full OWC placement. A weighting factor (WF) allows the ranking of all the nodes and the placement decision is based on the computed

values (nodes with higher WF should have full OWC. WF depends on the number of hops between nodes and the interference length taking into consideration the paths that are sharing one or more links with the considered path. The approach applies to static routing when traffic requests are known in advance and does not take into consideration the routing scheme and wavelength assignment.

The study in [MLZ01] considers distributed algorithms minimizing the number of wavelength conversions when establishing a connection on a given path. The approach is extendable to sparse wavelength conversion and limited wavelength conversion by applying different levels of aggressiveness in locking wavelength during path establishment. The reported results indicate that since wavelength availability is dynamic, adaptively assigning the wavelength to use is more crucial than the selection of the route for path establishment.

Some studies investigated other solutions for wavelength contention in WDM networks. The authors in [VSK99, YLE96] explore limited range OWC as a cost-effective solution instead of full OWC. The heuristic in [VSK99] is based on ranking the nodes by nodal degree. An auxiliary graph is built to capture the wavelength available per link as in [VRK98]. In [YLE96], an analytical model is used to estimate the network performance for unidirectional rings and mesh-torus topologies. The reported results suggest that with only 50% of the full wavelength conversion range, the same the blocking performance can be achieved as with full range conversion. The study in [RDH01] envisions that if certain nodes are capable of full OWC, broadcasting can be supported in WDM networks. The heuristic is based on the color covering

and the vertex color-covering problems; and it achieves the optimal solution 52% of the time with an average performance ratio of 1.169.

In what follows we describe in detail the considered switch designs allowing limited wavelength conversion and we introduce our placement heuristic. Our simulation results will cover the case of uniform distribution of traffic between (source, destination) pairs and also the case when the traffic is not uniformly distributed between node pairs for the NSFNET and the U.S Long Haul topologies.

## 3.2 OXC Switch Design with Limited Wavelength Conversion

Full wavelength conversion at a selected set of nodes improves the blocking performance of the network. This is referred to as the sparse full wavelength conversion. Further cost reduction can be obtained by deploying only a limited number of wavelength converter units at each selected node [JIM99, MSS02]. This is referred to as the limited wavelength conversion. The overall network performance achieved could be similar to the placement of sparse full wavelength conversion. This is due to the fact that at any given node only a portion of the wavelength conversion capability is used at any given time.

All of the proposed designs in [KLM93, KLJ93,VRK98, JIM99, MSS02, AAS02] use tunable multiplexers which do not yet exist and will not be available in the near future due to fundamental limitation of light propagation. Our optical switch designs are ideally suited for the case when fiber capacity or the size of the OXC is over-designed for future expansions so that

there are unused ports available. Consequently, the limited wavelength conversion does not incur any additional cost of switching. In addition to their scalability, our proposed designs ensure that no tunable multiplexers are needed as opposed to the previously proposed architectures in the literature.

In this section, we consider the case of limited wavelength conversion in the sense that the number of wavelength converter units $C_\lambda$ is smaller than F.W (needed for full conversion), where F is the number of fibers in the considered node and W is the number of wavelengths per fiber. These $C_\lambda$ any-to-any wavelength converter units are shared by all possible light paths that pass through the optical switch for the case of node-sharing designs. We will introduce a flexible and a strict implementation of node-sharing OXC design.

We also explore a design where the wavelength converters are statically mapped to an output link. With this simple optical switch design, there are two choices to make. The first step is to choose the node for placing the wavelength converter and the second step is to choose the output link to which this converter will be permanently assigned (statically mapped).

We will show via simulation that limited wavelength conversion achieves most of the benefits of full wavelength conversion while increasing the fault tolerance [JIM99]. We will also compare our optical switch designs with limited wavelength conversion taking into consideration the switch design complexity (cost) and the overall network performance achieved.

### 3.2.1 Flexible node-sharing OXC design

Our proposed architecture for the flexible node-sharing optical switch with limited wavelength conversion is shown in Figure 8. We propose a cost effective optical switch design using non-tunable optical multiplexers. The size of switch node is NxN where $N \geq F.W + C_\lambda$. Any light-path that needs wavelength conversion from input port i to output port j will be first routed to one of the output ports, F.W+k where $1 \leq k \leq C_\lambda$, for wavelength conversion. The wavelength-converted signal at input port F.W + k will then be switched to output port j.

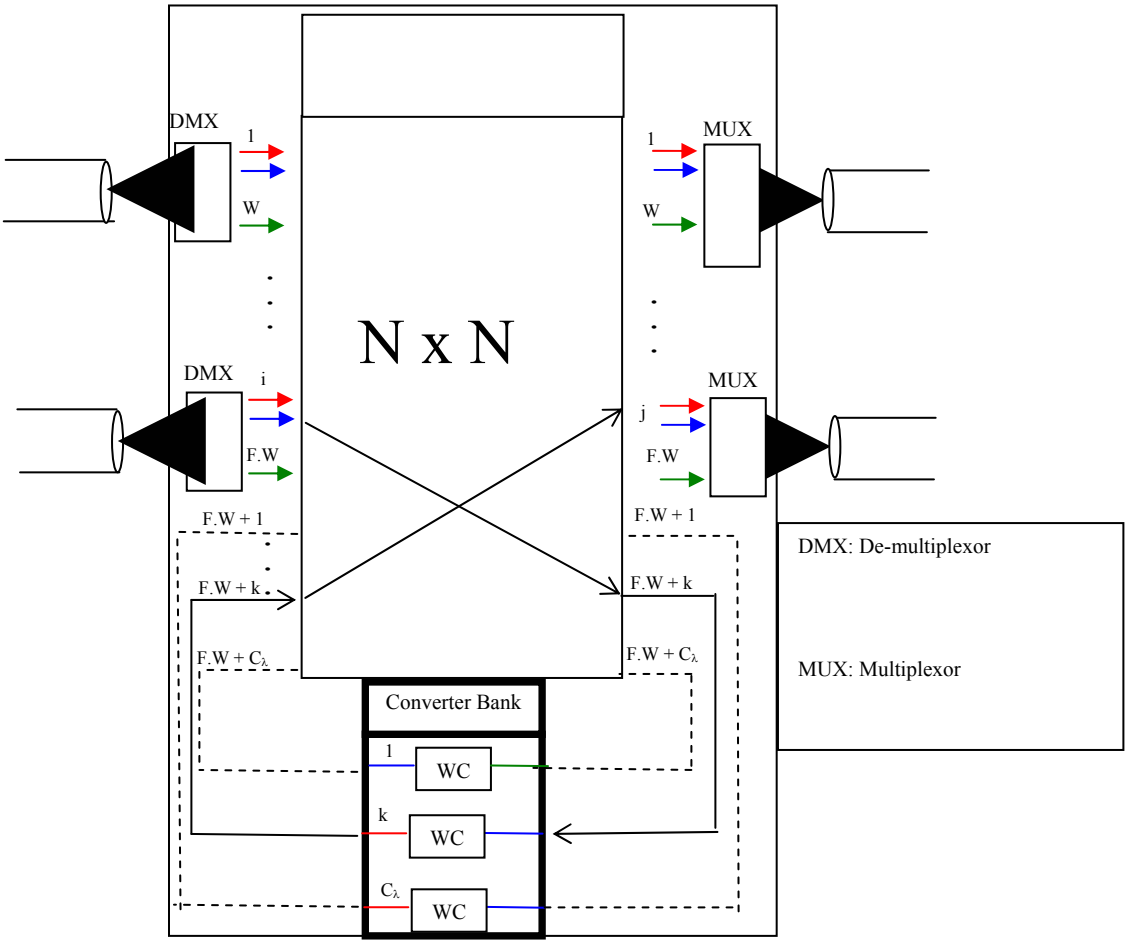


Figure 8: Flexible Node-sharing optical switch design

The flexible node-sharing switch design allows a centralized sharing at the node level of the wavelength conversion bank. The any-to-any wavelength converters are available to all output links and used by any connection requests.

### 3.2.2 Strict node-sharing OXC design

The strict node-sharing optical switch with limited wavelength conversion is shown in Figure 9. A wavelength converter $C_\lambda$ in this design has W sub-circuits for fixed wavelength conversion; each sub-circuit converts any incoming wavelength to one of the W different wavelengths. The wavelength converters are shared among all the outgoing links. However, we assume that once a converter is used for a given output link, it cannot be used for another output link at the same time; but it can be used to convert different wavelengths (up to W) on the same output link.

This assumption is not due to the limitation of the switch fabric but is made here for easy comparison with the static mapping OXC design described subsequently. When a converter becomes idle, it can be used with a different output link. Note that each conversion sub-circuit is specialized to convert to one unique output wavelength. The strict node-sharing design uses simpler conversion units (any-to-$\lambda$) as opposed to the flexible node-sharing that uses any-to-any wavelength conversion units.

In Figure 9, converter number 1 is used for output link number F. Sub-circuit 1, in converter 1, is used for wavelength conversion for the connection from input link number 1 to output link number F. Sub-circuit W, in converter 1, is used for the connection from input link F to output link F at the same time. Converter number $C_\lambda$ is idle since all its sub-circuits are unused and will be available to an output link if needed.

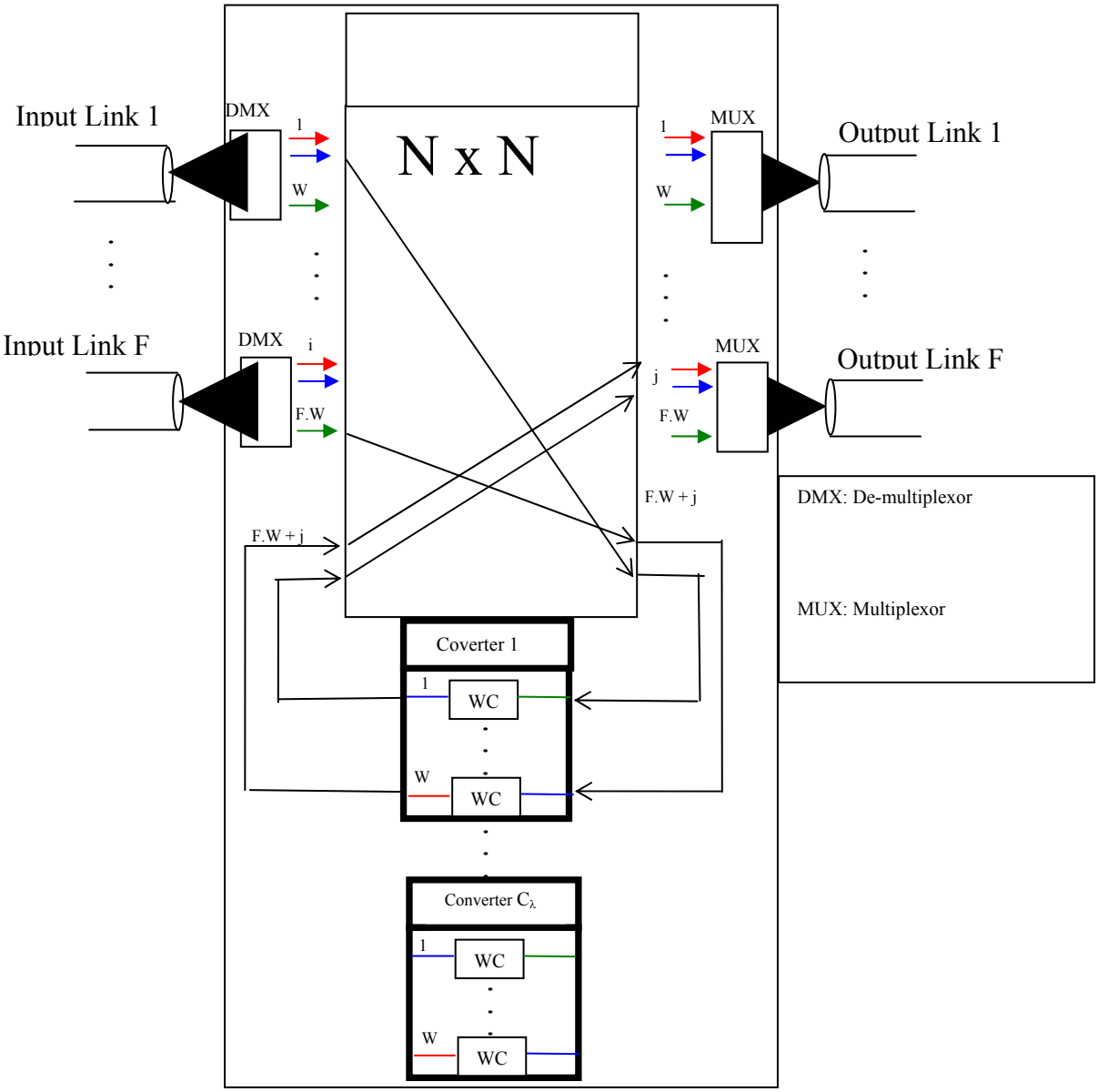


Figure 9: Strict node-sharing optical switch design

Note that our placement scheme for the flexible node-sharing design is based on one wavelength converter unit to be placed at each step. With the strict node-sharing design, we will be placing one converter containing W sub-circuits for wavelength conversion in each step. Our placement algorithm in either case will have to select a node where to place one single additional wavelength converter unit for the flexible node-sharing switch design; and will select a node where to place a converter containing W sub-circuits for the strict node-sharing switch design. Consequently, the number of conversion units available in the network will be increased by 1 at every step when the flexible node-sharing design is considered and will be increased by W after each step when the strict node-sharing design is studied.

### 3.2.3 Static mapping OXC design

In our static mapping optical switch design with limited wavelength conversion, a converter is attached to a specific output link on a permanent basis. A wavelength converter $C_\lambda$ in this design has W sub-circuits to convert to W different wavelengths (similar to the strict node-sharing design). The wavelength converters are not shared among all the outgoing links. A converter is dedicated to a given output link, it cannot be used for another output link, but it can be used to convert different wavelengths (up to W) on the link it is mapped to. Figure 10 describes the static mapping optical switch design for limited wavelength conversion. Wavelength converter 1 has W sub-circuits dedicated to output link F.

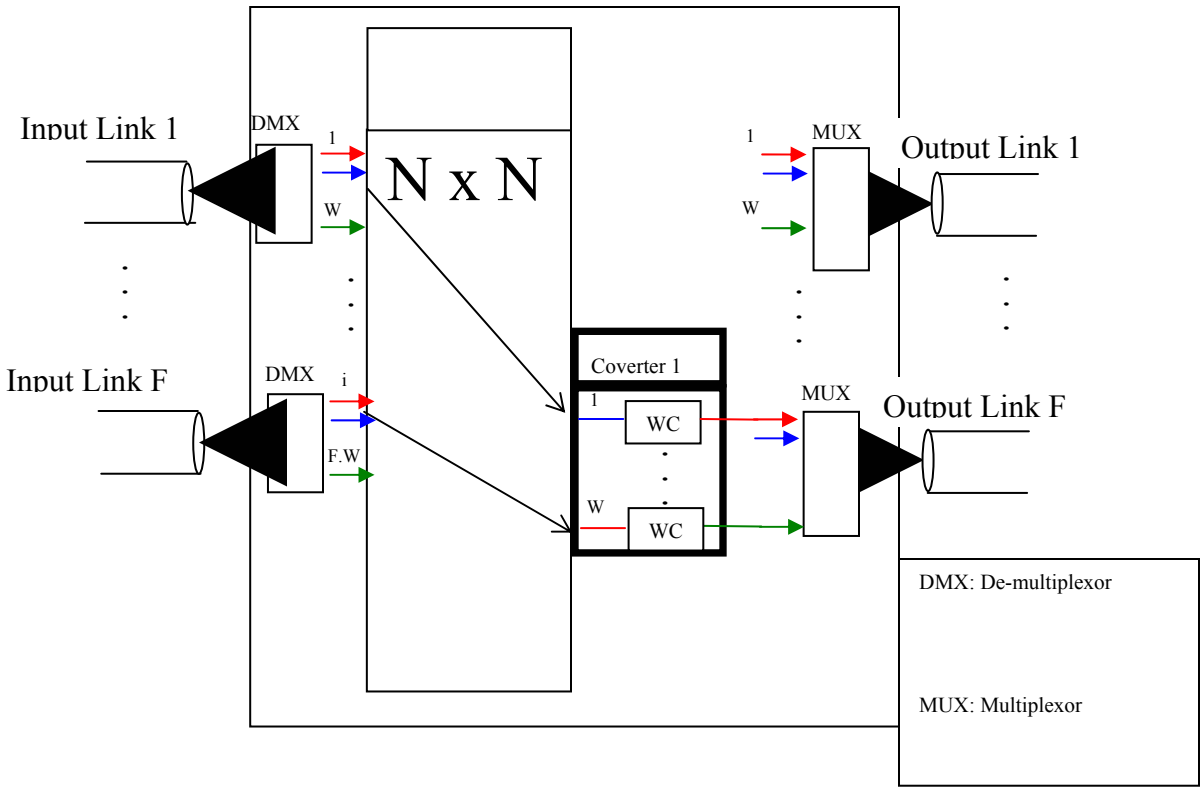


Figure 10: Static mapping optical switch design

The next step is to introduce our limited wavelength conversion placement algorithm; and apply it to each OXC design and compare its performance against the full search based heuristic introduced in [JIM99, MSS02].

## 3.3 k-DS Algorithm for Limited Wavelength Conversion

In this section, we propose the LIMITED algorithm for the placement of limited wavelength conversion based on our k-DS algorithm. Excluding the overhead of the simulation step as was done in [JIM99], the worst case complexity of LIMITED is $O(\Re.N^2)$ where $\Re < N$ as will be

explained shortly. Instead of trying all N possible placements for an individual converter unit as was done in the F-SEARCH heuristic [JIM99], our algorithm divides the nodes into ($\Re$+1) disjoints sets based on k-DS and runs the network simulation for the highest blocking node in each of those disjoint sets. The final placement decision will be made based on the node, out of the ($\Re$+1) selected, that provides the lowest overall network blocking percentage.

Given a network with Z existing converter units already placed semi-optimally, our LIMITED algorithm finds the placement for the next $(Z+1)^{th}$ converter in the network. As stated earlier, depending on the considered switch design, the converter to be placed will be one wavelength conversion unit for the flexible Node-sharing switch design; and it can be a wavelength converter containing W sub-circuits when the strict Node-sharing is considered. For the static mapping switch design, the algorithm will select a node and then a link to have a statically mapped wavelength converter. The LIMITED algorithm is described as follows:

1. Compute all k-DS sets, starting at k equals 1, until the last $\Re$-DS set has one member.

2. Initialize $\Re$+1 disjoint sets:

SET 1 = $\Re$-DS

SET 2 = ($\Re$-1)-DS – $\Re$-DS

SET 3 = ($\Re$-2)-DS – ($\Re$-1)-DS etc.

SET $\Re$ = 1-DS – 2-DS and SET $\Re$+ 1 has the rest of the nodes.

3. Run the network simulation with the existing Z individual converter units in the network.

4. Find the highest blocking node in each set of the $\Re$+1 computed sets.

5. For each one of the ($\Re$+1) nodes selected in step 4, run network simulation with the $(Z+1)^{th}$ converter unit placed in that node. For the static mapping case, place converter at the highest blocking link in the node.

6. Place the $(Z+1)^{th}$ converter unit in the node with the lowest overall network blocking computed in step 5.

Notice that the LIMITED algorithm avoids the greedy full search (examination of all possible combinations to place the $(Z+1)^{th}$ converter) as was done in the F-SEARCH heuristic [JIM99]. Instead, it uses a search based on the computed dominating sets k-DS. As we will see through simulation results, this makes the LIMITED algorithm more stable and less prone to the local minimum problem reported in [JIM99]. The reported complexity of F-SEARCH is reported to be $O(N^3)$.

## 3.4 Simulation and Results under uniform traffic

We compare the performance of each optical switch design using the U.S Long haul topology [VRK02] including 28 nodes and 45 links. Each link is a bidirectional fiber with 8 wavelengths (W equals 8). The connection holding time is exponentially distributed and the traffic is

uniformly distributed over all node pairs. When a connection request arrives to the network between a source, s, and destination, d, a pre-computed shortest path is taken to reserve a wavelength in each link in the path. The wavelength assignment is random and the reservation is done in the forward direction.

Our network simulation is based on a discrete-event model with a time-advance mechanism to the most imminent event to be processed. Each event processing affects the state of the system and the time of occurrence of future events. Our simulation models six different events: an arrival of a connection request to the network, a departure of a reserve control request from a particular node to the next hop node, the event of blocked connection request due to lack of resources, the event of establishment of the connection request at the destination node, the event of termination of an established connection allowing the release of resources and the event of ending the simulation after C connections processed. C is $10^6$ times the considered load of traffic in the network. The load, in Erlangs, is the product of the arrival rate and the average holding time. The simulation takes into consideration the control message processing time, P, at each node. P is assumed to be 10 μs. The propagation delay is estimated based on the kilometric distance between nodes and the speed of light. The hop based shortest paths between node-pairs are computed in advance using dijkstra's algorithm.

Our extensive simulation tests with randomly generated topologies have shown that the LIMITED algorithm provides excellent placement for nodes with limited wavelength conversion. We now apply our algorithm to a realistic topology: the U.S Long haul [VRK98] is described in Figure 5.

Our k-DS algorithm [BLJ03] produces the following results for the U.S long Haul network:

1-DS = {1,3,4,5,8,10,12,15,17,20,22,25,27}.

2-DS = {4, 8, 12, 17, 25}. Every node is at most 2-hops away from a member of 2-DS.

3-DS = {8, 12, 17}.

4-DS = {12}. Every node is at most 4 hops away from node 12.

With the U.S. Long Haul network $\Re$ is 4, and the computed disjoint sets are:

SET 1 = 4-DS = {12}

SET 2 = (3-DS) – (4-DS) = {8, 17}

SET 3 = (2-DS) – (3-DS) = {4, 25}

SET 4 = (1-DS) – (2-DS) = {1, 3, 5, 10, 15, 20, 22, 27}

SET 5 =contains the rest of the nodes, i.e., 15 nodes.

Our comparison results of LIMITED and F-SEARCH under different traffic loads are presented in Figure 11 for the flexible node-sharing switch design, in Figure 12 for the strict node-sharing switch design and finally in Figure 13 for the static mapping design. Under a fixed load of 50, we started with no wavelength conversion and at each step added a unit of conversion following the LIMITED algorithm. We continued to do so until we placed 50% of the maximum number possible of wavelength converters units, 720 in this case.

For the three proposed switch designs, the results show that the full search of all possible placements by F-SEARCH can miss-examine a combination of converter placements that reduce the blocking percentage. As it can be seen from the curves of F-SEARCH (in Figure 11, Figure 12 and Figure 13), the greedy full search frequently causes the blocking percentage to increase and decrease unexpectedly due to the local minimum problem (this problem was also reported in [JIM99]). On the other hand, the LIMITED algorithm is more stable since we base our search on k-DS sets; and it is also faster and less complex.

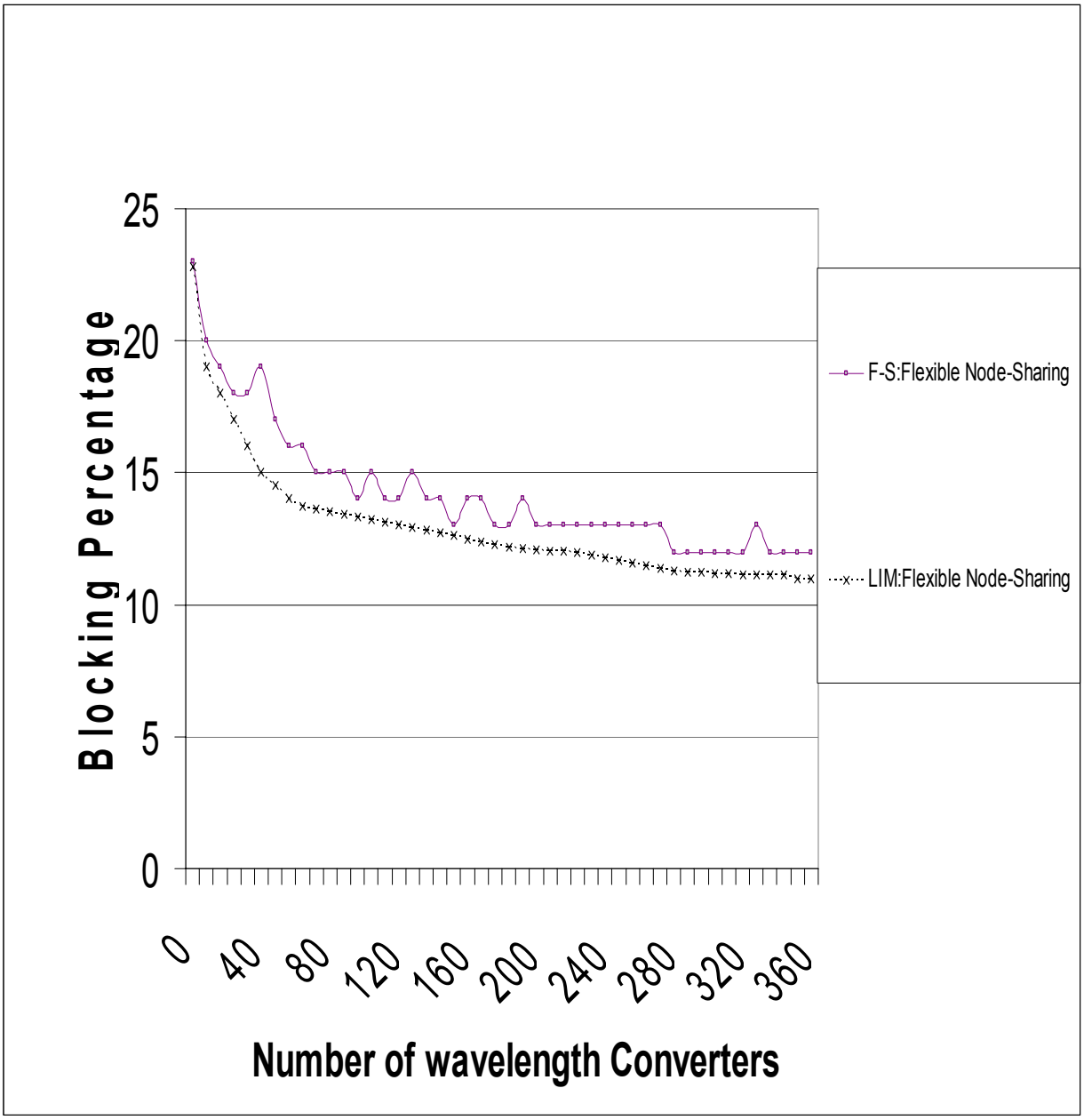


Figure 11: Flexible node sharing simulation results for U.S. Long Haul

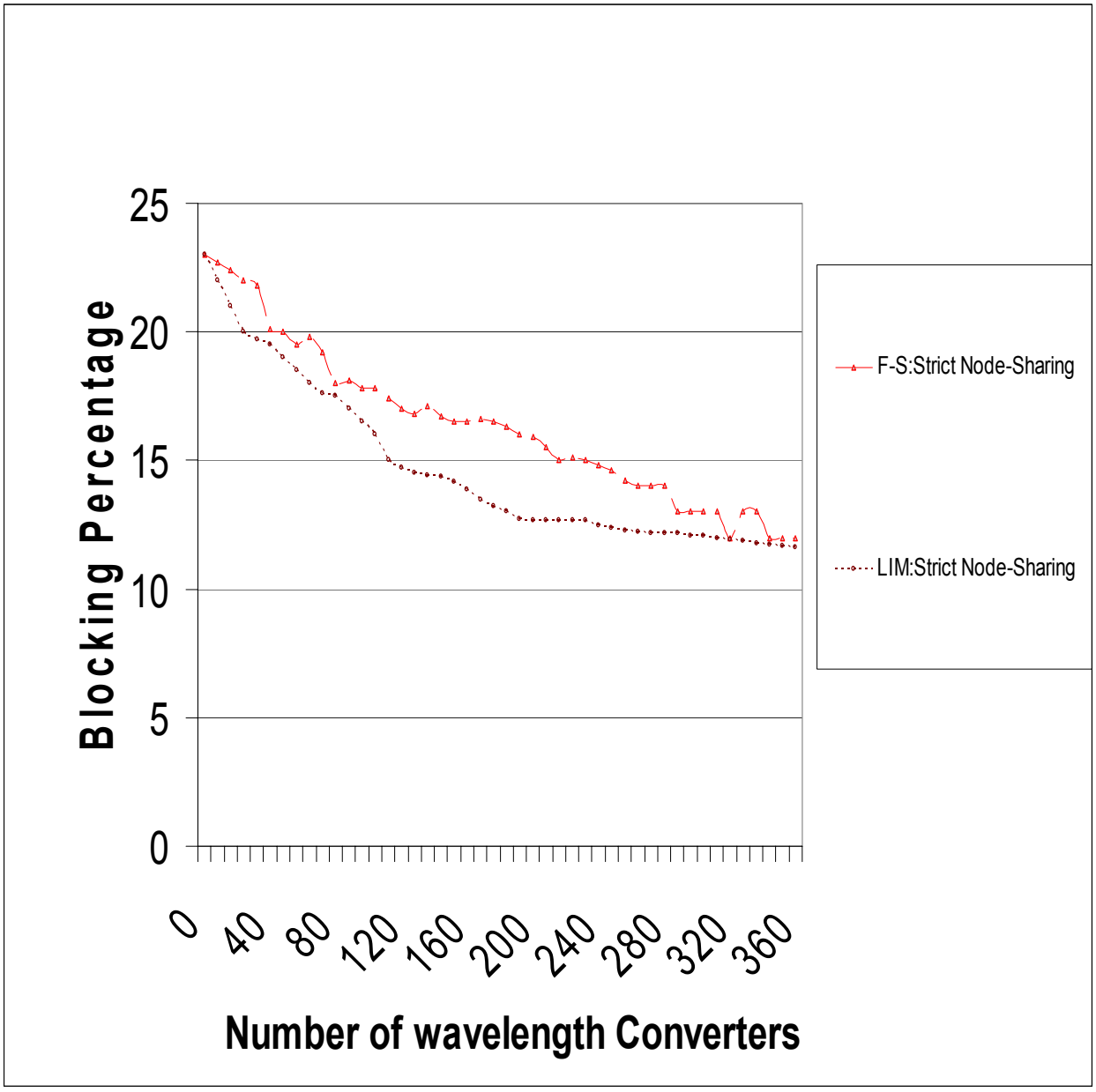


Figure 12: Strict node sharing simulation results for U.S. Long Haul

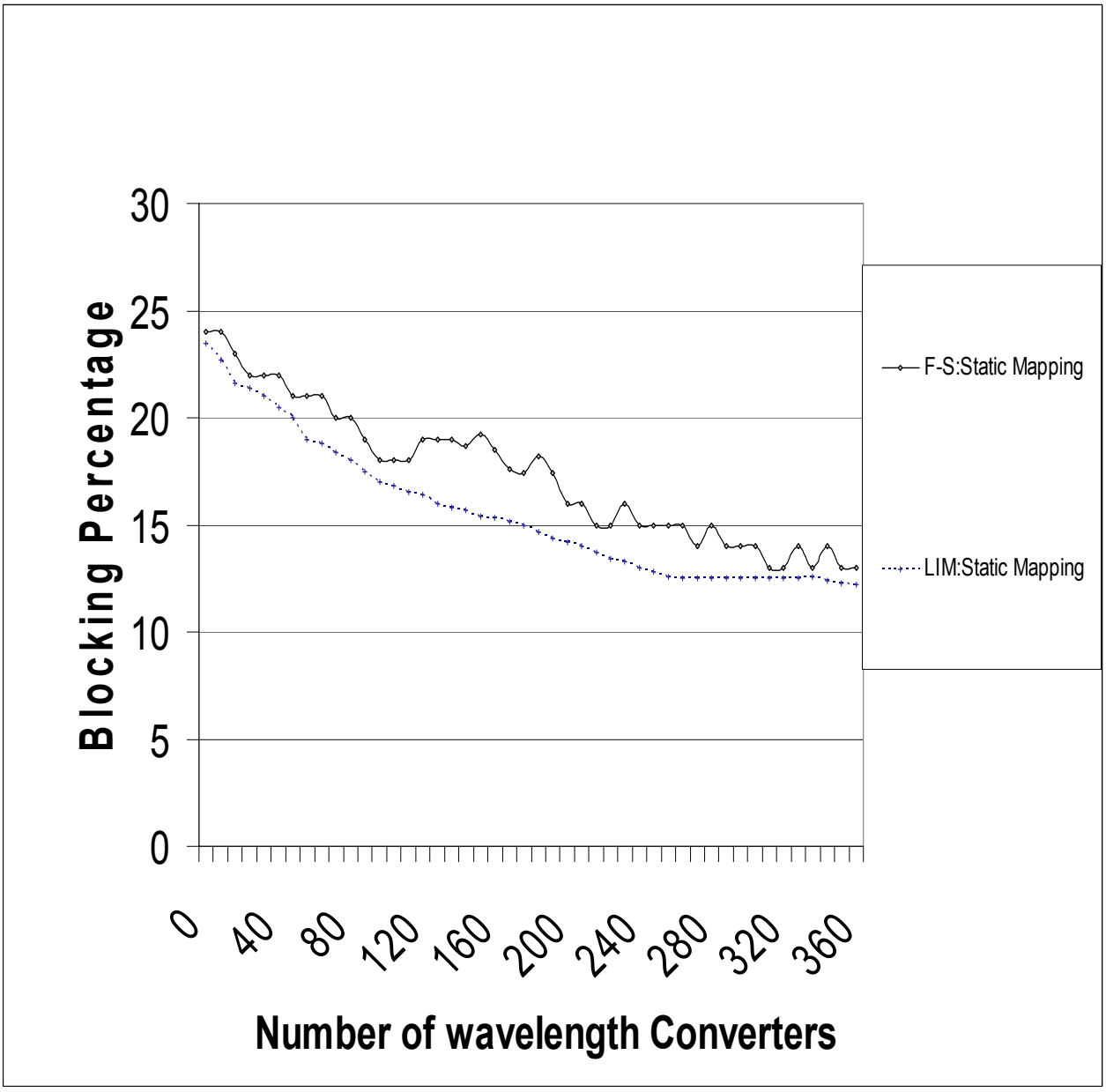


Figure 13: Static mapping simulation results for U.S. Long Haul

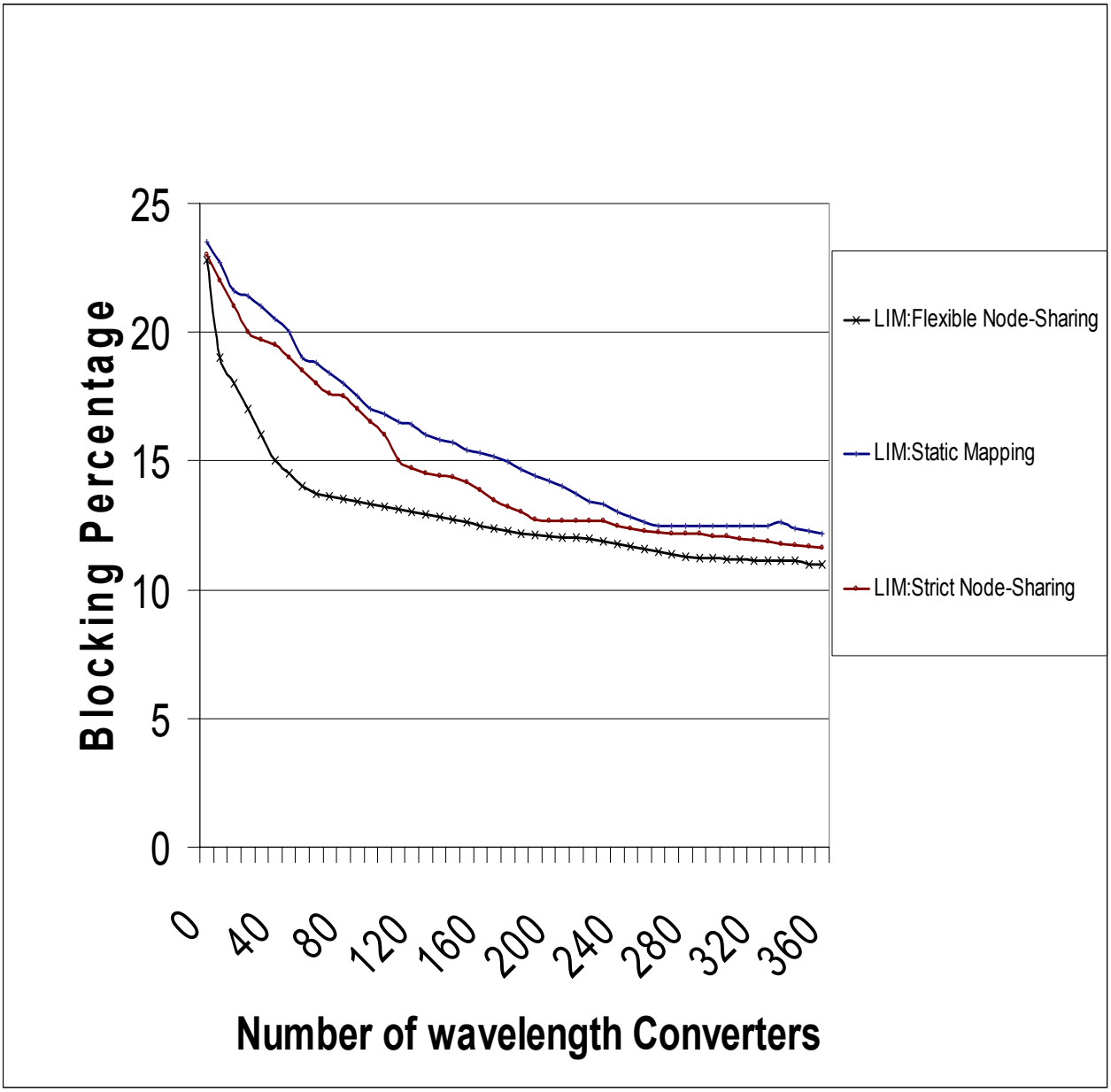


Figure 14: Combined simulation results for U.S. Long Haul

In Figure 14, we compare the proposed optical switch designs using the same method. The Flexible node-sharing outperforms the other design since it allows all output links to share the wavelength conversion bank. It fulfills the wavelength conversion needs of incoming connection

request in a centralized fashion. The Flexible node-sharing is suited when 200 or less wavelength converters are to be placed in the network (around 25% of the maximum of 720 converter units). The Flexible switch design uses any-to-any wavelength converters which make the switch fabric more expensive.

Also from Figure 14, we can see that the static mapping switch design is simpler and can provide comparable improvements as the strict node-sharing design. Both designs use simple wavelength converter with fixed wavelength output (any-to-λ converter). When more than 50% of the maximum possible conversion units are to be placed, all switch designs tend to have comparable performances.

So far we assumed that the traffic is uniformly distributed between node pairs and our placement scheme k-DS assumes that all nodes generate the same traffic in the network. In the next section, we apply the weighted k-DS, referred to as k-WDS, for the NSFNET topology and show its benefits for placing limited wavelength conversion.

## 3.5 Simulation Results under non uniform traffic

We consider the NSFNET topology (described in Figure 33) under non-uniformly distributed traffic between node pairs. We use k-WDS [BLO03], which differs from k-DS in the computation of $Connect_0$ (v). Under non-uniform traffic $Connect_0$ (v) is the product of Degree(v) and the weight of the node v:

$$Connect_0 (v) = Degree (v) . Weight(v)$$

We applied our voting algorithm to compute the k-WDS set as an approximation for the Weighted Dominating set for the NFS backbone.

The following table lists the randomly generated weights for each node in NSFNET:

Table 1: Placement of Limited Conversion: Assigned Node weights for NSFNET

| Node | Weight | Node | Weight |
|---|---|---|---|
| 0 | 6 | 8 | 7 |
| 1 | 12 | 9 | 2 |
| 2 | 7 | 10 | 7 |
| 3 | 12 | 11 | 15 |
| 4 | 5 | 12 | 3 |
| 5 | 8 | 13 | 15 |
| 6 | 1 | 14 | 9 |
| 7 | 11 | 15 | 2 |

The k-WDS algorithm provided the following results for the NSFNET:

1-WDS (NSF) = {1, 4, 5, 6, 9, 11, 14},

2-WDS (NSF) = {1, 4, 9, 14}, and

3-WDS (NSF) = {14}

With the NSFNET topology, $\Re$ is 3, and the computed disjoint sets are:

SET 1 = 3-DS = {14}

SET 2 = (2-DS) – (3-DS) = {1, 4, 9}

SET 3 = (1-DS) – (2-DS) = {5, 6, 11}

SET 4 = the rest of the nodes, i.e., 9 nodes.

Our comparison results of LIMITED and F-SEARCH under non-uniform traffic are presented in Figure 15 for the flexible node-sharing switch design, in Figure 16 for the strict node-sharing switch design and finally in Figure 17 for the static mapping design. Under a fixed load of 70, we started with no wavelength conversion and at each step added a unit of conversion following the LIMITED algorithm. We continued to do so until we placed 50% of the maximum number possible of wavelength converters units, 400 in this case.

For the three proposed switch designs, the results show that F-SEARCH miss-examines some combination of converter placements. The curves of F-SEARCH (in Figure 15, Figure 16 and Figure 17) show that this placement algorithm suffers from a local minimum problem. In comparison, the LIMITED algorithm is more stable since we base our search on k-WDS sets; and it is also faster and less complex.

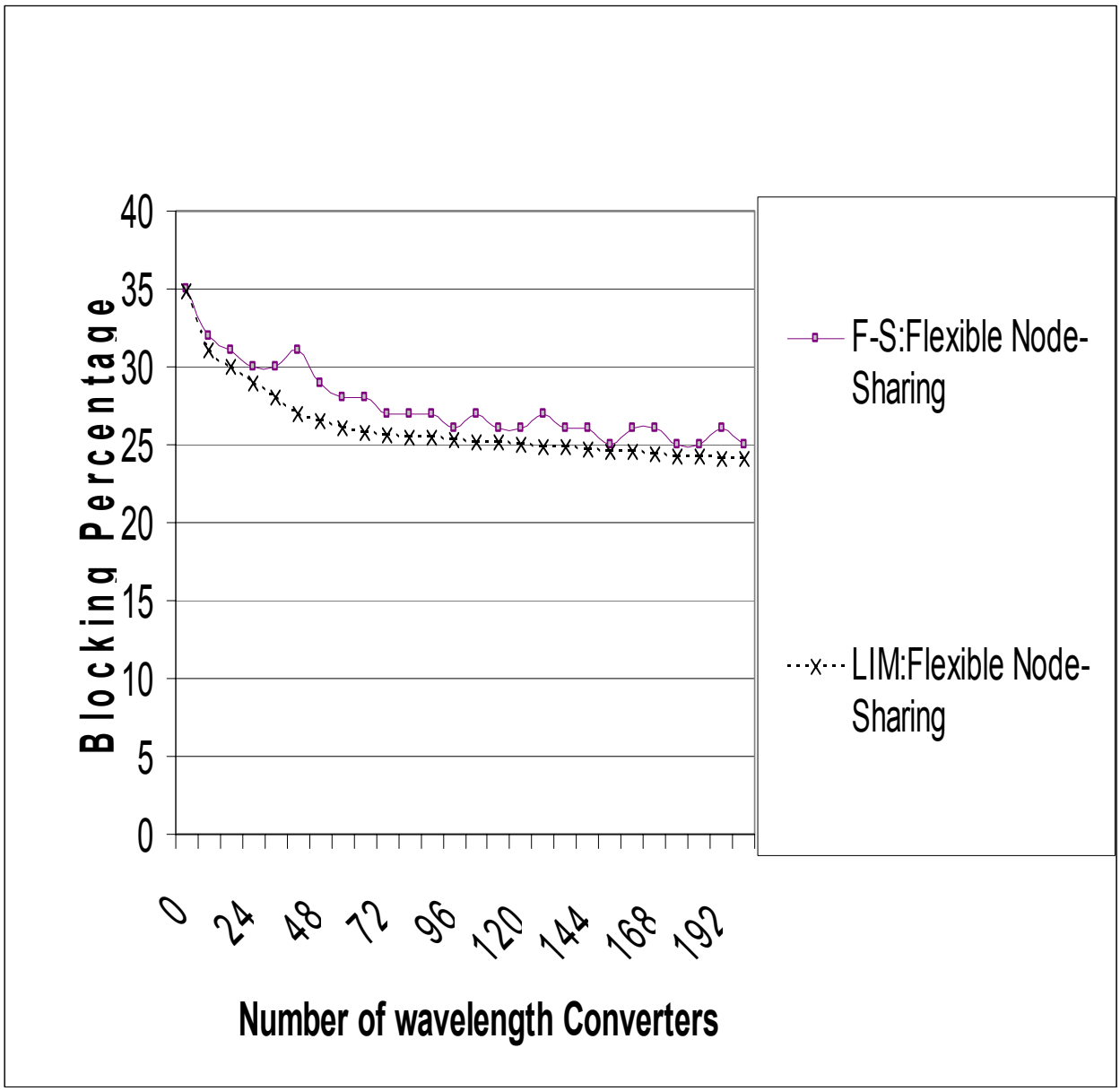


Figure 15: Flexible node sharing simulation results for NSFNET

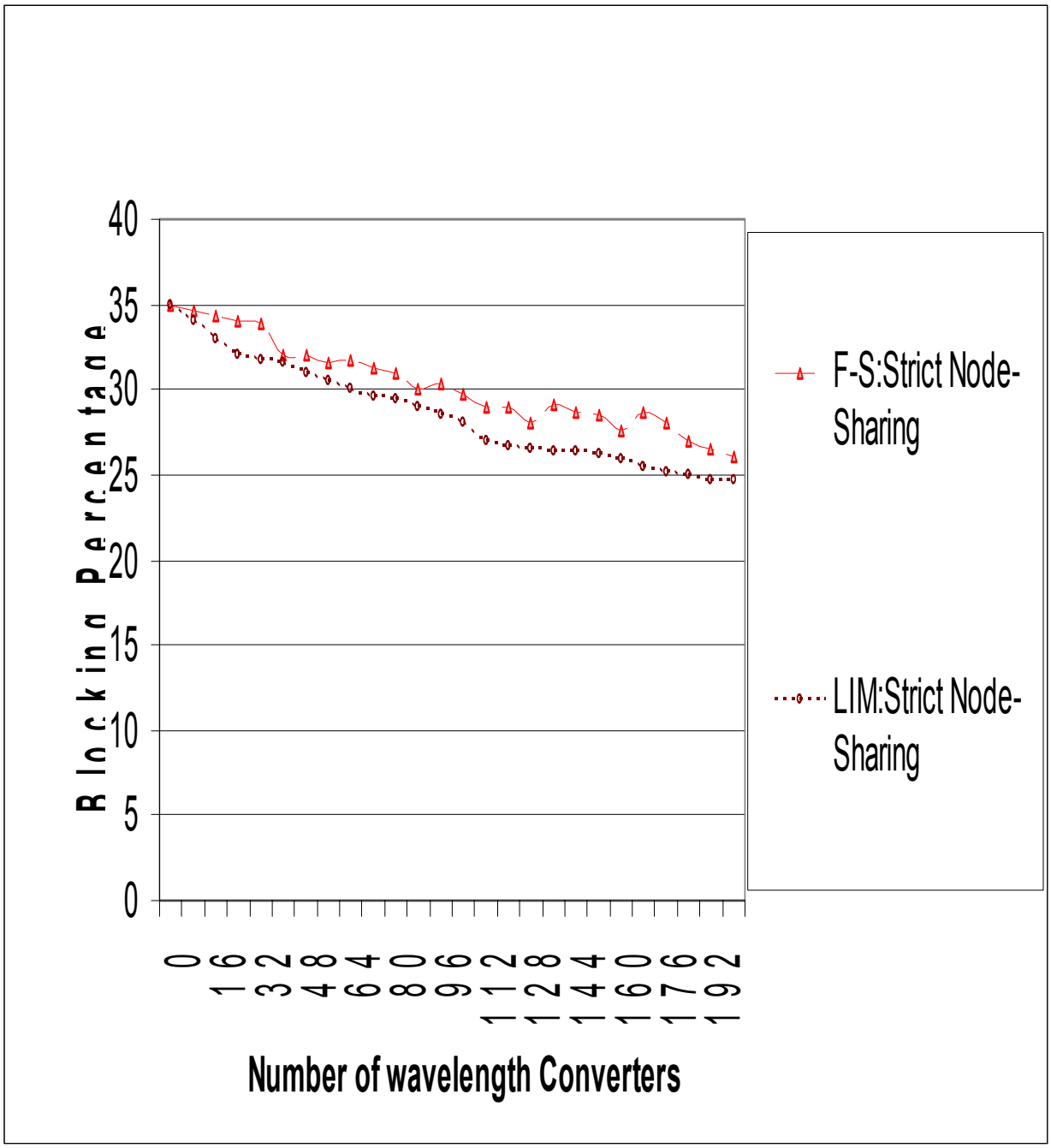


Figure 16: Strict node sharing simulation results for NSFNET

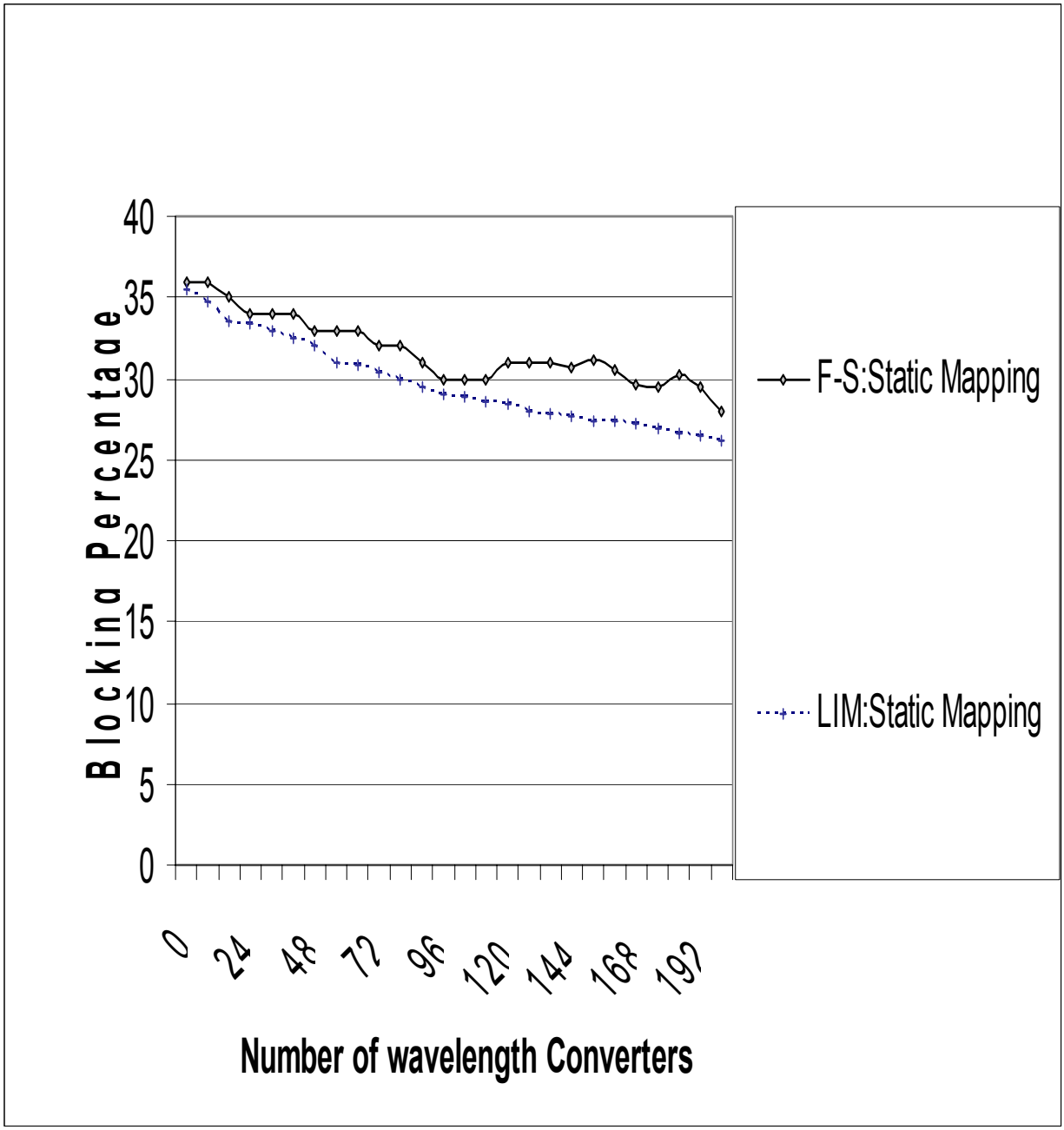


Figure 17: Static mapping simulation results for NSFNET

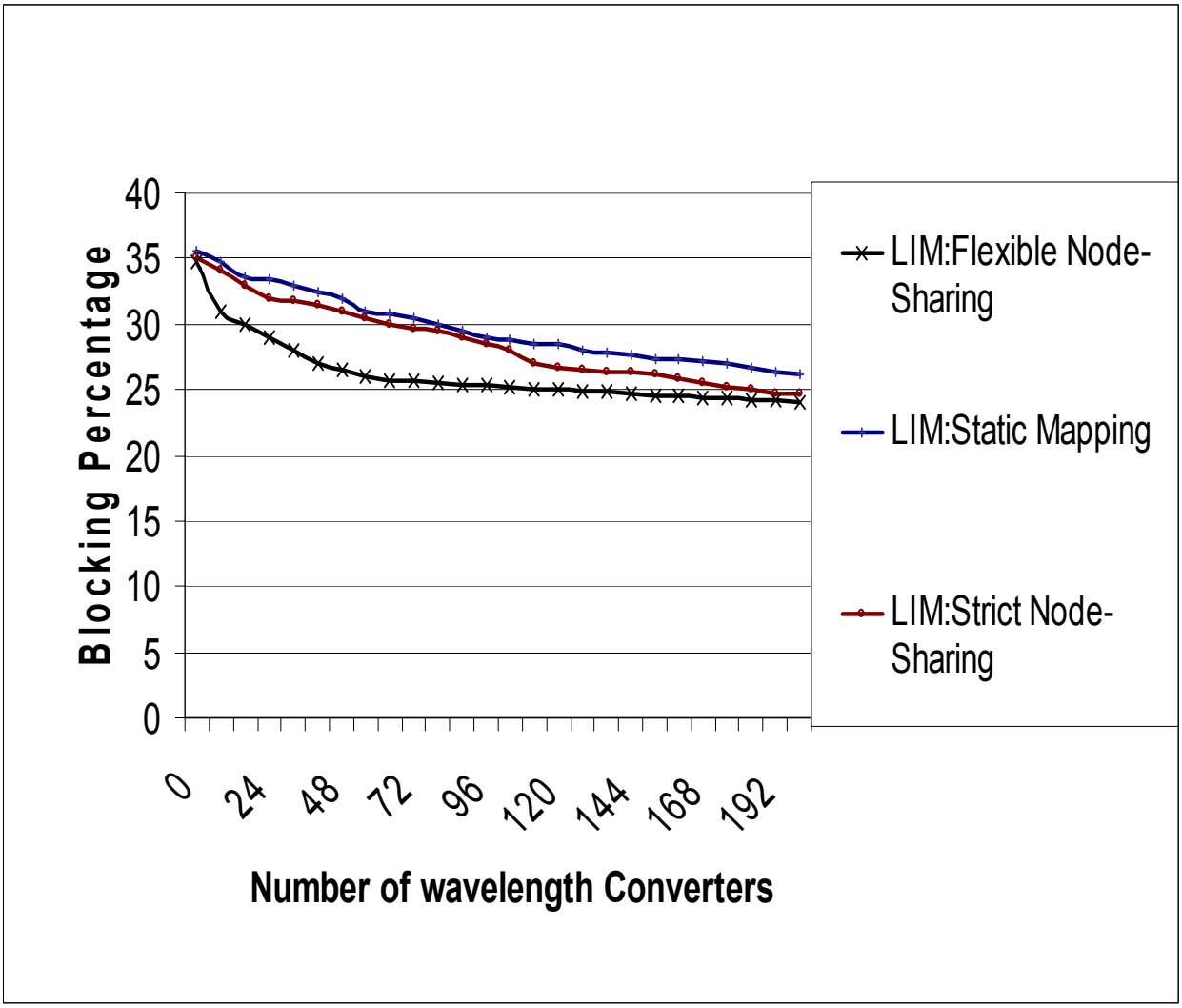


Figure 18: Combined simulation results for NSFNET

From Figure 18, we can see that the cost drives the decision making about which switch design to adopt. Static mapping with a cost effective switch fabric can achieve comparable improvement compared to the strict node-sharing design. This is due to the fact that the strict node-sharing allows converters, when idle, to be shared between links. This increases sharing of the wavelength conversion capability inside the node. The flexible node-sharing allows the

maximum sharing with its any-to-any wavelength converter units. When few wavelength converters are to be placed, the benefits of the flexible node-sharing switch design are very promising compared to the other two.

The flexible node-sharing design is suited for networks where the fiber capacity (dense network) or the size of the OXC is over-designed for future expansions with unused ports. The static mapping switch design is suited for sparse network with high number wavelength converters to be placed in the network.

## 3.6 Limited Range Optical Wavelength Conversion

Equipping all nodes of a large optical network with full wavelength conversion capability is prohibitively costly. To improve performance at reduced cost, sparse converter placement algorithms are used to select a subset of nodes for full conversion deployment [BLJ03, BLS03]. Further cost reduction can be obtained by deploying only limited conversion capability in the selected nodes [BLO03, BLJ04].

In this section, we explore the limited range wavelength conversion which can achieve performance very close to that of the full conversion capability; while not only decreasing the optical switch cost but also enhancing it's blocking performance and fault tolerance.

In the previous chapters, we assumed that wavelength conversion can be performed from any input wavelength to any other wavelength without any signal degradation. But wavelength

converters are generally only capable of limited range wavelength conversion. This is due to the fact that the output power decreases strongly with the increasing difference between the output wavelength and input wavelength. The decrease in the output power is nearly symmetrical around the input wavelength.

We will show through simulation using the NSFNET and the U.S Long Haul topologies that significant improvement in the blocking performance can be obtained when limited range wavelength converters with as little as 28% of the full range wavelength conversions are introduced and almost the entire network performance improvement obtained by the full range wavelength converters at all nodes is gained from converters with only 57% of the full range wavelength conversion.

The degree of wavelength conversion, D, is defined as follows: $D = r / (W - 1)$, W is the number of wavelengths and r is the permissible range of conversion on both sides of the input wavelength.

For instance in Figure 19 (NSFNET) and Figure 20 (U.S Long Haul), if there are 8 wavelengths per fiber (W=8) and two wavelengths on either side of the input wavelength are permissible for conversion (r=4), the degree of conversion is 57.14% and the blocking performance is similar to the full wavelength conversion (D = 100%).

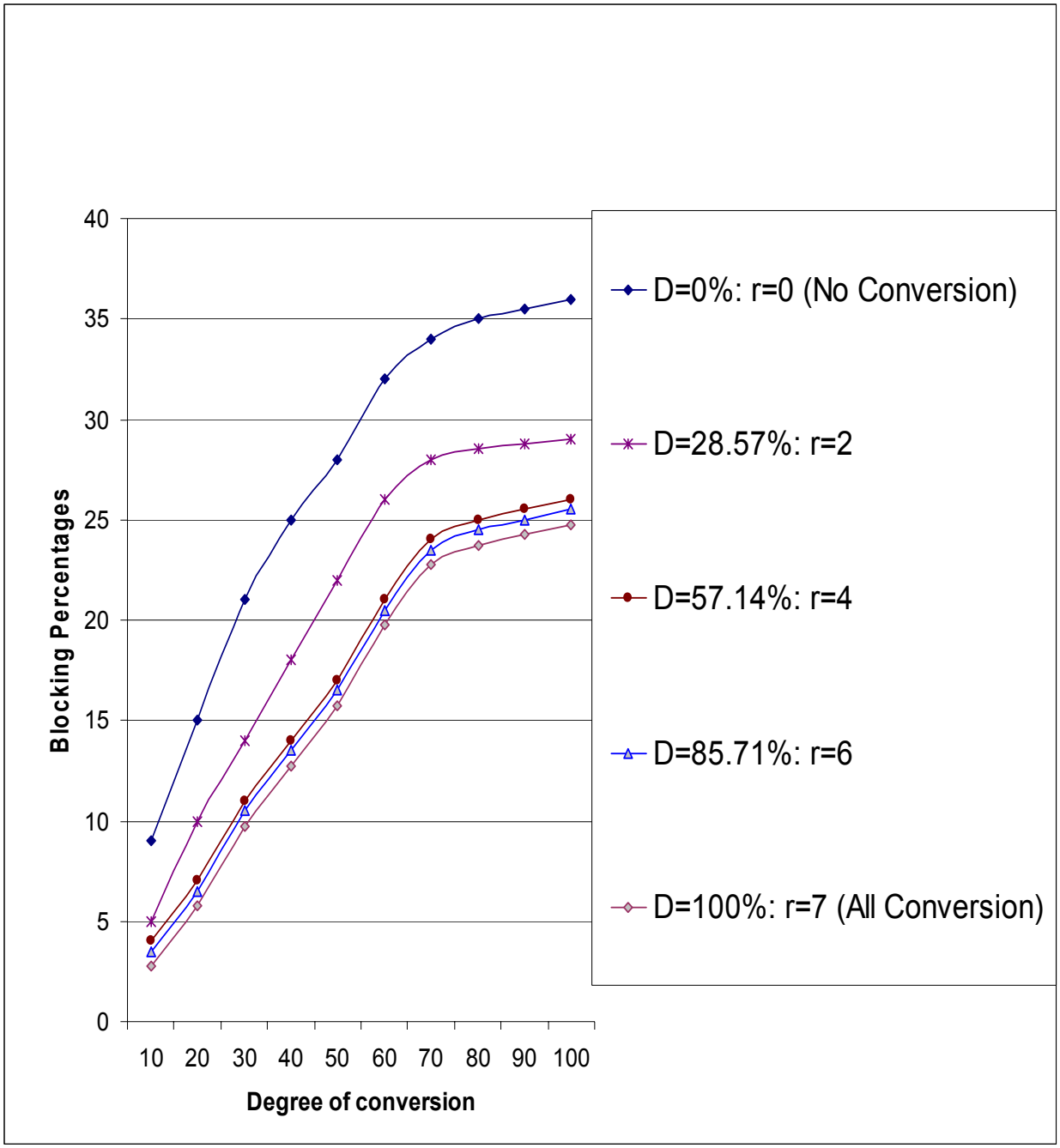


Figure 19: Limited Range Conversion for NSFNET topology (W=8)

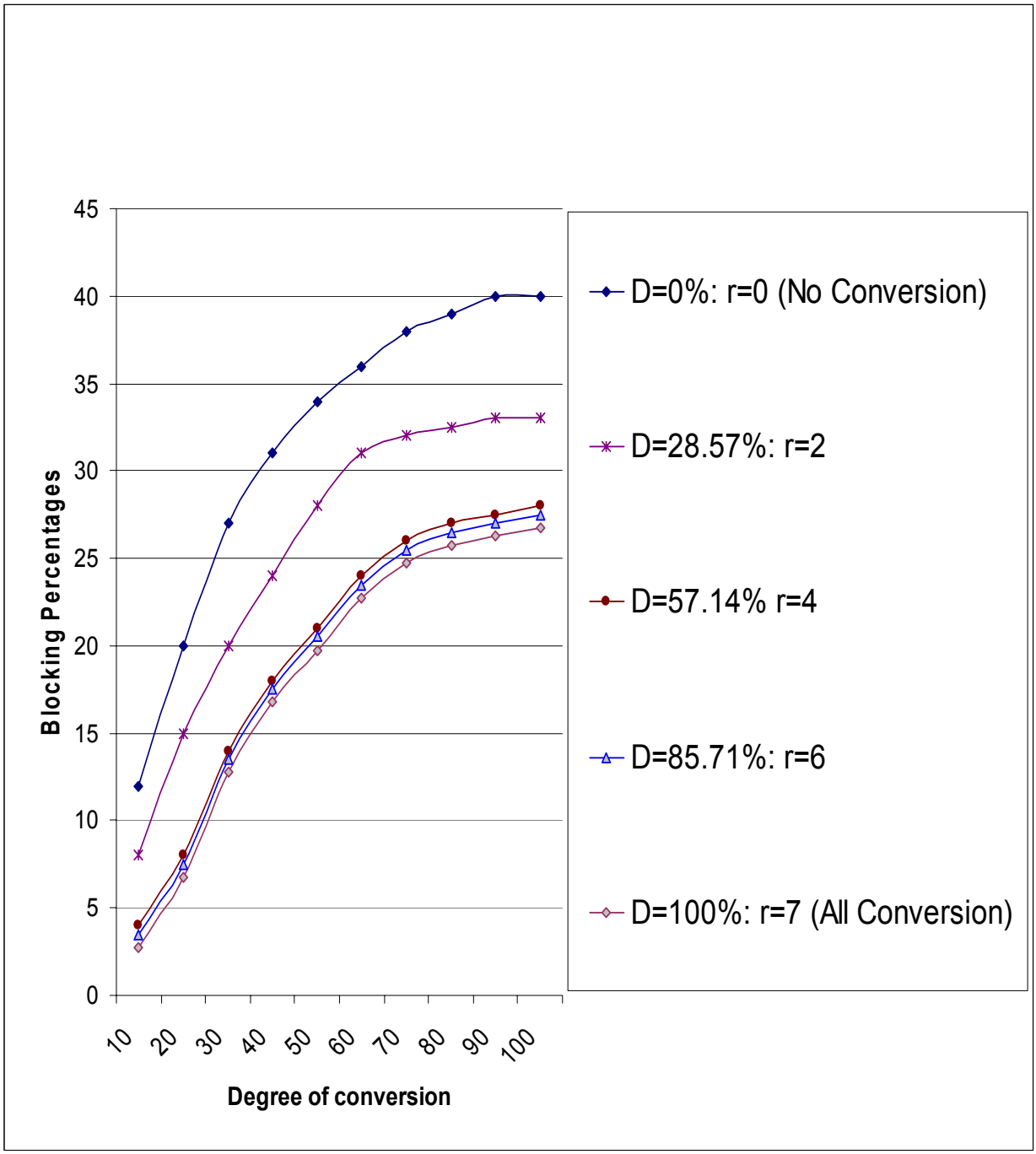


Figure 20: Limited Range Conversion for U.S Long Haul topology (W=8)

## 3.7 Conclusions and Future work

Our assumption in this chapter is that all nodes in the network have the same optical switch design. For future work, we are investigating the combination of the three designs in the network where certain nodes can have a flexible node-sharing switch design and other might have static mapping or strict node-sharing switch designs.

By combining all designs, we can reduce the total cost, improve the fault tolerance and provide better improvement. Since all three designs seem to achieve different performances, the decision about which switch design to use in each node depends on a number of factors related to the traffic flowing through the node.

We believe that nodes handling high traffic should use the flexible node-sharing design; and nodes under low traffic loads can benefit from the static mapping design; but further investigations and more simulation are needed.

Optical Wavelength Converters are generally only capable of limited range wavelength conversion. This is due to the fact that the output power decreases strongly with the increasing difference between the output wavelength and input wavelength. The decrease in the output power is nearly symmetrical around the input wavelength.

We showed through simulation using the NSFNET and the U.S Long Haul topologies that significant improvement in the blocking performance can be obtained when limited range wavelength converters with as little as 28% of the full range wavelength conversions are introduced and almost the entire network performance improvement obtained by the full range wavelength converters at all nodes is gained from converters with only 57% of the full range wavelength conversion.

# 4. OPTICAL BURST SWITCHING: CONTENTION RESOLUTION WITH SPARSE FIBER DELAY LINES AND THEIR CLASS-BASED ALLOCATION

We combine fiber delay lines (FDL) and optical wavelength conversion (OWC) as the solution for the burst contention problem in Optical Burst Switching (OBS). We present a placement algorithm, k-WDS, for the sparse placement of FDLs at a set of selected nodes. The algorithm can handle both uniform and non-uniform traffic patterns. Our extensive performance tests show that k-WDS provides more efficient placement of optical fiber delay lines than the well-known approach of placing the resources at nodes with the highest experienced burst loss. Performance results are also given to compare the benefit of using FDLs versus using OWCs as well as when both resources are used. A new algorithm, A-WDS, for the placement of an arbitrary numbers of FDLs and OWCs is presented and evaluated under different non-uniform traffic loads using network simulation of the NSFNET topology and randomly generated graphs. The dissertation is concluded by presenting the basic design and the performance evaluation results of a scheme to enhance just-enough-time (JET) signaling by introducing a QoS provisioning capability in OBS through controlling the end-to-end delay per burst class based on the availability of FDLs and OWCs.

## 4.1 Background

One of the candidates for next generation high speed network infrastructures will be based on optical burst switching (OBS) [JRT02, CQY99, YQD00, VWS03] that is envisioned to be able to combine the best of optical circuit/flow switching (OFS) and optical packet switching (OPS).

However it's been proven that under highly variable burst sizes, OBS suffers from excessive burst loss due to contention. This issue is due to the fact that the core nodes have very limited or no buffering capability and contending bursts for the same output link will suffer from losses. To reduce the burst loss in OBS, contention resolution is the main challenge to overcome in any OBS architecture.

Our work focuses on the sparse placement of FDLs at the core nodes of an OBS network as a solution to burst contention. Our proposed scheme places the FDL capabilities at key nodes, i.e., nodes that have good connectivity and are well placed within the network. We will show that when the nodes selected by our scheme are equipped with FDLs, they significantly reduce the burst loss rate and improve network throughput. In [BLJ03], we introduced a novel sparse placement algorithm of OWCs suitable for flow switching under uniform traffic and showed its benefits via simulation. In [BLO03], we introduced a placement algorithm for OWCs under non uniform traffic using k-Weighted Dominating set approach (k-WDS).

In this dissertation, we propose efficient and highly scalable algorithms for the sparse placement of FDLs in optical WDM networks. The algorithms use the k-weight dominating set concept [BLO03] and are particularly suitable for solving the contention resolution problem in OBS under JET control signaling. To our knowledge, our work is the first attempt to apply the weighted dominating set approach for solving a design and engineering problem in OBS networks in general and to the sparse FDLs placement in particular.

Under heavy tail traffic [VWS03] and high burst contention, we introduce a QoS capable JET using a simple scheduling scheme and allowing controlled burst loss and end-to-end delay for all classes of traffic. We also introduce a cost effective optical switch design with variable FDL capability and show its benefits via simulation under different classes of traffic.

The remainder of this Chapter is organized as follows: Section 4.2 presents our k-WDS algorithm for FDLs placement in JET-based OBS networks and compares its performance with that of another algorithm based on the ranking concept used in [JIM99, MSS02]. We also introduce a new algorithm, A-WDS, for the sparse placement of an arbitrary number of FDLs and full converters. Section 4.3 introduces an Enhanced QoS-capable JET (QEJET) based on FDLs availability. Our proposed burst contention resolution scheme can support QoS and lower the burst loss rate by controlling the end-to-end delay under different classes of service. Finally, we give concluding remarks in Section 4.4.

## 4.2 k-WDS algorithm for FDLs placement in OBS under JET

In this section, we propose a contention resolution scheme based on the sparse placement of FDLs at judiciously selected core nodes of the optical network. Our extensive performance results show that good improvement in network performance can be obtained by deploying FDLs in a relatively small number of nodes. Sparse FDLs placement, therefore, has benefits similar to those of sparse converters placement [BLJ03, JIM99, MSS02, BLO03, BLJ04, BLS03], namely, reducing blocking and improving throughput while reducing the cost of the added resources.

In [BLO03], we developed an approximation algorithm for the k-WDS problem which computes the set of nodes that should be equipped with full wavelength conversion capability for optical flow switching using a 2-way reservation scheme. Below, we explore the applicability of k-WDS to the sparse placement of FDLs in OBS networks using JET signaling.

### 4.2.1 k-WDS: Background and definitions

We model the considered topology as a graph G(V,E) where V is the set of vertices and E is the set of edges. Each node is assigned a weight modeling the amount of traffic originating from it. Based on these weights, the k-WDS algorithm computes a set D with the following property: every node $v \in V$ is either in D or is at most k hops away from a node in D. In [MDB02], the traffic model was assumed to be uniformly distributed between all node pairs. Since real-life networks may exhibit non-uniform traffic patterns, our algorithm provides an effective placement of FDLs in an OBS network under non-uniform traffic. The inputs to our algorithm are the topology of the network and the weights assigned to the nodes to model the non-uniform traffic pattern.

For example, if node v generates twice the amount of traffic generated by node w, then

$$\text{Weight}(v) = 2 \cdot \text{Weight}(w).$$

Given the traffic matrix ($T_{vw}$) describing the traffic intensity between all node pairs (v, w), the weight of node v used by our k-WDS scheme is computed as follows:

$$\text{Weight (v)} = \sum_{j=1}^{j=N} T_{vj} \Big/ \sum_{j=1}^{j=N} \sum_{i=1}^{i=N} T_{ij} \qquad \text{(Note That } T_{vv}=0\text{).}$$

Where N = |V| is the number of nodes in the graph. We first give the definitions and notations that will be used in our placement algorithm:

1. Neighbor (v): is the set of nodes sharing a link with a node v.

2. $\text{Connect}_k$ (v) represents a connectivity index based on nodes within k hops of the node v. This index reflects the fact that a node m can contribute more than once to the k-connectivity of a node v, since traffic can arrive from the same node, m, through different paths. Higher values of the k-connectivity of node v correspond to higher volumes of traffic passing through node v.

   To take the node's weight into consideration, it's defined as:

   $$\text{Connect}_0 \text{ (v)} = \text{Cardinality (Neighbor (v))} \text{ . Weight(v)}$$

   And recursively we define $\text{Connect}_k$ (v) as:

   $$\text{Connect}_k \text{ (v)} = \text{Connect}_{(k-1)} \text{ (v)} + \sum_{m \in Neighbor(v)} \text{Connect}_{(k-1)} \text{ (m).}$$

3. $Master_k$ (v) is the node p, within k hops from the node v, that has the highest $Connect_k$ value over all nodes m that are at most k hops away from node v. For k equals 0, $Master_0$(v) is the node v itself.

Our k-WDS algorithm [BLO03] implements a voting scheme based on the computed $Connect_k$ values of each node. A node v will vote for the node denoted as $Master_k$(v) since it has the highest $Connect_k$ over all nodes within k hops from v.

Our extension of k-WDS to the burst switching paradigm is that the elected nodes based on k-WDS should have FDLs available since they dominate the entire topology of the network. In [BLJ03], we showed that the time complexity of our placement algorithm is $O(k.N^2)$. We also showed [BLJ03, BLO03] that our algorithm is highly scalable, computationally efficient, gives better performance than the placement heuristics used in [JIM99, MSS02] and overcomes the local minimum problem reported in [JIM99].

To our knowledge, there has been no previous work on evaluating sparse placement algorithms of FDLs in optical networks. For the purpose of evaluating our k-WDS scheme described above, we adapted the simulation based approach used in [JIM99, MSS02] for sparse converters placement and applied it to the sparse placement of FDLs. The resulting scheme (which we call the k-LOSS scheme) solves the placement problem by iteratively selecting the node that experiences the highest burst loss at each simulation step. Since our work is the first attempt to explore the placement of FDLs, we have compared our algorithm to the k-LOSS scheme which

can be considered the best known simulation-based scheme for the sparse placement of resources in optical networks. Because of the simulation-based nature of the k-LOSS scheme, it is capable of handling uniform as well as non-uniform traffic. However, the results given in [JIM99, MSS02] are limited to uniform traffic; to our knowledge, no results have been reported in the literature about the performance of k-LOSS under non-uniform traffic.

In what follows, we apply our placement algorithm to the case of optical burst switching and compare its performance with the simulation-based heuristic k-LOSS.

### 4.2.2 Simulation results for FDL placement under non-uniform traffic

In order to evaluate the performance of our FDL placement algorithm, we use the NSFNET backbone with 16 nodes and 25 links (Figure 33). We first apply our voting algorithm to compute the weighted dominating sets k-WDS for the NFSNET backbone. To illustrate how k-WDS sets are computed, Table 2 lists an example of randomly generated weights (these weights reflect the amount of traffic generated a given node compared to the other nodes in the network ) for each node in NSFNET. The resulting set of nodes should be equipped with FDLs.

Table 2: Fiber Delay Line placement: Assigned Node weights for NSFNET

| Node | Weight | Node | Weight | Node | Weight | Node | Weight |
|---|---|---|---|---|---|---|---|
| 0 | 4 | 4 | 8 | 8 | 5 | 12 | 1 |
| 1 | 8 | 5 | 6 | 9 | 7 | 13 | 12 |
| 2 | 5 | 6 | 6 | 10 | 5 | 14 | 12 |
| 3 | 9 | 7 | 1 | 11 | 9 | 15 | 2 |

The k-WDS algorithm provides the following results (using the weights from Table 2):

1-WDS (NSF) = {1, 4, 5, 6, 9, 11, 14},

2-WDS (NSF) = {1, 4, 9, 14}, and

3-WDS (NSF) = {14}.

The computation of $Connect_k(v)$ is affected by the weight of the considered node v and the weights of all the nodes within k hops from it. As reported in [BLJ04], when the weights are all equal to 1, the k-DS sets become:

1-DS (NSF) = {1, 4, 5, 6, 9, 12},

2-DS (NSF) = {1, 4, 9, 12},

3-DS (NSF) = {12}.

Note that when k=0, 0-WDS (for NSFNET) contains all the nodes in the network. Also note that for k>0, k-WDS models non-uniform traffic between node pairs using weights assigned to each node based on the traffic intensity matrix . It also captures the fact that a node m can contribute more than once to the k-connectivity of a node v, since traffic can arrive from the same node

through different paths. Higher values of the k-connectivity of node v correspond to higher volumes of traffic passing through node v based on the traffic intensity matrix.

We now describe the performance results when the nodes selected by the k-WDS placement algorithm are equipped with FDL capability. A cost-effective design of an optical switch equipped with FDL is described in section 4.3. For all the tests reported in this dissertation, the simulation was run for a total of M bursts where M is $10^6$ times the considered load of traffic in the network ($M = 10^6 \times \lambda/\mu$.). As in [10], all simulation results are given with 95% confidence intervals using the batch means method with 50 batches. Our detailed simulation settings are provided in section 4.3.2 and to evaluate our k-WDS algorithm, we adopted a comparison method similar to that described in [JIM99].

Specifically we perform the following steps for a given network: We initially run our simulation assuming that FDLs are not available in any node (this is the case of no FDLs). Starting with k at 1, we next run simulations using the placement suggested by k-WDS and k-LOSS (the k-LOSS heuristic is made to select the same number of FDLs as k-WDS; this is the meaning of the prefix 'k" in the k-LOSS scheme). We then increase k and repeat the same process until k-WDS returns only one master node. For each simulation, we measure the experienced burst loss in the network. As shown in Figure 21, better results are obtained when we put FDLs in the nodes selected by the k-WDS algorithm instead of putting them in the nodes experiencing the highest burst loss on the basis of k-LOSS. For instance, under a typical normalized load of .70, without FDLs, the burst loss is 23%.

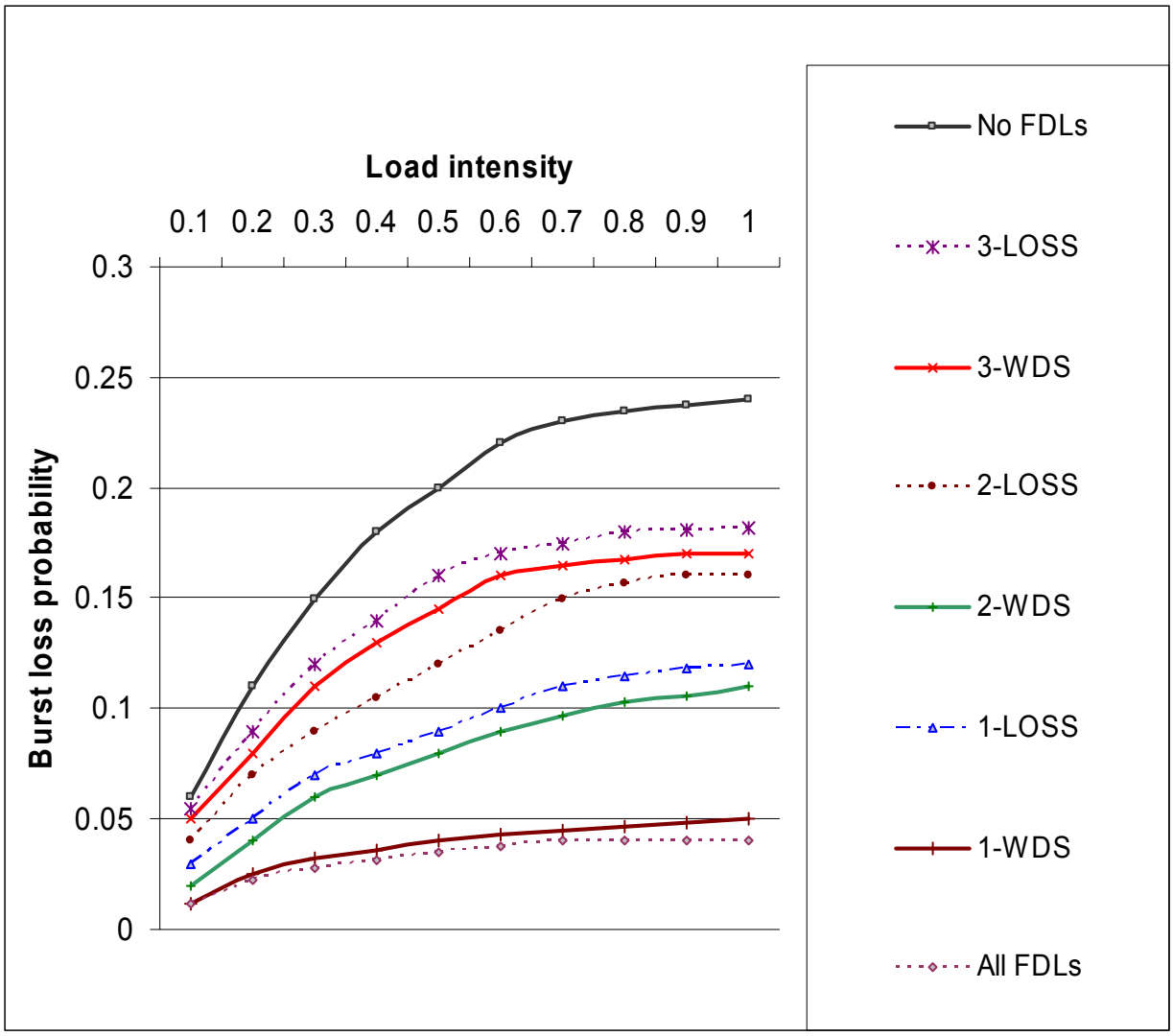


Figure 21: FDLs placement under JET using k-WDS

When we have FDLs at node 14, member of the singleton set 3-WDS, the burst loss becomes 16.5% (i.e. an improvement of 6.5%). However, when we put FDLs in node 8 selected by the 3-LOSS heuristic, the measured burst loss is 17.5%. The placement suggested by 3-WDS improves the performance by 28% and 3-LOSS only by 23%.

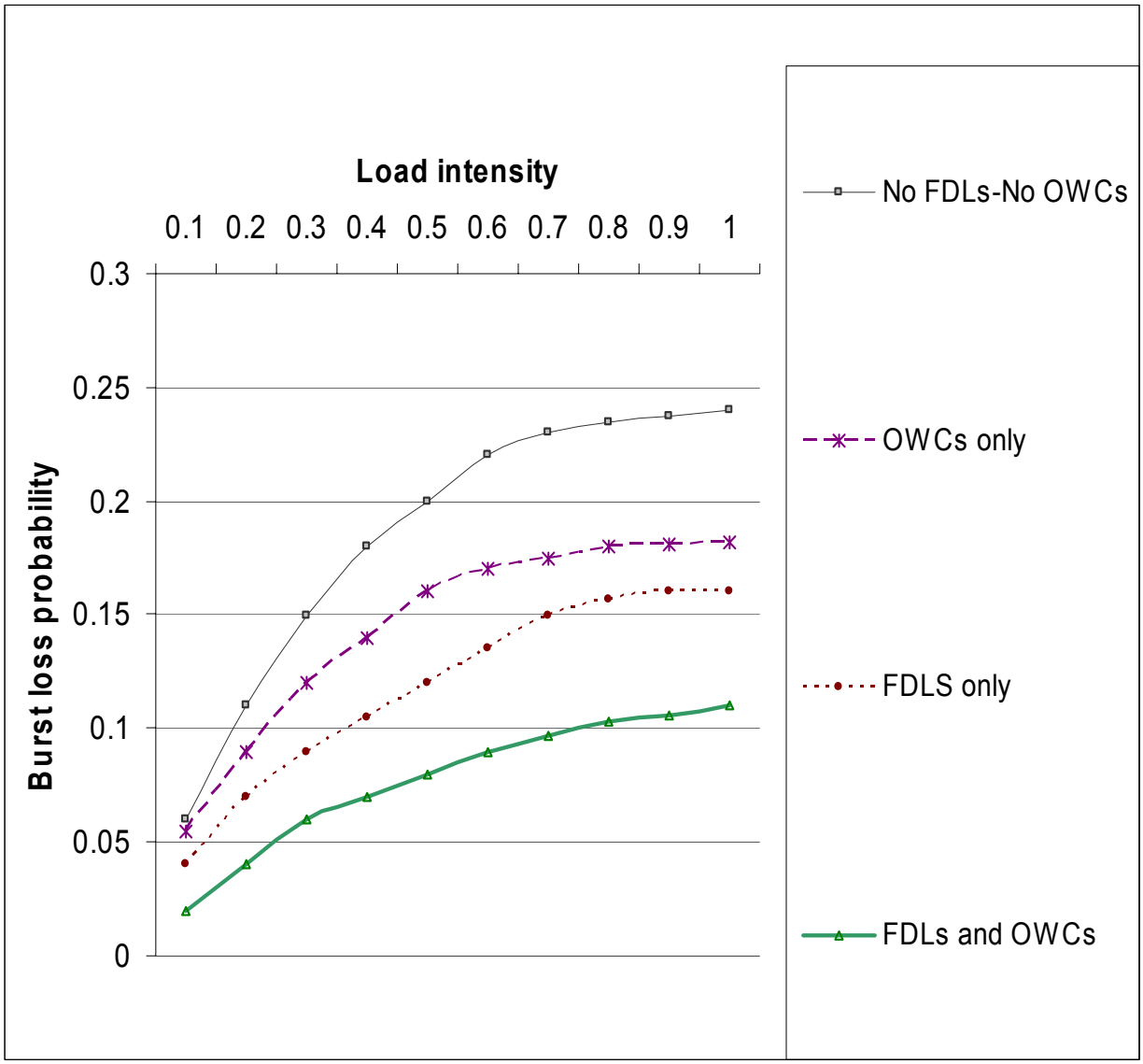


Figure 22: FDLs vs. OWC using JET and 2-WDS

Also, at load 0.7, 2-WDS with four nodes achieves 9.7% burst loss (equivalent to 57.8% improvement), whereas 2-LOSS achieves 15% burst loss (equivalent to 34.7% improvement). Thus we can achieve almost 60% improvement from the no-FDL case with only four nodes with

FDLs (selected by 2-WDS). Finally, 1-WDS with 7 nodes reduces the burst loss to 4.5% (80% improvement), whereas 1-LOSS reduces it to only 11% (52% improvement).

From the above results we can see that the k-WDS selection, based only on the network topology and node weights as input, provides better improvement than does the simulation-based k-LOSS heuristic introduced in [JIM99]. The k-WDS scheme is able to provide a better placement of FDLs, since its solution takes into account network-wide connectivity information as well as the traffic that goes through each node.

In Figure 22, we show the benefits of FDLs versus OWCs using the nodes in 2-WDS (NSF) = {1, 4, 9, 14}. We measured the burst loss for the following four cases:

1. When the four nodes of 2-WDS have neither FDLs nor OWCs.
2. When they have FDLs only.
3. When they have OWCs only.
4. When they have both OWC and FDL capabilities.

The switch control logic for the last case consists of using OWCs first (priority to conversion) and if not available then use FDLs. As predicted intuitively in terms of the burst loss, the performance is improved when the nodes have both resources combined. We also notice that the burst loss rate for the case of FDLs only is better than the loss rate for the case of OWCs only. However, the performance for EED (end-to-end delay) has the opposite trend, i.e., using FDLs only gives worse (higher) EED values than using OWCs only. This is due to the fact that

although more bursts will make it to the destination, the incurred delay due to sub-buffering at the intermediate nodes will negatively affect the end-to-end delay.

The simulation results for the EED (end-to-end delay) metric are shown in Figure 23 and Figure 24. The relative EED percentage given by the vertical axis is defined as the average end-to-end delay divided by the average burst length in microseconds. We measure the average delay from the time the burst is transmitted until it reaches the destination. Due to the nature of OBS, we do not have to include the setup time of cross-connects at each switch on the path of a burst and the processing of the control packets at each intermediate node.

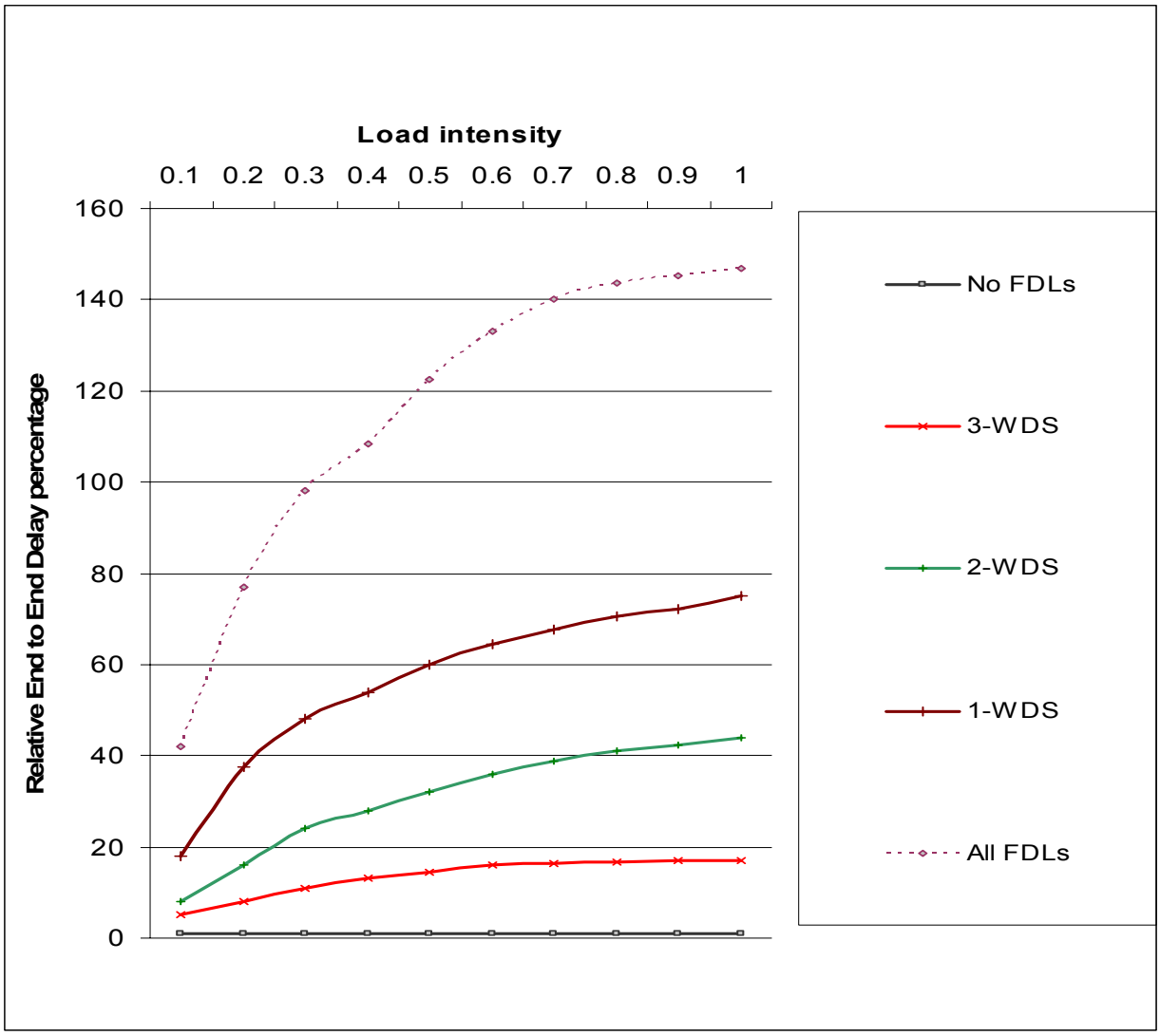


Figure 23: Relative EED percentage FDL only (k-WDS)

In Figure 23, we present the effect of FDLs on the relative end-to-end delay. When no FDLs are used, this metric is constant and depends on the propagation delay and the switching time (around 1% of the average burst length). Notice from Figure 23 that when more FDLs are placed in the network, the relative EED is increased by as high as 17% when only node 14, the only member of 3-WDS, has FDL. When FDLs are placed in nodes 1, 4, 9 and 14 (i.e., in the

members of 2-WDS) the relative EED is increased by as high as 44%. When FDLs are placed in the members of 1-WDS, the relative EED increases by 75%; and with all nodes equipped with FDLs, it increases by 147%. From these results, we were encouraged to explore QoS (Quality of Service) schemes to take advantage of both OWCs and FDLs in order to decrease the burst loss rate and also guarantee an acceptable end-to-end delay.

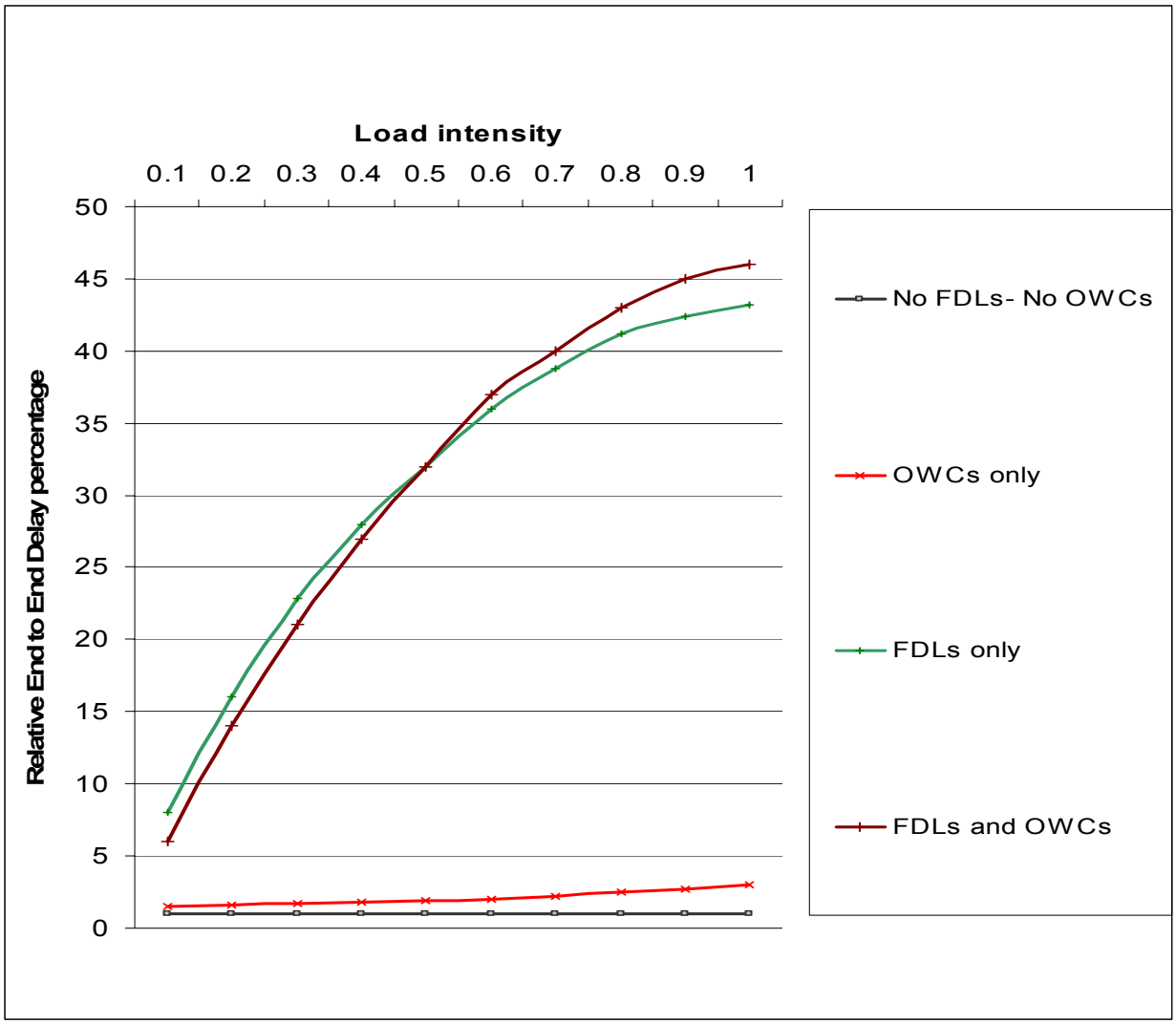


Figure 24: Relative EED percentage FDL vs. OWC (2-WDS)

In Figure 24, we show the benefits of FDLs versus OWCs using the nodes in 2-WDS (NSF) = {1, 4, 9, 14}. We measured the relative EED when these four nodes have neither FDLs nor OWCs; as before the relative EED percentage is constant around 1%. When they only have OWCs, the EED percentage increases linearly from 1.5% to 3%; this is due to the conversion time and also to the use of alternate routes under high loads. When the nodes have FDLs only, the relative EED increases sharply from 8% to 43.2% as the load increases from 0.1 to 1.0. Finally, when both FDLs and OWCs are available in all four nodes, the relative EED also increases sharply as the load increases. As shown in Figure 24, the case of combined capability has smaller EED values than the case of FDLs at low loads, but has higher EED values at loads higher than 0.5. This is due again to the use of conversion and the impact of re-routing via alternate routes under heavy loads.

Our FDL placement algorithm has the restriction that FDLs are only placed in the nodes of k-WDS for some index value k. In the next section, we extend this model to handle the case when the number of FDLs for deployment does not match the cardinality of any k-WDS. Furthermore, the results in Figure 24 for the case of combined FDLs and OWCs motivated us to investigate the placement of an arbitrary number of FDLs and OWCs to optimize the overall network performance.

### 4.2.3 Placement of arbitrary number of FDLs and OWCs under non-uniform traffic

Let C<N and F<N be the arbitrary number of full wavelength converters and the arbitrary number of fiber delay lines, respectively, to be placed in an optical network with N nodes. Our approach to solve this problem is to partition all the nodes in the network into 4 sets:

1. The first set of nodes, SET1 of size NCF, will be equipped with both FDLs and OWCs.

2. The second set of nodes, SET2 of size NF, will be equipped with FDLs only.

3. The third set of nodes, SET3 of size NC, will be equipped with OWCs only (an alternate design is to equip SET2 with OWCs and SET3 with FDLs).

4. Finally, the last set of nodes, SET4 of size NO, is without any capability.

Note that the following equations should hold:

1. C = NCF + NC
2. F = NCF + NF
3. N = NCF + NC + NF + NO

Set of all nodes = V = SET1 $\cup$ SET2 $\cup$ SET3 $\cup$ SET4

Our placement algorithm A-WDS to solve the above problem is as follows (we assume that C>0 and F>0):

1. Repeat starting at k =0

   Compute k-WDS

   Increment k by 1

   Until cardinality ( k-WDS) ≤ min(C, F).

   Let $\mathfrak{I}$ be the smallest k, such that the size of k-WDS ≤ min(C, F).

2. Set NCF = cardinality ($\mathfrak{I}$-WDS) and set SET1 = $\mathfrak{I}$-WDS

   Set NC = C – NCF and NF = F – NCF

   Set REM = V – SET1, the remaining nodes in V and not in SET1.

3. Repeat starting at k = $\mathfrak{I}$+1

   Compute k-WDS

   Increment k by 1

   Until cardinality (k-WDS) equals 1.

   Let $\wp$ be the smallest k, such that the size of k-WDS equals 1.

4. Sort all nodes, v, in REM based on Connect$_{\wp}$ (v)

   The first NF nodes of REM constitute SET2 and the next NC nodes of REM constitute SET3.

Our algorithm starts with the largest $\Im$-WDS set of size not exceeding C and F. This set constitutes the set of nodes equipped with full wavelength conversion and fiber delay line. Then the algorithm finds the smallest $\wp$ such that $\wp$-WDS is of size 1 and computes Connect$_{\wp}$ (v) for all remaining nodes v. We sort the remaining nodes v (i.e., all nodes in the graph excluding the members of $\Im$-WDS) based on Connect$_{\wp}$ (v). The remaining FDLs should be placed in the set SET2 whose nodes have the highest k-Connectivity and the remaining OWCs should be placed in the set SET3 whose nodes rank right after the members of SET2. The algorithm takes advantage of k-WDS by building an initial set and uses Connect$_{\wp}$ (v) to extend it without using any simulation.

To illustrate the benefits of our algorithm and for comparison purposes, we shall assume that C=F. We fixed the load intensity at 75% and ran our placement algorithm for C and F varying from 1 to the maximum number of nodes in the network (16 for the NSF backbone). Figure 25 shows the burst loss performance of our placement algorithm A-WDS, our simulation based algorithm HYBRID from [BLJ03] and LOSS from [JIM99]. The latter algorithm ranks the nodes of the network by blocking percentages (i.e., based on the burst loss percentage measured through simulation) and places the resource at nodes with high blocking.

In [BLJ03], we showed via simulation that the HYBRID algorithm performs better than the placement algorithm LOSS [JIM99] (we are omitting the prefix "k-"since it's not relevant in this case) HYBRID has better performance since it takes advantage of k-WDS (i.e., it starts with the largest k-WDS set and iteratively adds a node at each step). Note that with HYBRID and LOSS,

the fiber delay lines and full conversion are always combined in the selected nodes in each step. Our A-WDS placement algorithm places them independently as described earlier. Also in Figure 25, the A-WDS algorithm provides very good results compared to those obtained by the simulation based HYBRID algorithm. The complexity of A-WDS is order $O(N^2.\log N)$ due to the sorting step.

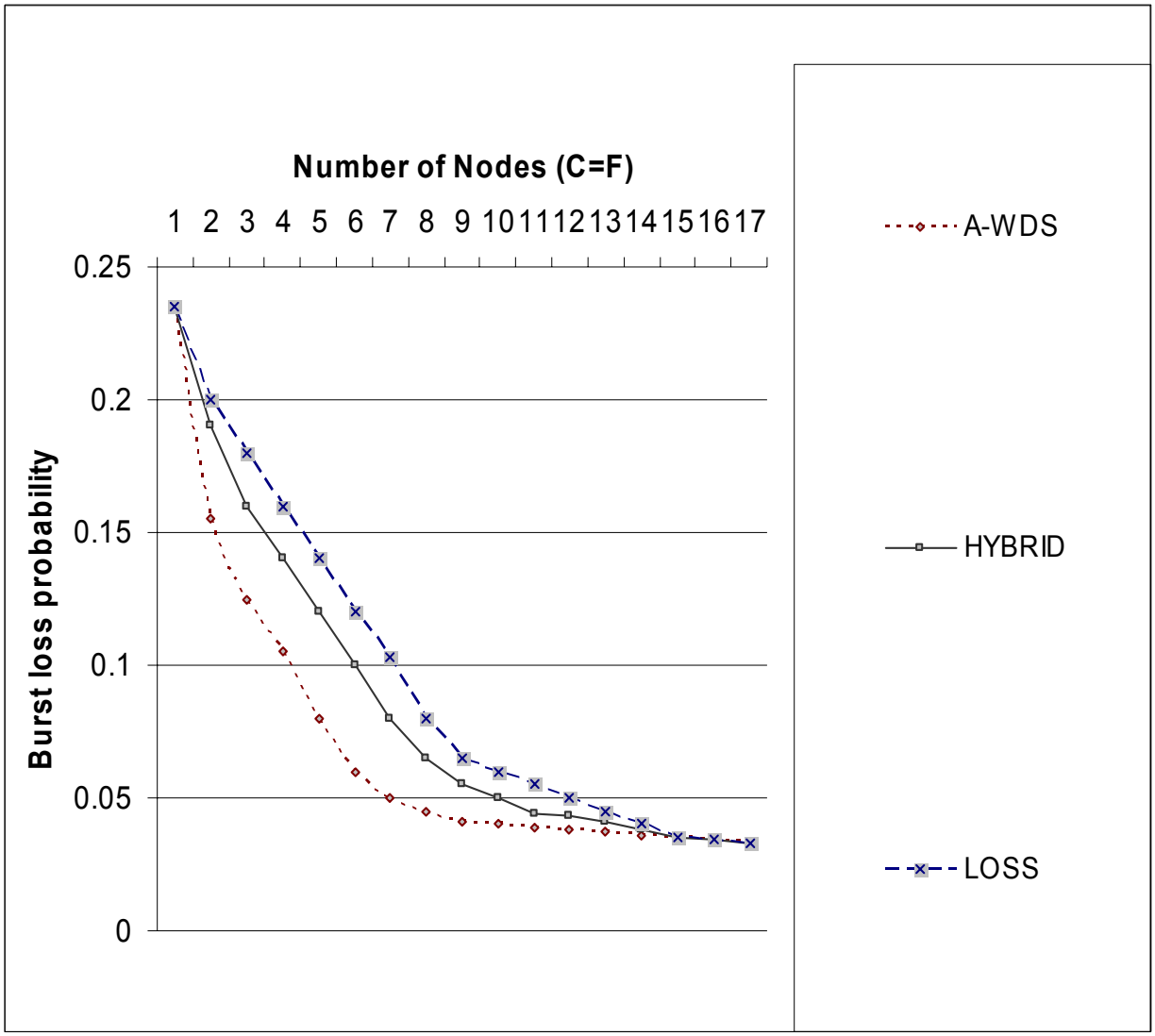


Figure 25: Burst Loss with A-WDS, HYBRID and LOSS

In Figure 26, we measure the relative EED percentage and we can see that the placement by A-WDS provide better performance than the simulation based placement algorithms HYBRID [BLJ03] and LOSS [JIM99]. The relative improvement of A-WDS versus LOSS has an average of 39.1%, a maximum of 83.6% and a standard deviation of .3055. The relative improvement of HYBRID versus LOSS has an average of 24.3%, a maximum of 69.1% and a standard deviation of .243.

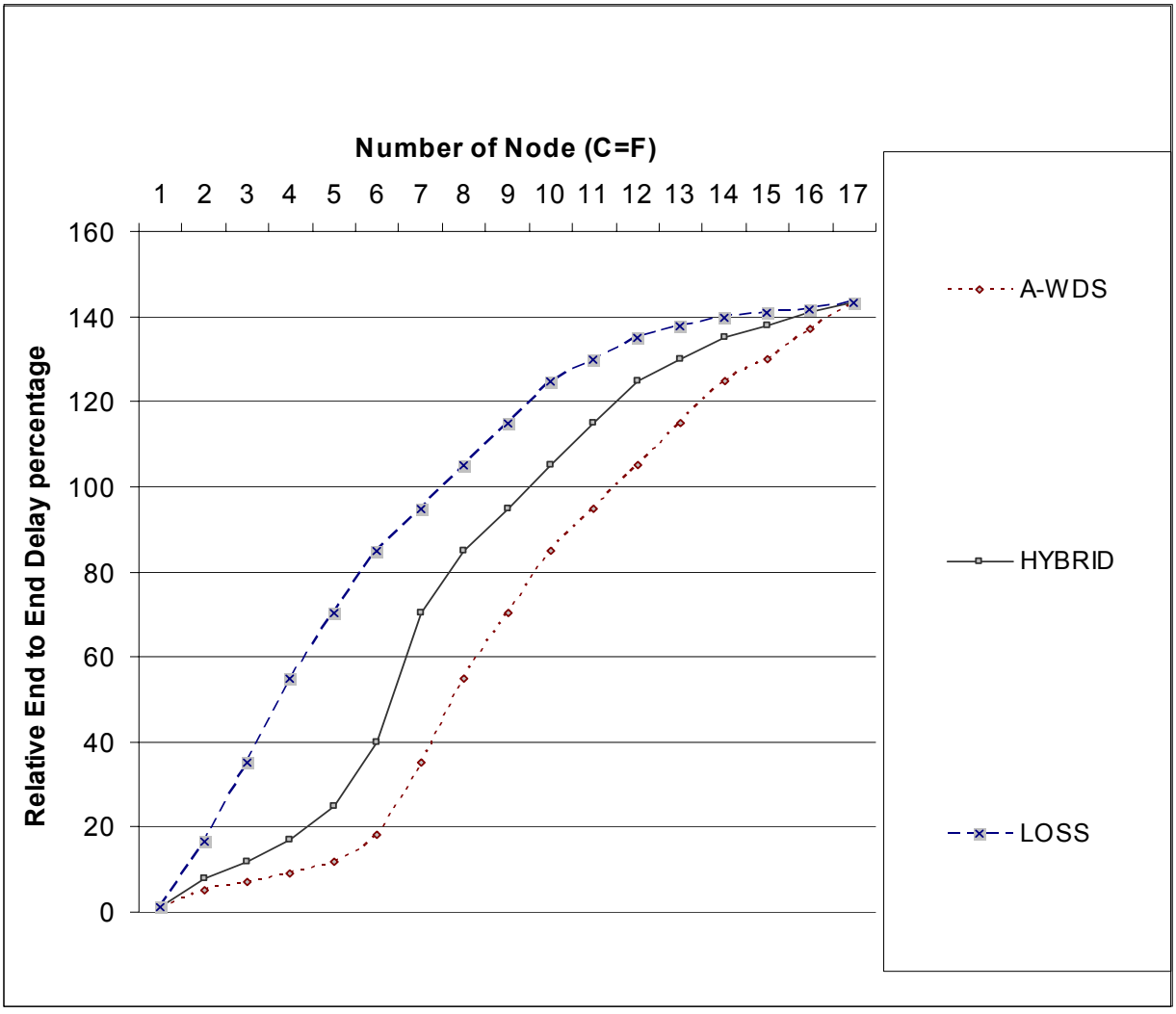


Figure 26: Relative EED with A-WDS, HYBRID and LOSS

Our next set of results uses randomly generated graphs using Boston University's BRITE tool [MMB00] by keeping the number of links per node ranging between 2 and 7. The number of nodes in the network, N, is increased by 10 in each iteration and the results of this iteration are obtained using a maximum of 1000 randomly generated topologies with N nodes. When N is increased, we increase the total load on the network accordingly to preserve the same fixed load per node. Similarly as before, we measured the burst loss and the relative end-to-end delay. We plot in Figure 27 the average measured burst loss rate over all tested graphs for a given iteration. Within any iteration, we test four scenarios by placing OWCs and FDLs in every node of the network; then in the case of $C + F = \frac{N}{3}$ (i.e., one third of the nodes can have the capability); then in the case of $C + F = \frac{2.N}{3}$; then without placing OWCs or FDLs in any node. The results show the accuracy of our placement algorithm A-WDS compared to the simulation-based scheme HYBRID. Our A-WDS placement scheme always provides good performance improvement for all considered cases. Note that with A-WDS, we use $C = F = \frac{N}{3}$ and $C = F = \frac{2.N}{3}$ to place full conversion and fiber delay lines in an independent fashion as opposed to HYBRID and LOSS that always place both capabilities combined when a node is selected.

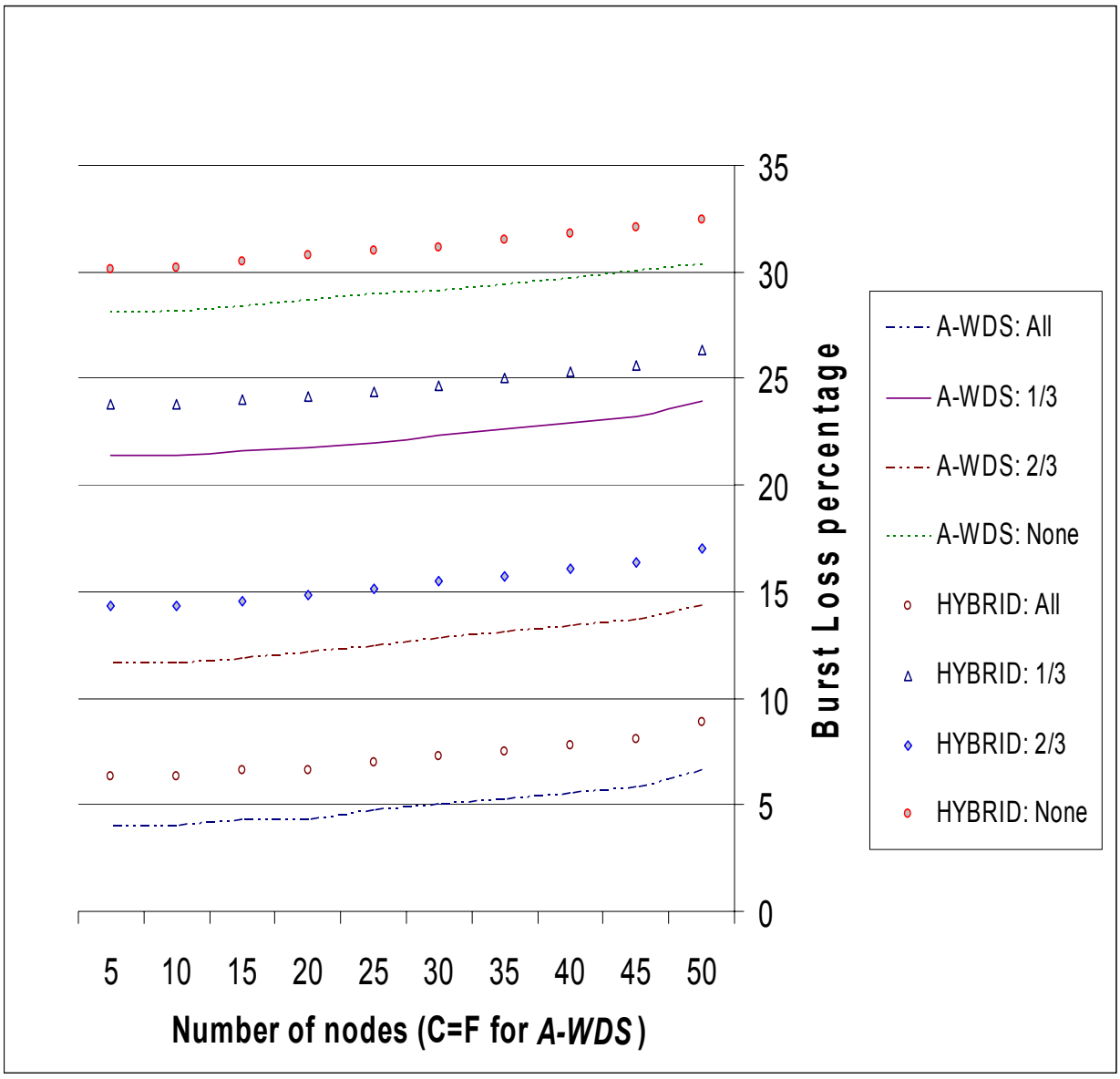


Figure 27: A-WDS's versus HYBRID's Burst loss using randomly generated graphs

The results in Figure 27 show that increasing N doesn't have a major impact on the burst loss if the load per node is kept fixed. Note the benefits of A-WDS compared to HYBRID for all examined scenarios (for clarity of the graphs, we omitted the performance of LOSS in Figure 27

since HBRID consistently outperforms LOSS). The average improvement of A-WDS over HYBRID is 19.1%, the maximum improvement is 34.9% and the standard deviation is .091.

We analyzed two key metrics in OBS networks: burst loss and end-to-end delay. Our placement algorithms k-WDS and A-WDS provide respectively an optimal placement of FDLs alone as well as combination of full conversion with fiber delay lines. We concluded that the burst loss can be reduced by using delay lines but the end to end delay is increased consequently. Our next section explores a QoS scheme that allows controlling both metrics at the burst class level.

## 4.3 Enhanced JET for QoS-capable Optical Burst Switching

It has been established, as in [VWS03], that Internet traffic is self-similar, bursty and has a heavy tail statistical nature (95% volume in 1% of traffic). This traffic pattern-based observation leads to the need for a signaling protocol not only suitable for long duration flows but that can also improve the network throughput and provision enough bandwidth and speed. OBS with its signaling protocol suite (JIT, JET …) is the switching paradigm of choice combining the best of OFS and OPS for high bit-rate transfer, providing real-time support for multi-media internet traffic, and fast switch configuration for short duration sessions.

In JET, the end-to-end delay can be controlled by the offset time at the source edge node based on the processing time along the path taken by the burst. The burst is buffered at the source edge node for the duration of offset time. JET does not support any QoS scheme that takes into

consideration the properties of the WDM layer and integrates contention resolution with a dynamic class-based allocation of resources (FDL and OWC).

In this section, we introduce a cost effective switch design and a QoS enhanced JET (QEJET) scheme using FDLs and OWCs at certain selected core nodes (A-WDS placement from previous section).

### 4.3.1 QEJET: switch design and benefits

We assume that FDLs and OWCs are available at selected core nodes of the OBS network. OWCs are used for high priority bursts where end-to-end delay needs to be kept to a minimum. FDLs are used to delay a burst at a core node to resolve contention for higher priority bursts. In Figure 28, we present our optical switch design based on cost effective and feasible any-to-λ optical wavelength converters, variable fiber delay lines and non-tunable optical multiplexers.

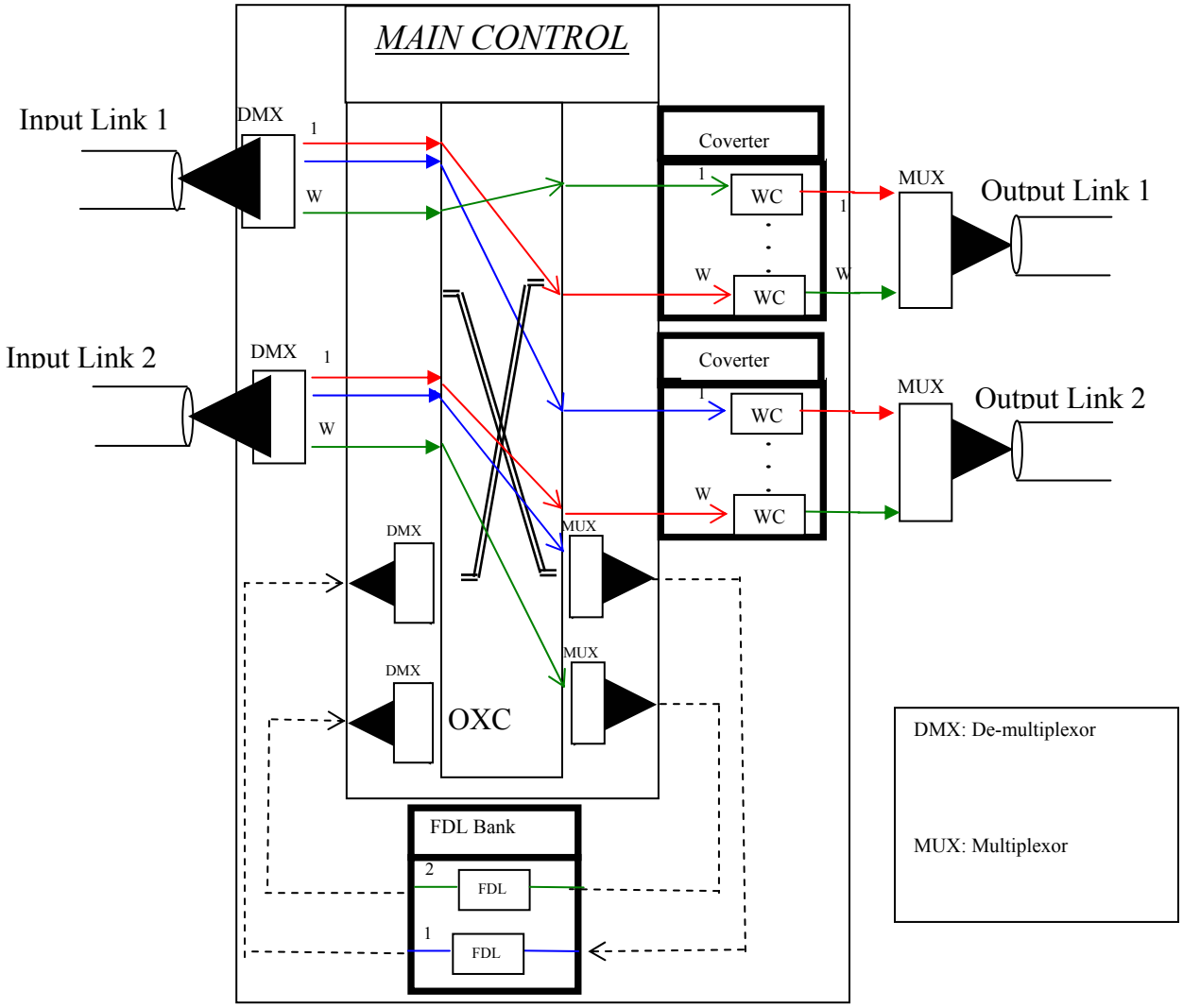


Figure 28: FDL based Optical Burst switch design

High priority bursts take advantage of wavelength conversion to incur minimal end-to-end delay and lower priority bursts will be delayed using a variable-delay FDL bank (each output fiber has a dedicated FDL). As in [HLH02], we adopt the variable-delay FDL design described in Figure 29.

Our design is cost effective compared to [HLH02]:

1. We don't use wavelength converters in the FDL.
2. We use only one optical cross-connect and it is symmetric.

The FDL consists of a number of stages (1+max_d stages shown in Figure 29) where the $k^{th}$ stage has $2^{k-1}$ fiber delay elements. Each fiber delay element (represented by a circle) can provide a delay of b time units. In each stage, the burst can either go through or bypass the delay elements of that stage. Therefore, a delay line can provide a variable delay ranging from zero to MAXD = $(2^0 + 2^1 + \ldots + 2^{(max\_d)})$.b units of time.

Note that bursts with different wavelengths can be delayed simultaneously using the WDM concept. Thus up to W bursts can concurrently exist in the same delay element where W is the number of wavelengths used in the network. We also allow the pipelining of multiple bursts with the same wavelength if there is no conflict. When a burst is to be delayed, the duration of the delay is computed based on the available stages of the FDL to ensure that no conflict exists with the bursts already being delayed. If there is no combination of stages allowing pipelining without collision, the burst will be dropped.

Note that if a burst requires a delay of 5.b, it will use stage 0 for a delay of duration b; then bypass stage 1 and go to stage 2 for a delay of duration 4.b.

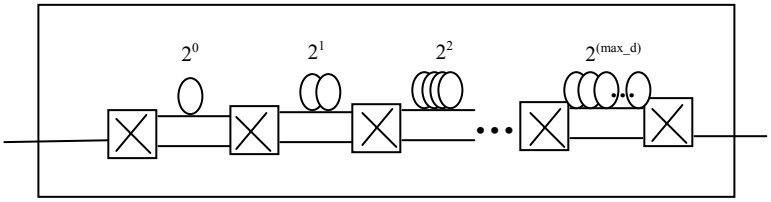


Figure 29: Fiber Delay Line (FDL) design

Our QoS enhanced JET scheme is based on the Horizon scheduling [JRT02]. The algorithm has an advantage in hardware implementation. Each class of traffic has a priority that drives the allocation of FDLs and OWCs. Higher priority bursts require minimal end-to-end delay and will use OWCs as much as possible (pre-emption of lower priority bursts is allowed). Low priority bursts will incur delays in FDLs. The scheduling algorithm is very simple and can be implemented in hardware. In the following section, we will show the benefits of QEJET compared to JET via simulation and investigate key design decisions to take full advantage of its features.

### 4.3.2 QEJET: simulation and results

In this section we consider the NSFNET topology. We show the benefits of QEJET supporting 4 classes of traffic. Each fiber link has W wavelengths. The burst length is exponentially distributed with an average of L μs and the normalized load intensity is ρ.

We assume that:

1. Switches are equipped with FDLs and OWCs based on A-WDS placement with $C = F = 6$.

2. max_d is 8 and consequently MAXD, representing the maximum delay, is 255.b μs.

3. The transmission rate is 10 Gbps, the cross-connect setup time is 10.b μs.

The considered performance metric is the burst loss probability and end-to-end delay as a function of the load intensity ρ, the delay ratio DR defined as MAXD/L = 255.b/L and the number of wavelengths W. Figure 30 and Figure 31 show the relationship between the burst loss probability and the load intensity ρ ranging from 0.2 to 0.9. We fixed burst length to L = 100xb and b = 1 μs. We measured the experienced burst loss as a probability for classless JET and also when QEJET is supporting 4 classes of traffic (class 0 has the lowest priority and class 3 has the highest). The performance tests are done using W=4 in Figure 30 and W=64 in Figure 31. All classes of traffic have equal mean burst length, i.e. $L_3=L_2=L_1=L_0=L$; and generate an equal amount of traffic. Our results show that QEJET achieves a class differentiation in term of incurred burst loss: class 3 experienced a reduction of burst loss as compared to the classless JET: 50 and 600 orders of magnitude when W=4 and 64, respectively. For the case of 4 wavelengths per fiber, we observe that class 3 under QEJET has lower burst loss probability than the classless JET for all values of the load intensity and class 2 achieves lower burst loss than the

classless JET only when the load intensity is higher than 0.4. We also note that class 0 and 1 experience higher burst loss than the classless JET scheme for all considered loads.

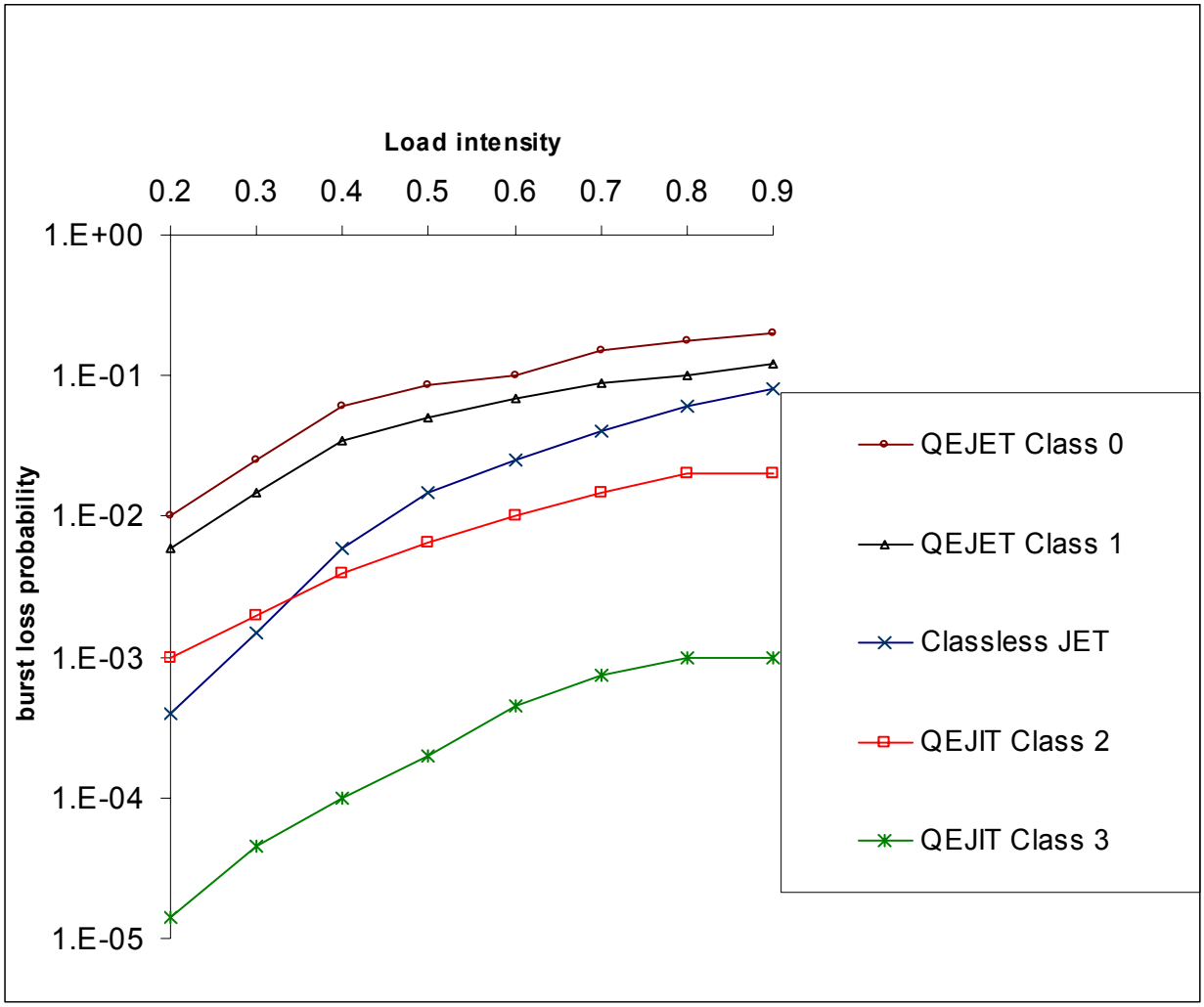


Figure 30: QEJET: burst loss versus load (W=4)

When we use 64 wavelengths per fiber, we notice that the QoS performance can be significantly improved by increasing the number of wavelengths: Only class 0 incurred higher burst loss than the classless JET, Class 2 and 3 for all loads and class 1 when the load is higher than 0.6.

The overall average burst loss probability for QEJET is slightly higher than JET for low loads but for loads higher than .4 for W=4 and than .7 for W=64, JET experiences higher burst loss.

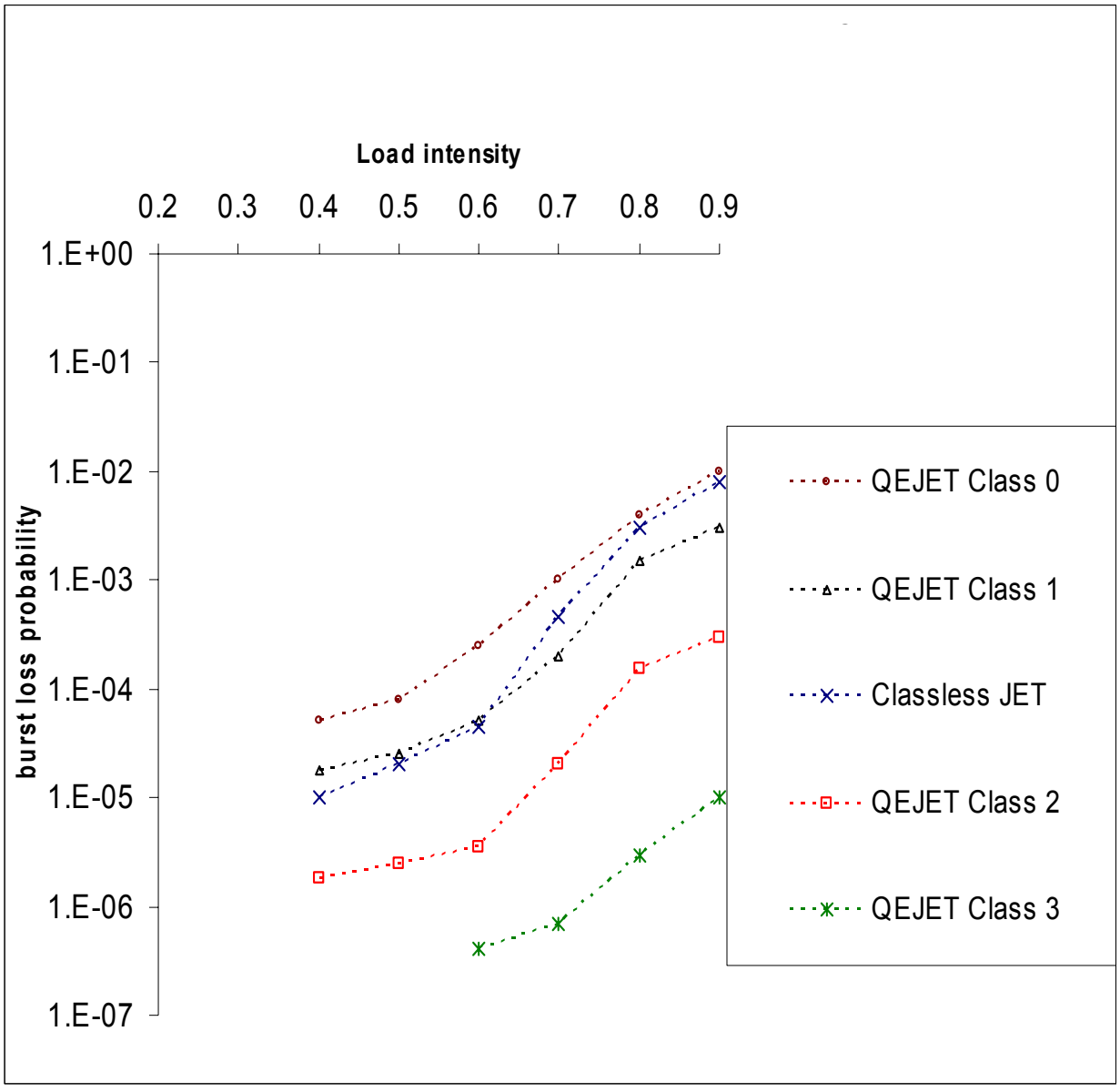


Figure 31: QEJET: burst loss versus load (W=64)

In Figure 32, we explore the effect of the delay ratio DR, defined as MAXD/L, on the burst loss probability when the load intensity is 0.8 with W=4. For each class ranging from 0 to 3, we measured the experienced burst loss when DR ranges from 0 (No FDLs) to 5 (a burst can be delayed in an FDL for a duration up to 5 times the average burst length). We also measured the burst loss under the classless JET.

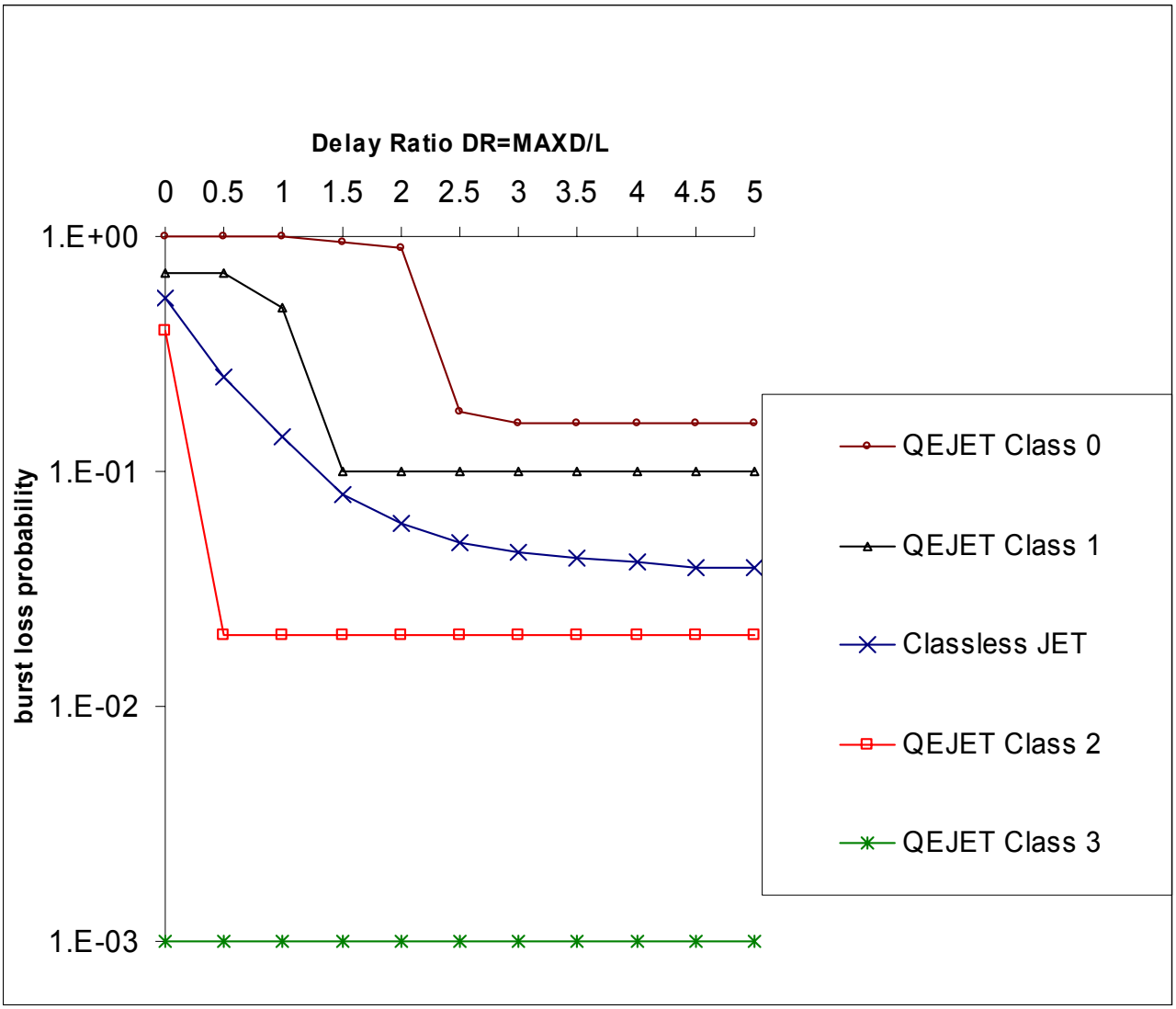


Figure 32: QoS Enhanced JET: burst loss percentage versus the Delay ratio

Intuitively, one can argue that with higher delay durations, our QoS enhancement in JET allows better performance in terms of burst loss for high priority bursts and the end-to-end delay incurred gets higher for low priority bursts. Consequently, the low priority bursts will be dropped more frequently after being pre-empted by higher priority bursts. For instance, class 0 traffic is almost blocked 100% of the time when DR is less than 2, then the burst loss sharply decreases to 18% and then eventually becomes equal to 16% when DR is greater than 2.5. We also notice that bursts of class 0 can be delayed up to 4 times their average length. In other words, for DR higher than 2, there is less contention between classes 0 and 1. The same observation applies between class 2 and class 1 when DR is higher than 1; and between class 3 and class 2 when DR is higher than 0.5. For class 3, it seems to be unaffected by the delay ratio since it has the highest priority and its bursts will take advantage of all available OWCs.

In conclusion, our simulation results show that classes of traffic can be differentiated based on our QoS enhanced JET (QEJET) contention resolution. With low wavelength (W=4), QEJET is unfair to low priority traffic: Higher priority classes experience less burst loss compared to lower priority classes. We also showed that by using more wavelengths (W=64), classes of low priority are less affected by the unfairness of QEJET.

Another property of QEJET is that increasing the delay ratio doesn't always improve the overall performance across all classes of traffic. This is due to the fact that a delayed burst gets the end-to-end delay increased and will get pre-empted under contention with a higher class burst.

## 4.4 Conclusions

The work presented in this chapter dealt with the sparse FDLs placement problem. We modeled non-uniform traffic between node pairs by assigning weights to the nodes. Our simulation results showed that our placement algorithm, k-WDS, captures the non-uniformity nature of the traffic in OBS. With the NSFNET topology, the k-WDS algorithm achieves almost 60% improvement in burst blocking over the no-FDL case with only four nodes selected for FDLs deployment. An extended version of the algorithm, called A-WDS, is presented to handle the placement of an arbitrary number of FDLs and full converters. The effectiveness of this algorithm has been demonstrated by extensive performance tests using the NSFNET network topology and randomly generated graphs. We focused on the burst loss rate and relative end-to-end delay as the key metrics for evaluating network performance, and we presented comparison results for the tradeoffs of combining fiber delay lines and wavelength converters in solving the contention problem.

This chapter was concluded by presenting cost-effective optical switch and FDL designs along with a QoS-enhanced JET (QEJET) protocol suitable for optical burst switched WDM networks. QEJET allows classes of traffic to benefit from FDLs and OWCs while minimizing the end-to-end delay for high priority bursts. Extensive simulation results were presented showing that QEJET can achieve a clear QoS-based separation between the different classes of service and at the same time provide a good overall performance.

The work presented in this dissertation can be extended in several ways. Two of the issues that we plan to investigate in the near future are:

1. Applying QEJET to other OBS architectures with a limited number of OWCs and FDLs [BLJ04, BLS03].

2. Developing an analytical model that take into consideration the dependency and correlation of FDLs usage in order to improve the speed and blocking performance of our algorithms for FDLs placement.

# 5. DEPENDENCY BASED ANALYTICAL MODEL FOR BLOCKING RATES COMPUTATION

We present a new analytical model that captures link dependencies in all-optical WDM networks under uniform traffic and enables the estimation of connection blocking probabilities more accurately than previously possible. The basic formula of the dependency between two links in this model reflects their degree of adjacency, the degree of connectivity of the nodes composing them and their carried traffic. Our validation tests have shown that the analytical dependency model gives accurate results and successfully captures the main dependency characteristics observed in the simulation measurements. The usefulness of the model is illustrated by showing how to use it in enhancing a simulation-based algorithm that we recently proposed for the sparse placement of full wavelength converters in WDM networks. To analytically handle the presence of wavelength converters, a lightpath containing converters is divided into smaller sub-paths such that each sub-path is a wavelength continuous path and the nodes shared between these sub-paths are full wavelength conversion capable. The blocking probability of the entire path is obtained by computing the probabilities in the individual sub-paths. We validate the analytical-based sparse placement algorithm by comparing it with its simulation-based counterpart using a number of network topologies.

## 5.1 Background

In WRON (Wavelength-Routed Optical Networks), when a connection request is initiated at the source node, the RWA (Routing and Wavelength Assignment) protocol should set up a lightpath between the source and destination nodes using the same wavelength in each link traversed by

the connection. This restriction is referred to as the wavelength continuity constraint (no wavelength conversion is required at any intermediate node). However, if there is no path from the source to destination with the same wavelength available in every link of the path, the call is blocked. When the continuity constraint is removed by using wavelength converters, the network blocking performance is reduced, higher loads are supported and the network throughput is enhanced [ABR96, SAS96, SAS99, JIM99].

Performance evaluation models of WDM networks represent an important research area that has received increased attention. A new analytical model that captures link dependencies in all-optical WDM networks under uniform traffic is presented. The model enables the estimation of connection blocking probabilities more accurately than previously possible.

Existing analytical models for WRON's performance evaluation suffer from accuracy and scalability problems (e.g., the complexity of the model in [LLS00] is intractable for general network topologies, the model in [RBM95] tends to over-predict the blocking probabilities under high loads or with a large number of wavelengths, the tractability of the model in [ABR96, MKA96] is guaranteed only for networks with a small diameter). Models that take the correlation between links into consideration are more accurate than models that assume link independence but are also more computationally intensive.

In this dissertation, we develop a link dependency model that improves our ability to capture the correlation of wavelength availability among different network links. To analytically handle the presence of wavelength converters, a light path containing converters is divided into smaller sub-

paths such that each sub-path is a wavelength continuous path and the nodes shared between these sub-paths are full wavelength conversion capable. The blocking probability of the entire path is easily obtained by computing the probabilities in the individual sub-paths.

Our analytical model captures link dependencies in all-optical WDM networks under uniform traffic and enables the estimation of connection blocking probabilities more accurately than previously possible. The basic formula of the dependency between two links in this model reflects their degree of adjacency, the degree of connectivity of the nodes composing them and their carried traffic.

The remainder of this Chapter is organized as follows. In Section 5.2, we describe our proposed link dependency model, present its validation results and discuss its advantages and its limitation. Section 5.3 introduces the A-BLOCK analytical model and applies it to the sparse wavelength conversion problem. Section 5.4 discusses the impact of the network topology, the traffic pattern, the routing scheme and the number of wavelengths per link. We make concluding remarks in Section 5.5.

## 5.2 Dependency and correlation model

In this section, we present our link dependency model. We first present the basic definitions used in our model then proceed to present the details of the dependency formula. Given a graph G(V,E), a k-dominating set (k-DS) in G is a set $D \subset V$ such that every node in the graph is either a member in D or is at distance k or less from at least one member in D. In [BLJ03], we

presented a heuristic approximation algorithm for the k-Minimum Dominating Set problem (an NP-hard problem) and used it in solving the sparse wavelength converters placement problem. The heuristic algorithm computes k-dominating sets (k-DS) that are used to guide the selection of wavelength conversion sites (i.e., nodes that are to be equipped with full wavelength conversion capability). The index k of k-DS represents the maximum distance allowed between a node in the network and the nearest conversion site. For example, k=2 means that a wavelength converter is guaranteed to exit at a distance of no more than 2 hops from any node in the network. Figure 33 shows the NSF backbone topology along with the three k-DS sets (k=1,2,3). The nodes with double circles in Figure 33 represent the conversion sites selected by the 2-DS set. The k-DS heuristic algorithm uses a metric, called $Connect_k(v)$, that measures the connectivity of node v based on the index k. We have used the $Connect_k(v)$ metric in the formula of the link dependency model proposed in this dissertation. The recursive definition of $Connect_k(v)$ is given in [9] and will be explained in this dissertation using an example of the ring topology. For any node v, the value of $Connect_0(v)$ is the degree of node v (i.e., the number of neighboring nodes sharing a direct link with node v). Thus in the ring topology, $Connect_0(v)$ is always 2. The value of $Connect_1(v)$ is obtained by summing up $Connect_0(v)$ and $Connect_0(u)$ for each node u that is at a distance of 1 hop from v. Thus in the ring topology, $Connect_1(v)$ is 6 for any node v. The value of $Connect_2(v)$ is obtained by summing up $Connect_1(v)$ and $Connect_1(u)$ for each node u that is at a distance of 1 hop from v. Thus in the ring topology, $Connect_2(v)$ is 18 for any node v. $Connect_k(v)$ for higher values of k can be evaluated using the same recursive logic. For a ring, it is easy to establish: $Connect_k(v) = 2 \cdot 3^k$, for all nodes v.

1-DS (NSFNET) = {1, 4, 5, 6, 9, 12}

2-DS (NSFNET) = {1, 4, 9, 12}

3-DS (NSFNET) = {12}

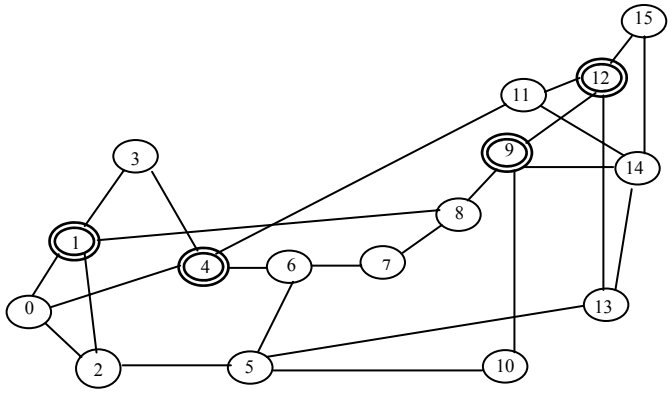


Figure 33: NSFNET and k-DS sets

The 1-DS and 2-DS sets shown in Figure 33 are redundant in the sense that a node or more (e.g., node 1 in 2-DS) can be removed from the set without affecting its dominance property. A polynomial time procedure can be used to remove this redundancy but we have found that sub-optimal k-DS sets are good enough for the converters placement problem. We have observed from numerous simulation tests on different topologies that when the value of k increases, the size of the k-DS set computed by the heuristic algorithm decreases until k-DS becomes a singleton set. We define $\Re$ as the smallest value of k such that the size of k-DS computed by the heuristic algorithm is 1. For the NSFNET topology of Figure 33, the value of $\Re$ is 3 (the set 3-DS is singleton and node 12 is at a distance 3 or less from any other node). We next proceed to present our analytical dependency model.

Consider a network with an arbitrary topology represented by a graph G(V,E) with a set of nodes V, a set of links E and W wavelengths per link. The traffic is uniformly distributed among all node pairs. A connection request originating from source node s to destination node d arrives as a Poisson process with rate $\frac{\lambda}{N(N-1)}$ (thus the total arrival rate in the entire network is λ). The connection holding time is exponentially distributed with mean μ. The offered load of the network is $\rho = \lambda/\mu$. The arrival process to link i when it has n available wavelengths is Poisson with arrival rate $\lambda_{in}$. A connection request is established using a path P if there is a wavelength available on all links of the path P. If wavelength conversion is available along the path, the wavelength used could be different in different portions of the path. The choice of the wavelength when more than one is available is random. We implemented the well known fixed alternate routing (FAR) approach [HMH97] by pre-computing three link-disjoint shortest path routes between every pair of nodes. If a connection is blocked on the first route, the second alternate route is examined, and if still blocked, the third alternate route is examined. A new request is discarded (blocked) if it cannot be served by one of the three pre-computed alternate routes.

### 5.2.1 Formulation of the correlation model

Let $X_i$ be the random variable representing the number of available wavelengths on link i. In our model, we assume that the dependence between $X_i$ and $X_j$ is formulated as follows:

$$P[X_j = m \mid X_i = n] = r_{ij}(n,m) + P[X_j = m] \qquad (5.1)$$

The term $r_{ij}(n,m)$ in the above equation is a correction term that captures link dependency. Note that making $r_{ij}(n,m) = 0$, for $\forall i, j$ and $\forall m,n$ is equivalent to assuming that the variables $X_i$ and $X_j$ are independent. If we sum up both sides of equation (5.1) over m (from m=0 to m=W), then the left side sums up to 1. Also the term $P[X_j=m]$ in the right side sums up to 1. Thus for proper probability values, we must have the following condition:

$$\sum_{m=0}^{W} r_{ij}(n,m) = 0 \qquad (5.2)$$

As will be shown later, the correction term $r_{ij}(n,m)$ depends on three factors:

1. A(i,j) which is the degree of adjacency of the directed links $i=(s_1,d_1)$ and $j=(s_2,d_2)$ defined as the number of hops in the shortest path between nodes $d_1$ and $s_2$.

2. The value of the connectivity metric for the two links.

3. The carried traffic. The value of $r_{ij}(n,m)$ is carefully chosen to accurately reflect the dependence of wavelength availability and we always ensure that "$r_{ij}(n,m)+P[X_j=m]$" is a valid probability value between 0 and 1.

The value of $r_{ij}(n,m)$ is obtained by a two-step procedure as follows:

*Step 1: Initial Assignment*

$$r^{*}_{ij}(n,m) = f \,.\, \alpha \,.\, (W/2 - \mathrm{Abs}(n-m)), \tag{5.3.a}$$

$$\text{where } \alpha = \frac{1}{W} * \frac{\lambda_{in}}{\lambda} * \frac{C\Re(i \cap j)}{\max(C\Re(G))} * \frac{1}{1 + A(i,j)} \tag{5.3.b}$$

The term $r^{*}_{ij}(n,m)$ denotes the initial estimate of $r_{ij}(n,m)$. The term α depends on the adjacency of links i and j, A(i,j) defined earlier. If A(i,j)=0, then links i and j share a common node, denoted by i∩j. If there is no common node (i.e, A(i,j)>0 ) then $C_{\Re}(i \cap j)$ is defined to be 1. The notation $\max(C_{\Re}(G))$ denotes the maximum value of $C_{\Re}(v)$ over all nodes, v, in the graph G. When links i and j are far from each other, i.e., A(i,j) is large, then $P[X_j=m]$ and $P[X_i=n]$ are nearly independent and the value of $r_{ij}(n,m)$ is close to zero.

If links i and j are adjacent, then A(i,j) equals 0, and α has a relatively larger value that depends on the connectivity value $C_{\Re}(i \cap j)$. The above model makes the impact of $r_{ij}(n,m)$ stronger when A(i,j) is zero.

The scale factor f is given a value between 0 and 1 depending on the topology. The purpose of this term is to improve the accuracy of the dependency model for various topologies. Note that if f=0, then all $r_{ij}(n,m)$ values are zero, i.e., we get the no-dependency case.

When links i and j share a common node denoted by $i \cap j$, we define f as: $f = 1/(\text{degree}(i \cap j)-1)$. If there is no common node (i.e, $A(i,j)>0$ ) then f and $C_k(i \cap j)$ are defined to be 1. Notice that for the ring topology, the degree of any node is 2 and the scale factor f will always attain its maximum value of 1, thereby contributing to larger values of link dependencies $r_{ij}(n,m)$. The validation tests presented later in this section will provide more clarification on the impact of the various factors used in equation (5.3.b).

*Step 2: Normalization*

In the second step, the initial values $r^{*}_{ij}(n,m)$ are adjusted to satisfy relation (5.2). A corrective shift Z is first computed as follows:

$$Z = \frac{\sum_{m=0}^{W} r^{*}_{ij}(n,m)}{W+1} \qquad (5.4)$$

To satisfy relation (5.2), the initial estimates of $r_{ij}(n,m)$ are adjusted by subtracting Z.

$$r_{ij}(n,m) = r^{*}_{ij}(n,m) - Z \qquad (5.5)$$

We further test the $r_{ij}(n,m)$ values to make sure that the probabilities of equation (5.1) are valid probability values. Next, we describe the simulation tests used to validate the above dependency model.

### 5.2.2 Validation of the correlation model

In this section, we present the validation tests for the link dependency model using NSFNET, 8-node ring and 16-node ring topologies under uniform traffic. For all the tests reported in this dissertation, the simulation was run for a total of M connection requests (events) where M is $10^6$ times the considered load of traffic in the network ($M = 10^6 \times \lambda/\mu$.). For analysis purposes, the wavelength assigned to a path (or to a sub-path after wavelength conversion) is chosen randomly from the set of free wavelengths. As in [BLJ03], all simulation results are given with 95% confidence intervals using the batch means method with 50 batches (confidence intervals are shown as vertical bars on the plotted curves). Let us start by considering the two directed links i and j in the NSF network of Figure 33, i=(8,9) and j=(9,12). Notice that these two directed links share a common node (i.e, A(i,j)=0). Under a load of 50 Erlangs, we keep track of the durations when link i has n wavelengths available and link j has m wavelengths available, $0 \leq n , m \leq W$. Based on the simulation measurements, we then compute:

$$r_{ij}(n,m) = P[X_j = m \mid X_i = n] - P[X_j = m]$$

In Figure 34, we present the simulation measurements and the analytical values of $r_{ij}(2,m)$ and $r_{ij}(8,m)$ for the links i=(8,9) and j=(9,12). When n is fixed at n=W/4=2, the dependency between the links has the highest value (of 0.0569) at m=n=2. The average error of the model is 3.86%, the maximum error is 5.24% and the standard deviation is .02654. When n is fixed at n=W=8, the dependency between the links has the highest value (of 0.08536) at m=n=8. The average error of the model is 4.12%, the maximum error is 4.97% and the standard deviation is .02471.

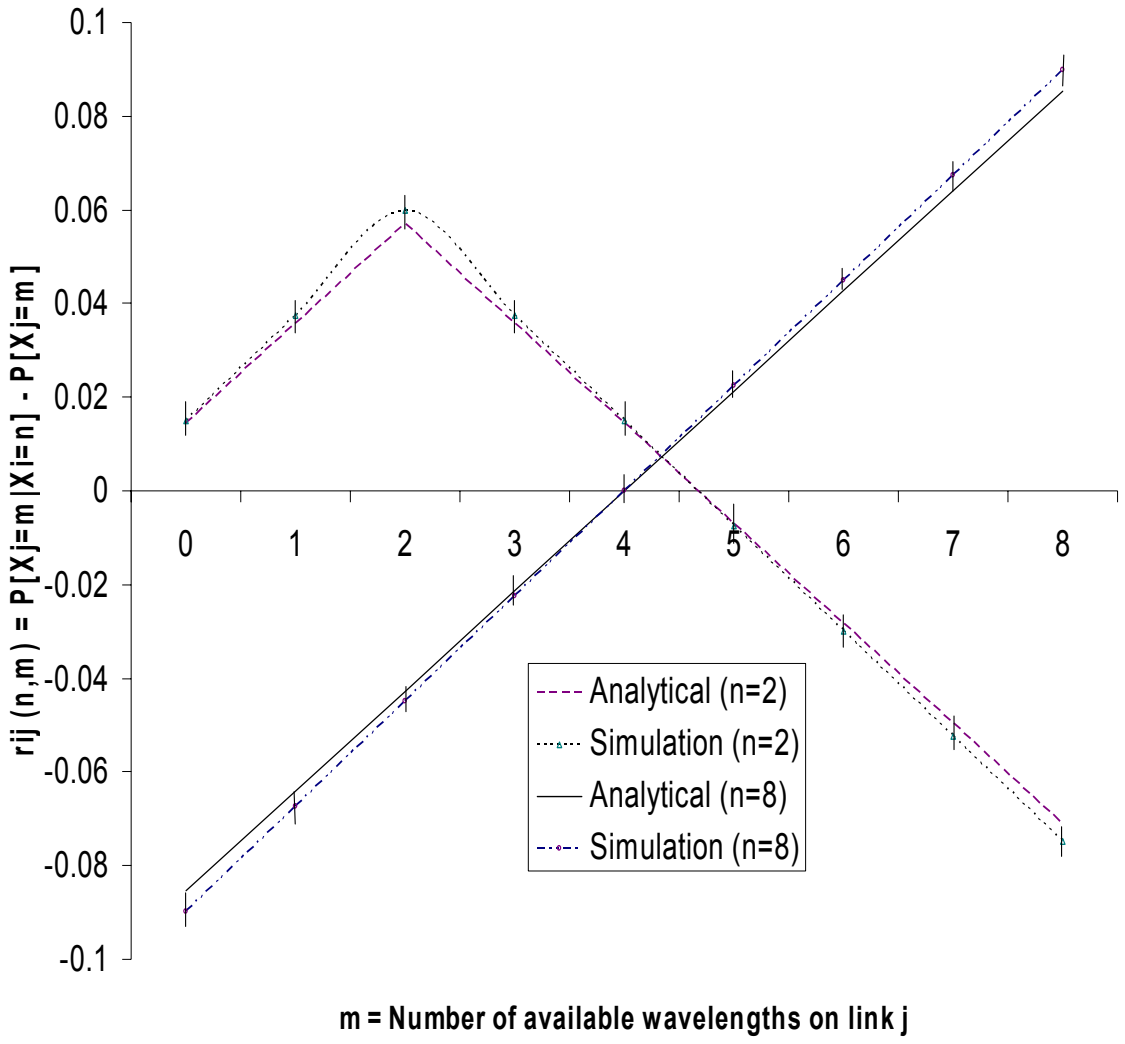


Figure 34: $r_{ij}(W/4=2,m)$ and $r_{ij}(W=8,m)$ when i=(8,9), j=(9,12) and W=8, NSFNET

We are not presenting the validation graphs for NSFNET when n is fixed at n=0 and at n=W/2=4 (these graphs have the same shape and general trends of the graphs for the ring topology with n=0 and n=W/2 presented below in Figure 35).

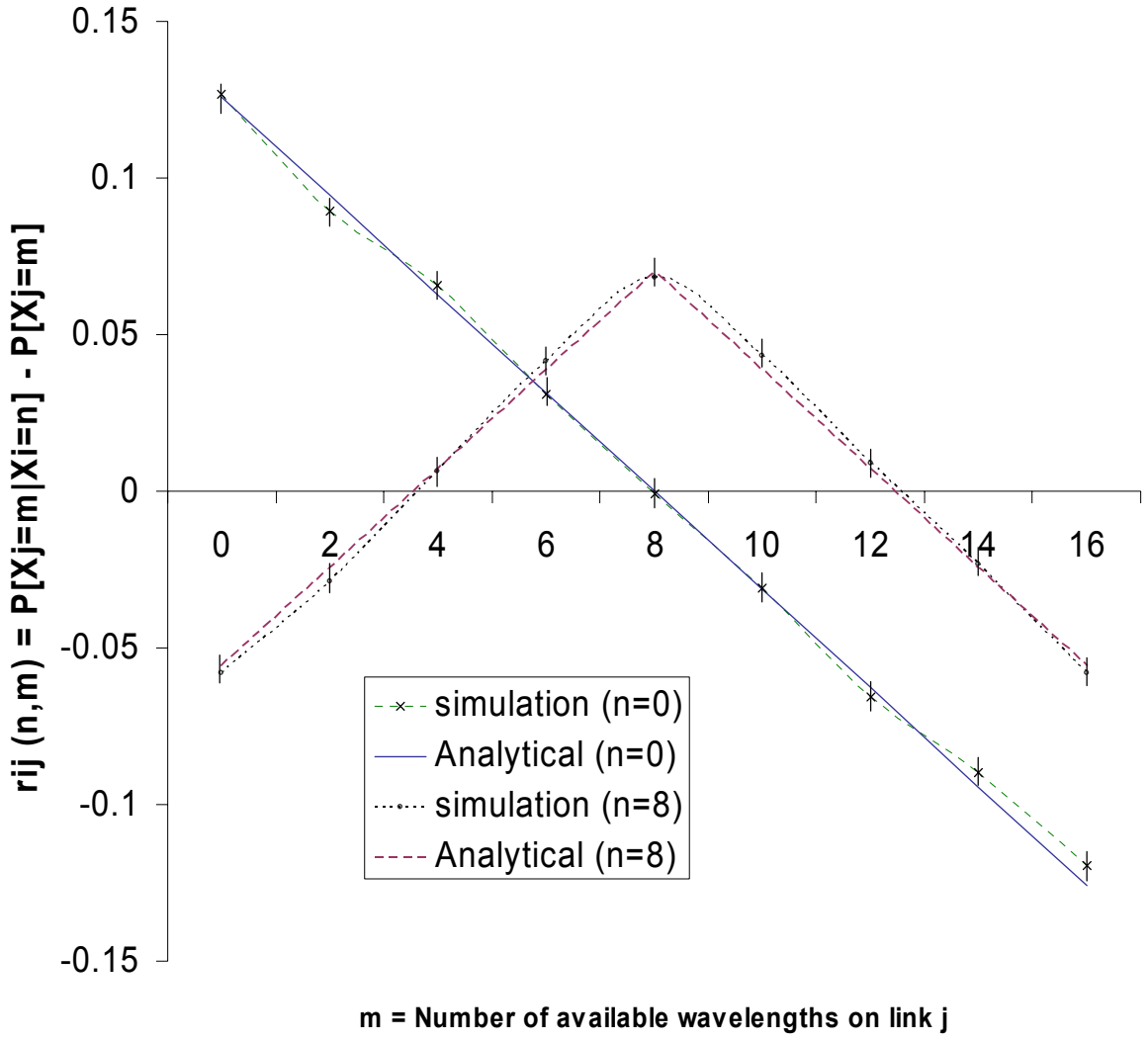


Figure 35: $r_{ij}(0,m)$ and $r_{ij}(W/2=8,m)$ in 8-node ring and W=16

We next consider the case of the highly sparse ring topology. Due to the symmetric nature of the ring, we consider two arbitrary adjacent links in an 8-node ring with W=16 under uniform traffic. We plot $r_{ij}(n,m)$ for m ranging from 0 to 16 and present the case of n=0 and n=W/2=8 in Figure 35. For the case of n=0, the dependency between the two links has the highest value (of 0.125) when m=n=0. The average error of the model is 4.74%, the maximum error is 5.67% and the standard deviation is .07986. Similar accurate results was obtained for the case of n=W/2=8 shown in Figure 35. As was pointed earlier for the ring topology, the degree of any node is 2 and the scale factor f (of equation 5.3.a) is at its maximum value of 1, thereby contributing to larger values of $r_{ij}(n,m)$.

So far, we looked at adjacent links to validate the link dependency model that captures the correlation of wavelength availability. For all cases (n ranging from 0 to W), our measurements show that $r_{ij}(n,m)$ has a maximum at m=n indicating that the dependency is strongest when the two links have nearly the same number of available wavelengths. We conducted tests for the dependency between link pairs i and j when these links are not adjacent (A(i,j)>0).

The results obtained by these tests showed similar trends as those found in Figure 34 and Figure 35 but the highest values of $r_{ij}(n,m)$ were much smaller. The further away the two links are from each other (i.e., the higher the value of A(i,j)) the smaller the value of maximum $r_{ij}(n,m)$. In Figure 36, we plot the peak value of $r_{ij}(n,m)$ for 8-node ring at load 30 Erlangs when n = 0 and m = 0 corresponding to $r_{ij}(0,0) = P[X_j = 0 \mid X_i = 0] - P[X_j = 0]$ for different values of A(i,j) ranging from 0 to 3. Note that the impact of $r_{ij}(w,m)$ is stronger when A(i,j) is zero. If A(i,j) is

large (the two links are far away from each other), then $P[X_j=m]$ and $P[X_i=n]$ are nearly independent and the value of $r_{ij}(n,m)$ is close to zero.

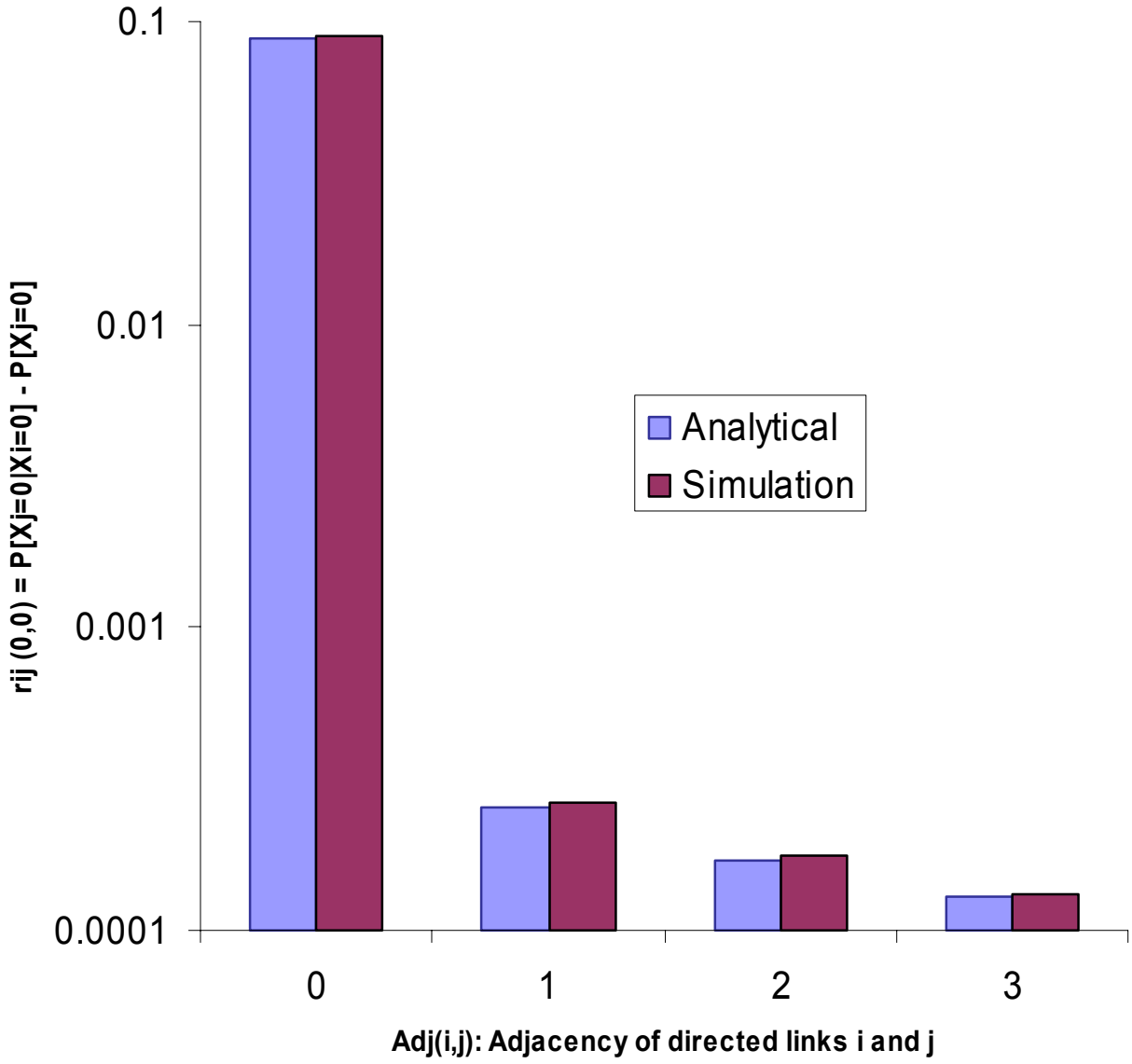


Figure 36: rij(0,0) when A(i,j) ranges from 0 to 3 and W=16 (8-node ring)

Our tests showed that the dependency model matched the simulation results with good accuracy for the NSFNET topology (presented in Figure 33) and the U.S LongHaul topology [BLJ04] (presented in Figure 5) under both low and high loads.

For the ring topology, accurate match is obtained at loads of 25 Erlangs or higher for 8-node ring with W=16 and loads of 40 or higher for 16-node ring. With random wavelength assignment, the strongly sequential nature of the ring topology causes connections with larger number of hops to be dropped more often at moderate and high loads. In this case, most of the active connections are very short (mostly affecting no more than two adjacent links) and there is a significant drop in the value of $r_{ij}(n,m)$ when A(i,j) increases from 0 to 1, conforming to the exponential increase in the value of $C_{\Re}$ for ring in the denominator of equation 5.3.b.

As we can see in Figure 37, at lesser loads such as 15 Erlangs, the drop becomes smaller deviating form the formula and at loads smaller than 8 Erlangs for the 16-node ring there is no drop whatsoever in the value of $r_{ij}(n,m)$ when A(i,j) increases from 0 to a higher value.

In the case of 8-node ring and loads less than 3 Erlangs, there is no drop whatsoever in the value of $r_{ij}(n,m)$ when A(i,j) increases from 0 to a higher value

Further research is needed to investigate replacing $C_{\Re}$ by a slow growing term for the ring topology under low loads.

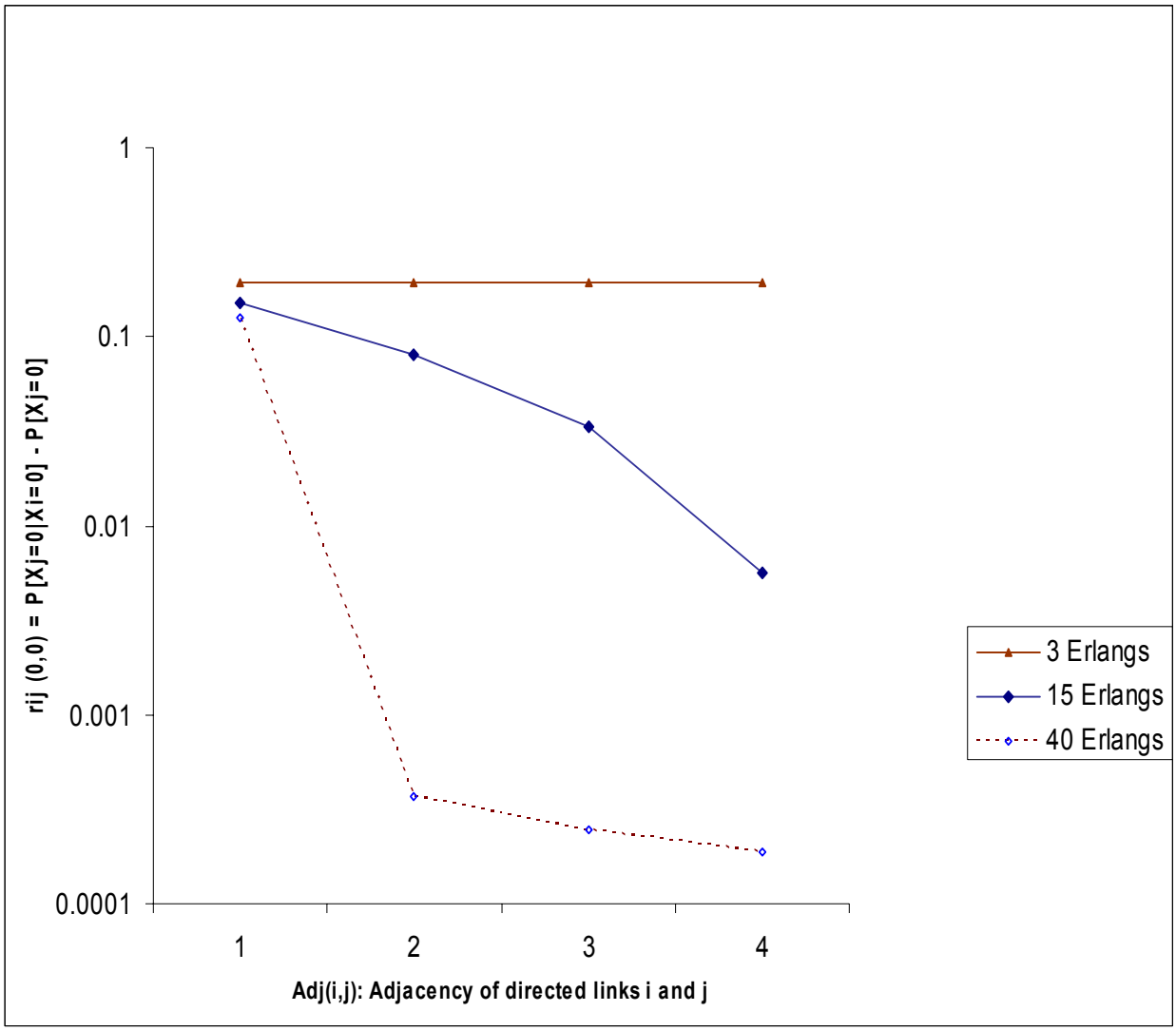


Figure 37: Ring topology, Drop in the value of $r_{ij}(n,m)$ when A(i,j) increases

We now investigate the impact of the connectivity of the common node that joins two adjacent links. In Figure 38 we look at the case when links i and j are adjacent (A(i,j)=0) and their common node has degree of 2 or 4. The value of n in this test is fixed at n=W/2=4. The

dependency between links i and j is clearly proportional to the connectivity of their common node v captured by the term $C_{\Re}(v)$.

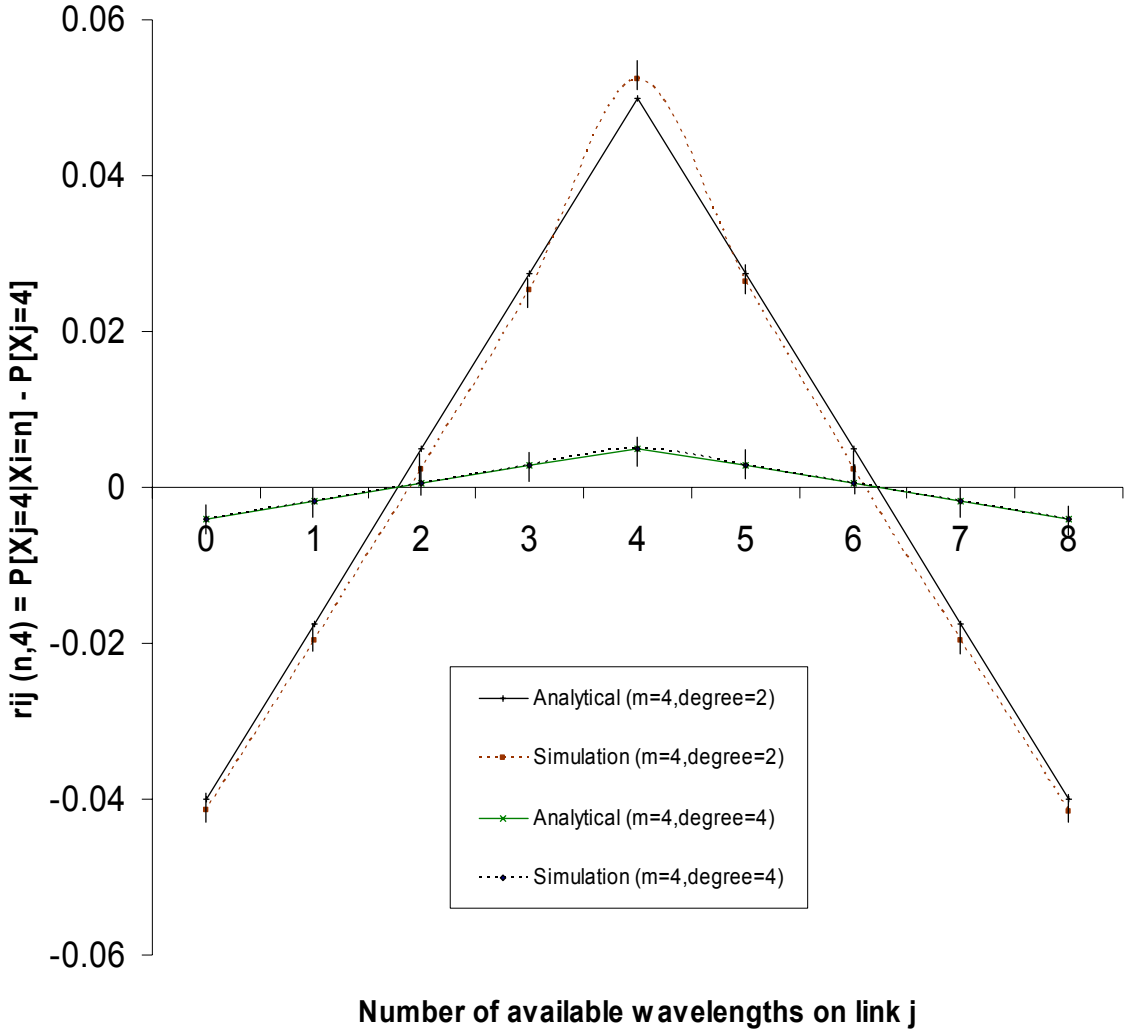


Figure 38: $r_{ij}(4,m)$ when Adj(i,j)=0, common node has degree of 2 or 4 (W=8), NSFNET

In concluding this section, it is important to notice that sparse wavelength conversion is not directly incorporated in the formula for $r_{ij}(n,m)$ but it indirectly affects $r_{ij}(n,m)$ via the arrival rate

on link i (defined as $\lambda_{in}$ in equation 5.3.b). Placing a full wavelength converter in a node forces the analytical model presented in Section 5.3 to perform path decomposition at this node for any path that goes through it. This affects the computation of $\lambda_{in}$ and indirectly affects the link dependencies $r_{ij}(n,m)$. Our tests have shown that this indirect incorporation of wavelength conversion gives reasonably accurate results. An approach for directly incorporating wavelength conversion in the link dependency model is a topic worthy of further research but is beyond the scope of this dissertation.

## 5.3 Analytical Model: A-BLOCK

In this section, we use the dependency model in computing the blocking probabilities for an arbitrary network topology. Let $X_i$ denote the random variable representing the number of available wavelengths on link i. The arrival process on link i, when it has n available wavelengths, is Poisson with arrival rate $\lambda_{in}$ (we will shortly show how to compute $\lambda_{in}$). The rate at which connections terminate and free up wavelengths when there are W-n active connections (i.e., n available wavelengths) on link i is $(W - n)\mu$. The number of available wavelengths on link i could be modeled as a continuous time death and birth model with the following solution.

$$p_i(n) = P[X_i = n] = \frac{\prod_{j=1}^{n}(W-j+1).\mu}{\prod_{j=1}^{n}\lambda_{ij}} p_i(0) = \frac{(W-n+1).\mu}{\lambda_{in}} p_i(n-1) \qquad (5.6)$$

$$p_i(0) = P[X_i = 0] = \left[ 1 + \sum_{n=1}^{W} \frac{\prod_{j=1}^{n} (W - j + 1).\mu}{\prod_{j=1}^{n} \lambda_{ij}} \right]^{-1} \quad (5.7)$$

Let $X_P$ denote the random variable representing the number of available wavelengths on a path P with t links and let $w_P = (w_1, w_2, \ldots w_t)$ be a vector representing the number of available wavelengths on each of the t links composing P. We will provide the detailed derivations to determine $P[X_P = m]$ and $P[X_P = m \mid X_1 = w_1, \ldots, X_t = w_t]$ for t ranging from 1 to 3.

We follow the same logic used in [RRM02] to compute $\lambda_{in}$, the arrival rate to link i when it has n available wavelengths, i.e., we sum up the arrival rates on all paths P that use the link i in question (with a probability equals to $P[X_P>0 \mid X_i=n]$):

$$\lambda_{in} = \sum_{P \text{ such that } i \in P} \frac{\lambda}{N(N-1)} (1 - P[X_P = 0 \mid X_i = n] \quad (5.8)$$

Notice that because of the uniform traffic assumption, the total arrival rate $\lambda$ in the above equation is distributed equally among N(N-1) source-destination pairs.

We can compute the blocking probability $B_P$ on any given path P, corresponding to the probability that a connection is blocked on route P.

$$B_P = P\,[X_P=0] \tag{5.9.a}$$

Shortly, we will derive the computation of $P\,[X_P>0 \mid X_i=n]$, $\lambda_{in}$ and $B_P$, where P is a path with one link, two links and three links, respectively. When there are nodes with full wavelength conversion on a path P; P is divided into S smaller sub-paths $P= P_1P_2...P_S$. Each sub-path $P_s$, $1\leq s\leq S$, is a wavelength continuous path (i.e., the same wavelength is used in all links in $P_s$). The nodes shared between sub-paths $P_s$ and $P_{s-1}$ (or $P_s$ and $P_{s+1}$) are full wavelength conversion capable.

The blocking probability on any given sub-path $P_s$, $B_{Ps} = P\,[X_{Ps} = 0]$, is computed the same way as in equation (5.9.a). The blocking probability of the entire path P is given by the following equation:

$$B_P = 1 - \prod_{s=1}^{s=S} (1 - B_{P_S}) \tag{5.9.b}$$

We utilize the framework presented in [ABR96] and modify it to include our proposed dependency model presented in Section 5.2. We look first at the case of path with 2 links and establish the following equations:

$$P\,[X_P=m \mid X_1=w_1,\ X_2=w_2] = \begin{cases} \dfrac{\binom{w_1}{m}\binom{W-w_1}{w_2-m}}{\binom{W}{w_2}}, & if\ \max(0, w_1+w_2-W) \le m \le \min(w_1, w_2) \\ 0, & otherwise \end{cases}$$

Notice that m is obviously smaller than $w_1$ and $w_2$. The above expression can be easily understood if we multiply both the numerator and the denominator by $\binom{W}{w_1}$. This makes the denominator equal to the number of combinations where there are $w_1$ free wavelengths in link 1 and $w_2$ free wavelengths in link 2. The numerator in this case is equal to the number of combinations in which exactly m wavelengths are common among the free wavelengths in the two links.

$$\text{And} \quad P[X_P = m\,] = \sum_{w1=m}^{W}\sum_{w2=m}^{W} P[X_P = m \mid X_1 = w_1, X_2 = w_2\,].P[X_1 = w_1, X_2 = w_2\,] \qquad (5.10)$$

We will use the following notation: $q_m(w_1,w_2) = P\,[X_P=m \mid X_1=w_1,\ X_2=w_2]$ (5.11)

For paths of any arbitrary number, t, of links composing the path P, the same logic will apply and the generalized formulation of $q_m(w_1, w_2 \ldots w_{t-1}, w_t)$ is:

$$q_m(w_1, w_2, \ldots, w_{t-1}, w_t) = \sum_{k=m}^{\min(w_1, w_2, \ldots, w_t - 1)} q_m(k, w_t).q_k(w_1, w_2, \ldots, w_{t-1}) \qquad (5.12\text{-a})$$

and

$$P[X_P=m] = \sum_{w=m}^{W} \sum_{w_t=m}^{W} P[X_P = m \mid X_{P_{t-1}} = w, X_t = w_t] P[X_{P_{t-1}} = w, X_t = w_t] \qquad (5.12\text{-b})$$

$P_{t-1}$ denotes the sub-path containing the first t-1 links of the path P.

For paths with two links, we will refer to $P[X_P=0 \mid X_1=w_1, X_2=w_2]$ as $q_0(w_1, w_2)$ and for paths of three links, $P[X_P=0 \mid X_1=w_1, X_2=w_2, X_3=w_3]$ as $q_0(w_1, w_2, w_3)$; see equation 5.10 with m equals 0.

The computation of P [$X_P$>0 | $X_i$=n], $\lambda_{in}$ and $B_P$, where P is a path with one link, two links and three links is as follows:

*1. For a Path P with one link i:*

If n>0 then P [$X_P$=0 | $X_i$=n] = 0.

$$\text{So,} \quad \lambda_{in} = \sum_{P \text{ such that } i \in P} \frac{\lambda}{N(N-1)} \qquad \text{for n>0} \tag{5.13}$$

$$B_P = P\,[X_P=0] = p_i(0). \tag{5.14}$$

Notice that $p_i(0)$ is computed using equation 5.7 given earlier in section 5.3

*2. For a Path P with two links i and j:*

$$P\,[X_P>0 \mid X_i=n] = \sum_{m=o}^{W} P[X_P > 0 \mid X_i = n, X_j = m].\, P[X_j = m \mid X_i = n].$$

$$= \sum_{m=o}^{W} (1 - P[X_P = 0 \mid X_i = n, X_j = m]).(r_{ij}(n,m) + P[X_j = m])$$

$$= \sum_{m=1}^{W} (\, r_{ij}(n,m) + p_j(m)\,).(1 - q_0(n,m)) \tag{5.15}$$

Note that the link dependency $r_{ij}$ (n,m) is defined earlier by equation 5.3 in section 5.2.

$$\text{So,} \quad \lambda_{in} = \sum_{P \text{ such that } i \in P} \frac{\lambda}{N(N-1)} \sum_{m=1}^{W} (r_{ij}(n,m) + p_j(m)).(1 - q_0(n,m)) \tag{5.16}$$

$$B_P = P\,[X_P=0] = \sum_{n=0}^{W} P[X_P = 0 \mid X_i = n]\, P[X_i = n]$$

$$= \sum_{n=0}^{W} \sum_{m=0}^{W} (r_{ij}(n,m) + p_j(m)) p_i(n) q_0(n,m) \tag{5.17}$$

*3. For a Path P with three links: i, j and k:*

$$P\,[X_P>0 \mid X_i=n] = \sum_{l=1}^{W} \sum_{m=1}^{W} (r_{ij}(n,m) + p_j(m))\,(r_{jk}(m,l) + p_k(l))\;\;(1 - q_0(n,m,l)) \tag{5. 18}$$

So,

$$\lambda_{in} = \sum_{P \text{ such that } i \in P} \frac{\lambda}{N(N-1)} \sum_{l=1}^{W} \sum_{m=1}^{W} (r_{ij}(n,m) + p_j(m))(r_{jk}(m,l) + p_k(l))(1 - q_0(n,m,l)) \tag{5.19}$$

$$BP = P[X_P=0] = \sum_{n=0}^{W} P[X_P = 0 \mid X_i = n]\, P[X_i = n]$$

$$= \sum_{n=0}^{W}\sum_{m=0}^{W}\sum_{l=0}^{W} (r_{ij}(n,m) + p_j(m))(r_{jk}(m,l) + p_k(l))\, p_i(n) q_0(n,m,l) \qquad (5.20)$$

### 5.3.1 A-BLOCK algorithm for blocking probabilities computation

The blocking probabilities for the entire network can be computed using the following algorithm referred to as A-BLOCK:

*Initialization Routine: r=0*

0. Depending on the adopted routing (shortest path, FAR), compute route(s) for all node pairs.

1. For all paths P, initialize $B_P(r)$ to 0.
2. For all links Li and available wavelengths n, initialize $\lambda_{in}$ to $\sum_{P \text{ such that } i \in P} \frac{\lambda}{N(N-1)}$. In the case of FAR, P is the primary path of a source-destination pair

*Iterative Loop: r=r+1*

1. For all links Li and available wavelengths n, compute $p_i(n)$ using equations (5.6)-(5.7).

2. For all links Li and available wavelengths n, compute $\lambda_{in}$ using equations (5.8).

3. For all paths P, compute $B_P(r)$ using equations (5.9.a) and (5.9.b).

4. For all paths P, if the difference between $B_P(r-1)$ and $B_P(r)$ is small enough, stop.

*else* repeat the Iterative Loop.

The Iterative Loop of the A-BLOCK algorithm is executed until the difference between $B_p(r)$ and $B_p(r-1)$ is smaller than $10^{-5}$. As the dependency model is applied repeatedly in the loop, the influence of link dependencies on the solution increases until A-BLOCK converges to the correct values.

Our algorithm uses path decomposition, which allows a significant reduction of the time complexity of the model and captures the correlation of wavelength availability and link loads. As stated earlier, when there are nodes with full wavelength conversion on a path, the path is reduced to sub-paths having no wavelength conversion in their intermediate nodes. We further divide these sub-paths into smaller sub-paths of length one, two or three links. For example a

sub-path of 5 links will be further divided into a sub-path of 3 links and another sub-path of 2 links (note that path decomposition is not applicable to the NSFNET topology since its diameter is only 3).

We analyze each sub-path in isolation and then the individual results are combined appropriately to obtain a solution for the overall path. Let N=|V| be the number of nodes in the network, $\xi$=|E| be the number of links (edges), P be the number of paths, and D be the diameter of the network.

The worst-case time complexity of A-BLOCK is analyzed below:

1. Step 1 is of order O(P ) for the case of shortest path routing (1 path per source-destination pair) and O(3.P ) for the case of FAR (3 alternate routes per source-destination pair).

2. Step 2 is of order O($\xi$. W. P).

3. Step 3 can be implemented in order O($\xi$ . ($W^2$ + W))= O($\xi$ .$W^2$) since $p_i(0)$ can be computed from equation (5.7) in O($W^2$) then $p_i(n)$ can be computed from $p_i(n-1)$ in O(1) using the iterative version of equation (5.6) . Note that, $\lambda_{in}$ in equation 5.6 is initialized previously in step 2 (for all $0 \leq n \leq W$).

4. Step 4 is of order $O(\xi . P . D/3 . W^3)$ since we divide the paths into sub-paths of at most one, two or three links. Equation 5.13 is of complexity O(P), equation 5.16 is of complexity O(P.W) and equation 5.19 is of complexity $O(P.W^3)$.

These equations provide the detailed computation of $\lambda_{in}$ for paths with one, two and three links, respectively. The term $q_0(n,m)$ in equation 5.16 is of order O(1) and $q_0(n,m,l)$ in equation 5.19 is of order O(W). Equation 5.19 (case of three-link sub-path) has the highest complexity and the maximum number of 3-link sub-paths in a route is D/3 where the diameter D is the maximum possible length of a route. Thus the time complexity of step 4 is $O(\xi . D/3 . P. W^3)$.

5. Step 5 is of order $O(P. D/3. W^3)$. Equation 5.14 is of complexity O(1) since pi(0) was already computed in step 3, equation 5.17 is of complexity $O(W^2)$ and equation 5.20 of is of complexity $O(W^3)$. These equations provide the detailed computation of BP for paths with one, two and three links, respectively. The worst-case time complexity of step 5 is obtained from the three equations using logic similar to the logic explained above in step 4.

6. Finally, Step 6 is of order O(P ).

For a worst case analysis, $\xi$ is of order $O(N^2)$, P is of order $O(N^2)$ and D is of order O(N). Thus the iterative algorithm A-BLOCK evaluates the blocking probabilities in order $O(N^5.W^3)$ per iteration compared to the model in [RRM02] which has order $O(N^5. W^4)$.

We have observed in our numerous tests that the A-BLOCK iterative algorithm converges after 7 to 10 iterations. Even though the A-BLOCK algorithm has the inherent complexity of incorporating the link dependencies $r_{ij}(n,m)$ (as opposed to algorithms that assume link independence), the algorithm has been reasonably fast for all the network topologies and tests reported in the next section.

### 5.3.2 A-BLOCK simulation results

In Figure 39, we applied our analytical model by varying the load from 0.1 to 20 (low load conditions) using the NSF backbone topology. The horizontal axis in Figure 39 represents the load and the vertical axis represents the average network-wide blocking probability (expressed as a percentage). There are four curves in Figure 39 as explained below.

We first consider the network when all nodes are capable of full wavelength conversion and use A-BLOCK to compute the network blocking probability (in this case, every link forms a separate sub-path). We also run a simulation with a full wavelength converter placed in every node and measure the average network-wide blocking percentage for every considered load.

We can see that our analytical model is a good approximation of the experienced connection blocking. The average error of the analytical model for the "All Converter" curve is 3.77% and the maximum error is 6.53%. Similar accurate results are obtained for the case when no wavelength conversion is available (i.e., none of the nodes is capable of wavelength conversion).

The analytical model estimates accurately the blocking probabilities in the "No Converters" case for all considered loads with an average error of 2.68% and a maximum error of 4.32%.

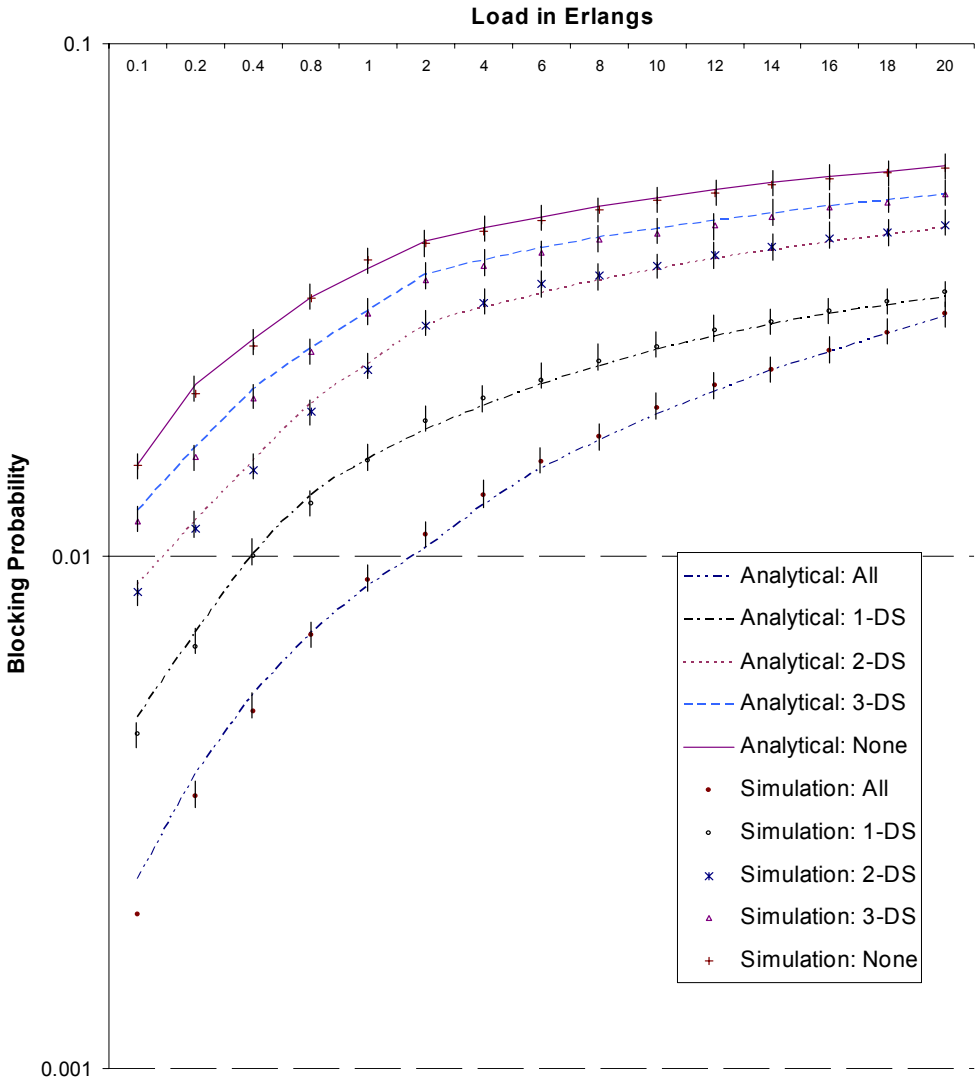


Figure 39: Simulation and model comparison using NSFNET under low load (W=8)

Using our k-DS heuristic algorithm [BLJ03], we then find a 1-Dominating set for the NSF network. In this case, 1-DS is the set of nodes {1, 4, 5, 6, 9, 12}. The set of nodes in 1-DS are then made capable of full wavelength conversion. Note that this 1-DS set is not optimal but this is not important here; this 1-DS is simply used to guide the placement of 6 converters in order to compare the analytical model with the simulation model.

We obtain the networking-wide blocking percentage both analytically and by simulation. The analytical model approximates accurately the correct blocking probabilities; the average error for the 1-DS curve is 3.15% and the maximum error is 5.42 %. The 2-DS set has nodes {1, 4, 9, 12} as members. Again this 2-DS set is not optimal but this is not important as was explained for 1-DS. The accuracy of the model for the 2-DS curve is high with an average error of 2.15 % and a maximum error of 3.27%. Finally, the 3-DS set has only one node in it, namely node 12. The accuracy of the model for 3-DS is also very good with an average error of 2.41% and a maximum error of 4.56%.

In Figure 40, we compare two types of analytical results, namely, the results obtained by our dependency based analytical model and those obtained by adopting the link independence assumption, i.e., by setting $r_{ij}(n,m)=0$ for all i, j, n and m.

Note that the link independence assumption has been used in previous relevant work [2, 8, 14]. The results in Figure 40 are based on the NSFNET topology when the members of 2-DS (i.e. nodes: 1, 4, 9 and 12) have the wavelength conversion capability.

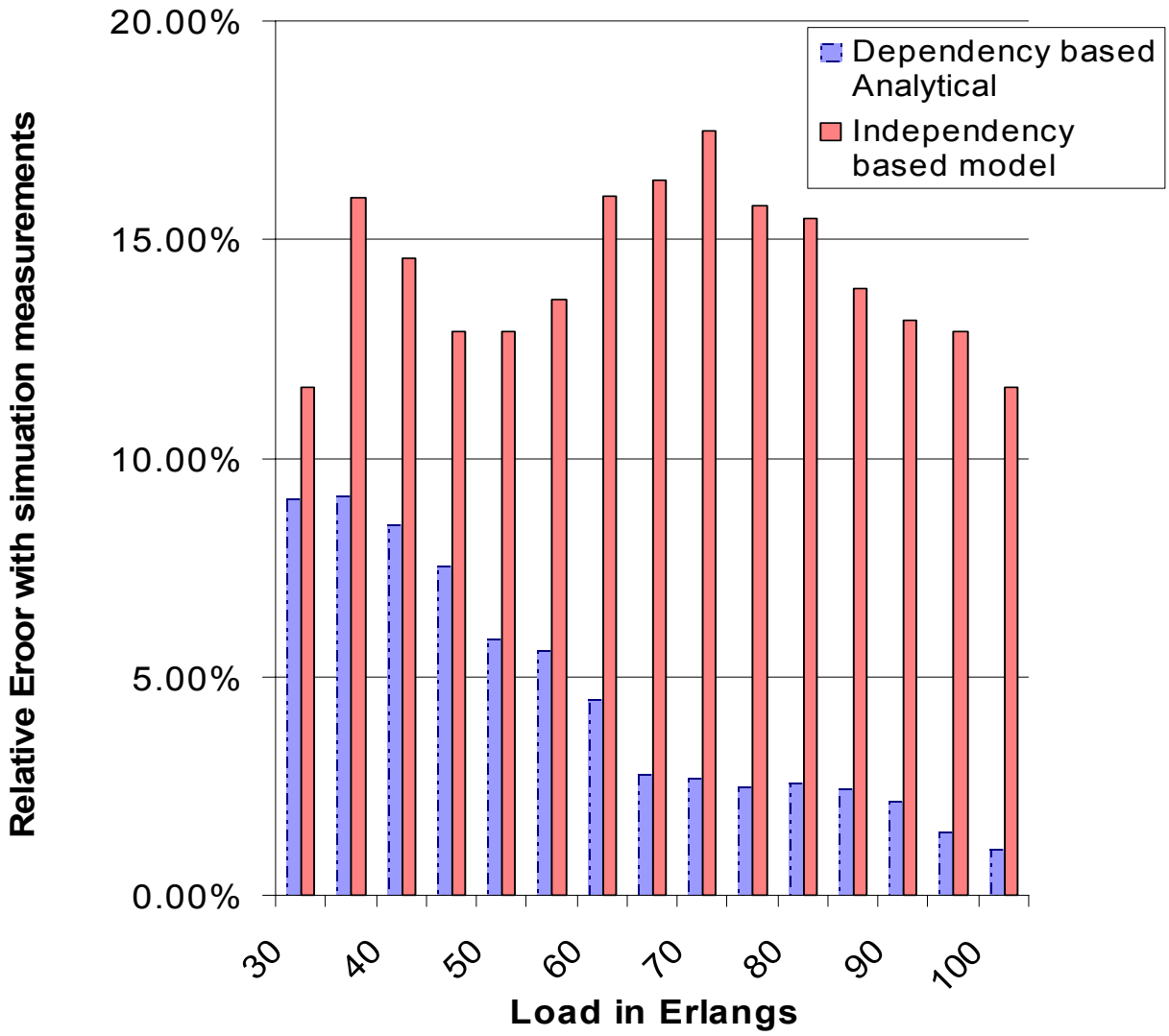


Figure 40: Relative error of Dependency model compared to independence (W=8)

The relative error in Figure 40 is a percentage error based on the absolute value of the difference between the blocking probability obtained by the analytical model and the blocking probability obtained by simulation measurements. We also investigated the accuracy of our model using NSFNET under high loads ranging from 30 to 100 Erlangs. As in the case of low load traffic, the

analytical model gives very accurate estimates of the blocking probabilities under high load traffic.

In the next section, we further extend the validation of our analytical model and explore the effect of the topology, the traffic load, the routing scheme, and the number of wavelengths W.

## 5.4 Analytical Model Applicability and validation

In the following sections, we consider the applicability of our analytical model. We investigate effect of the network topology, the traffic load, the routing scheme and the number of wavelengths per link.

### 5.4.1 Effect of the network topology and traffic load

The U.S Long Haul Network (USLH) [15] has 28 nodes and 45 links (Figure 5). Note that the diameter of USLH has a length of seven links and that of NSFNET (Figure 33) has only 3 links. For USLH, the percentage of paths with number of links equals to 1, 2, 3, 4, 5, 6, and 7 is 12%, 20%, 23%, 21%, 14%, 8%, and 2%, respectively; for NSFNET, the percentage of paths with number of links equals to 1, 2 and 3 is 23%, 40%, and 37%, respectively.

Figure 41 shows the corresponding results for the U.S Long Haul topology under low loads ranging from 0.1 to 12 Erlangs. As in the case of the NSF network, the proposed analytical model with link dependencies gives accurate estimates (for all k-DS sets) of the blocking

probabilities for the U.S. Long Haul network (the results for the U.S Long Haul topology under high loads are omitted).

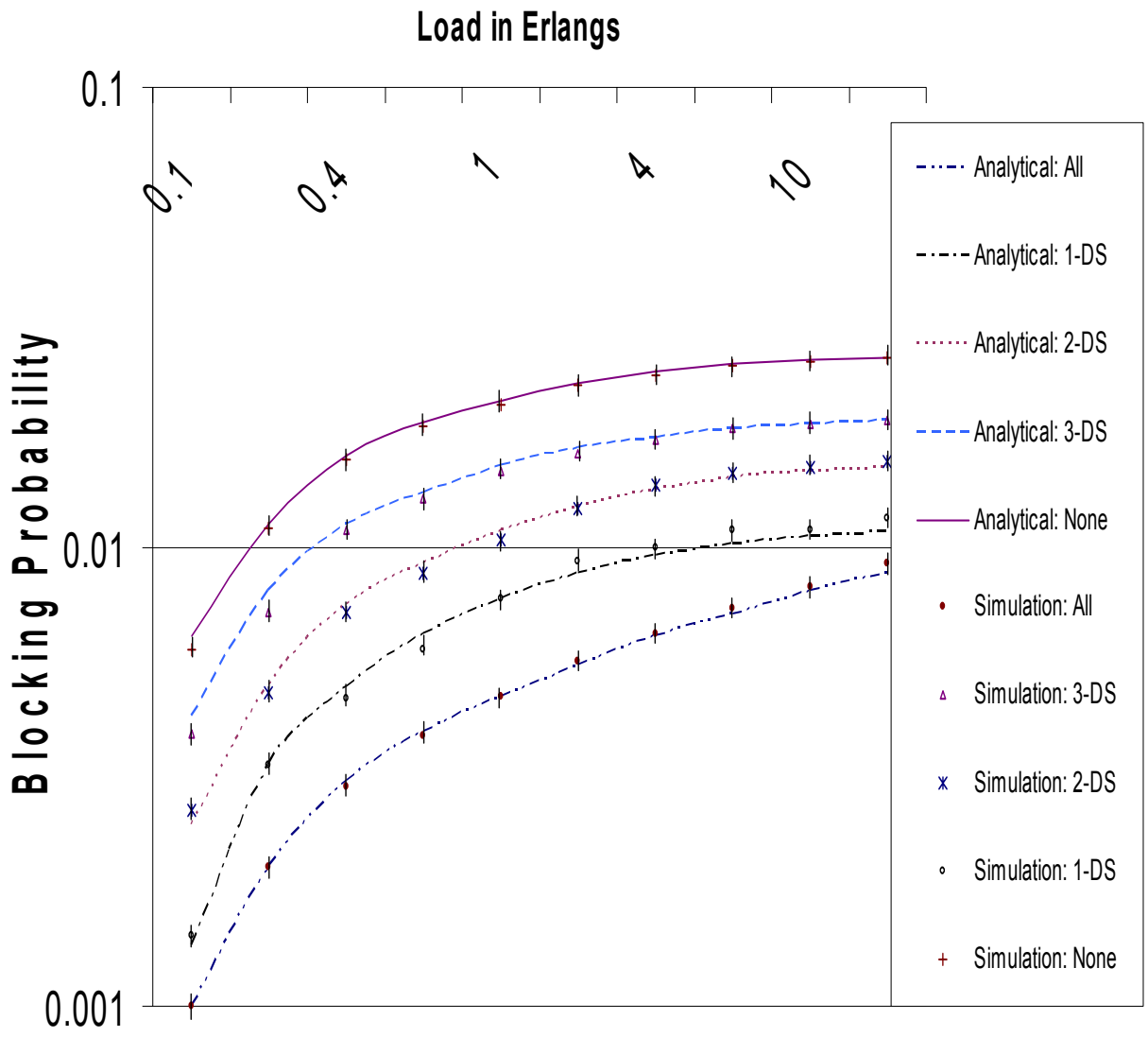


Figure 41: Simulation and model comparison using the U.S Long Haul at low load (W=8)

### 5.4.2 Effect of the routing scheme

To show the applicability of our model under shortest path routing (i.e., only one route is assigned to each source-destination pair), we randomly generated different graphs using Boston University's BRITE tool [MMB00] by keeping the number of links per node ranging between 2 and 7. This topology generator is proven to accurately reflect many aspects of the actual Internet topology (e.g. hierarchical structure, degree distribution, etc.).

The number of nodes in the network, N, is increased by 5 in each iteration and the results of this iteration are obtained using 1000 randomly generated topologies with N nodes. We fixed the load at 50 Erlangs and measured the blocking percentages with $50.10^6$ connections arriving to the network. We plot the average of the measured blocking percentage via simulation and via A-BLOCK overall graphs for a given iteration. Within any iteration, we test five scenarios by placing full wavelength converters in every node of the network, then in the members of the 1-DS, 2-DS and 3-DS sets, then without placing converter in any node.

Figure 42 shows the accuracy of our analytical model using the shortest path routing. Note that as the number of nodes in the graph increases (but the total load is fixed at 50 Erlangs), the network becomes more lightly loaded and the blocking probability decreases. The analytical model successfully captures the blocking performance for graphs with various values of N.

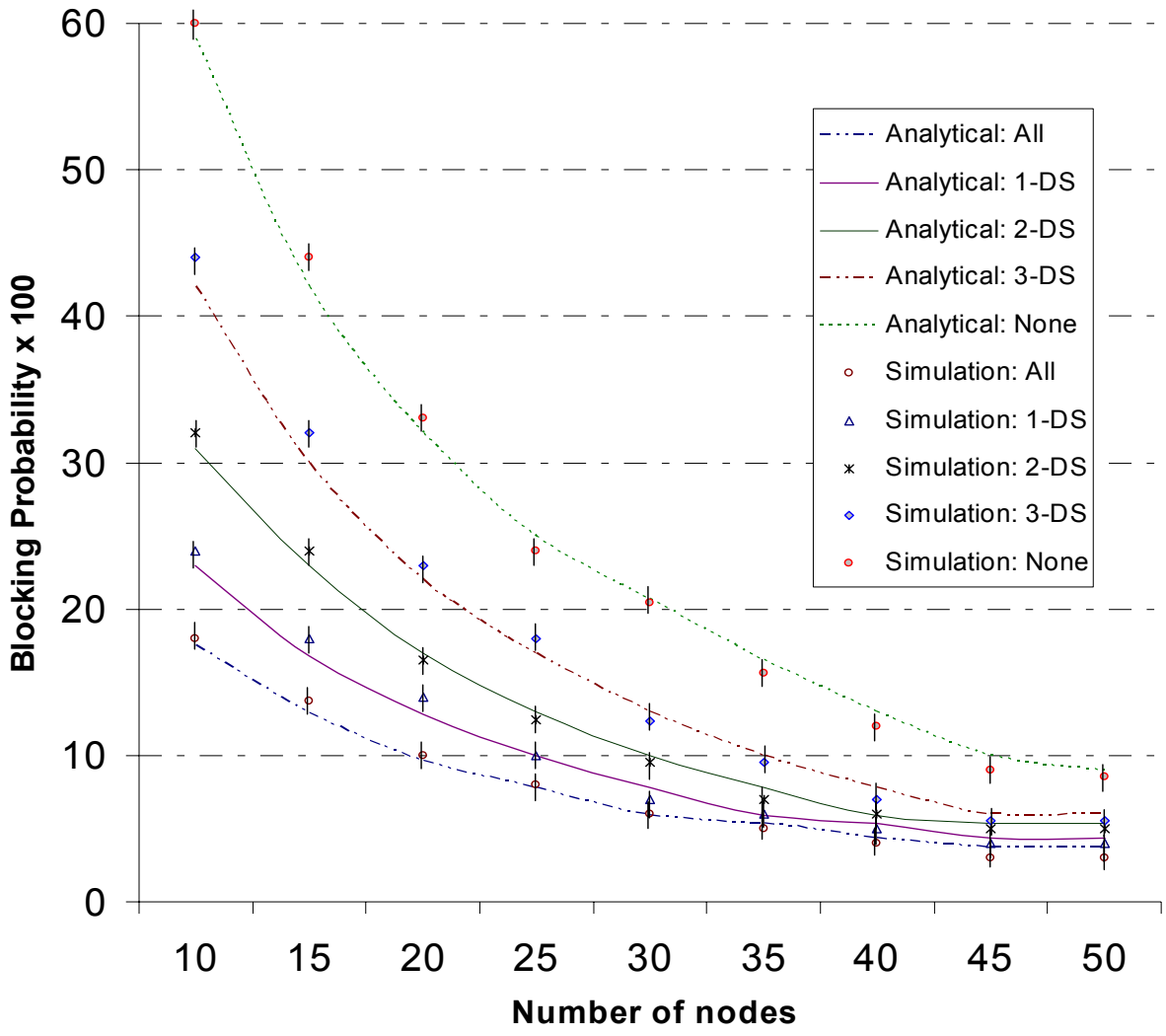


Figure 42: Simulation and model comparison using the randomly generated graphs (W=8)

### 5.4.3 Effect of the number of wavelengths per link

In this section, we study the ring topology (16 nodes) and analyze the effect of W on our model. For W=8, 16 and 32, we measure the blocking probability for light load ranging from 1 to 15 Erlangs. Full wavelength conversion is placed at every other node of the ring. Note that our

analytical model incorporates W in evaluating the arrival rate to any given link i (defined as $\lambda_{in}$). The value of W is also used in evaluating the link dependencies $r_{ij}(n,m)$ as shown earlier in equations (5.3.a, 5.3.b) and (5.4). Figure 43 shows that our correlation-based analytical model is quite accurate for ring topologies under light traffic loads.

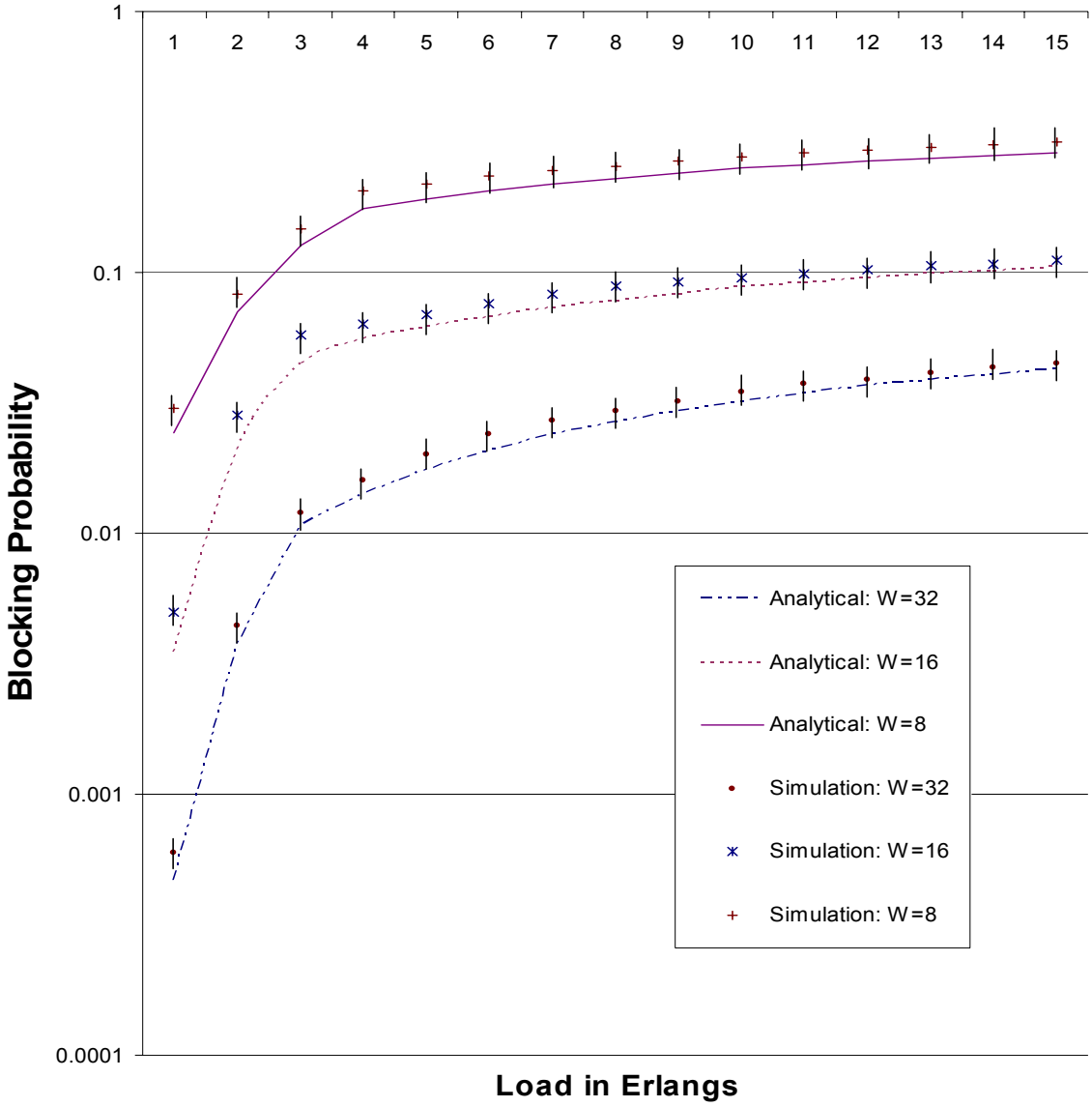


Figure 43: Simulation and analytical model comparison 16-node ring (W=8, 16 and 32)

## 5.5 Conclusions

We presented an analytical model to capture link dependencies and compute the blocking probabilities in all-optical WDM networks. We validated the analytical model via simulation tests using several topologies. The model is generally accurate in capturing link dependencies and estimating the blocking probabilities with and without wavelength converters available in the network. The A-Block algorithm presented in section 5.3 is reasonably fast; it divides longer paths into smaller ones and computes the results iteratively. The algorithm has provided accurate results and reduced the computational overhead of the simulation-based algorithm. Further research is needed to enhance the robustness of the link dependency formula by adapting/extending it to handle special topologies, very low loads, non-uniform traffic [BLO03] or non-random wavelength assignment.

# 6. ALARM BASED ROUTING AND PATH PROTECTION IN SURVIVABLE WAVELENGTH ROUTED ALL-OPTICAL MESH NETWORKS

We present a new Fault Tolerant Path Protection scheme, FTPP, for WDM mesh networks based on the alarming state of network nodes and links. Our extensive simulation results show that FTPP outperforms known path protection schemes in terms of loss of service ratio and network throughput. The simulation tests used a wide range of values for the load intensity, the failure arrival rate and the failure holding time. The effectiveness of our method has been demonstrated by using the US Long Haul and the NSFNET topologies.

We next extend the FTPP scheme to the differentiated services model and evaluate its connection blocking performance. We introduce a QoS-enhanced FTPP (QEFTPP) routing and path protection scheme in WDM networks. QEFTPP uses preemption to minimize the connection blocking percentage for high priority traffic. Extensive simulation results show that QEFTPP can achieve a clear QoS differentiation among the traffic classes and at the same time provide a good overall network performance.

## 6.1 Background

In wavelength routed all optical networks (WRON), there is a need for fault tolerant routing mechanisms to protect network performance against link failures and optical cross-connect (OXC) failures. A wide range of protection and restoration schemes for WDM networks have been investigated in the literature. Some researchers in the area of protection have mainly considered the static model (i.e. offline routing) [ZOM03, RSM03, SSY04, GKS04]. Those

models are reasonable only when connection demands are known in advance. We consider the dynamic routing scenario with random connection arrivals to the network. As in [XCQ04, OZZ03, WLY04, QZM03, GCS03, PHM02], when a new connection request arrives to the network, our scheme establishes the active and the protection resources according to the traffic already present in the network.

In path protection schemes, the backup (protection) route is reserved during the connection setup such that the active path and the protection path are link-disjoint. The authors in [TFP03, EMN02, JFL04, SYR04] consider the single failure case. In reality, multiple failures can occur at the same time due to the nature of fiber bundling or to destructive natural events. Path protection schemes focus on the fact that the active capacity cannot be shared, but the protection capacity can be shared among multiple connections. The first category of solutions is formulated as an integer linear program (ILP) [ZOM03, RSM03, GCM03, EMN02, DSS03, JFL04, WGD02, SRM02]. The complexity of these approaches (when large networks are studied) prompted researchers to consider heuristics for implementing efficient protection schemes [SSY04, GKS04, XCQ04, AKM03, HES04, OZZ03, WMC04, TFP03, QMJ03, GCM03, DSS03, JFL04, WGD02, IAM03, SYR04, CLS02]. We classify path protection heuristics into three main categories:

1. The first category, referred to as Dedicated Path Protection (DPP), is a greedy approach that reserves a link-disjoint protection path. It is also called 1:1 protection [RSM03]. The protection path is not shared with any other working or protection paths. The shortest routes are computed for working and protection paths (cost function for each link is 1).

2. The second category of heuristics, referred to as Disjoint Shared Path Protection (DSPP), selects the active path using a shortest path route. It then selects the protection paths using a shortest path algorithm in which wavelengths already assigned for protection can be used at no cost [RSM03, PHM02]. This means that the protection links are multiplexed among multiple working paths which makes DSPP schemes more capacity efficient than DPP schemes.

3. The third category, referred to as Joint Shared Path Protection (JSPP), is a greedy approach that establishes the active and protection paths jointly. Wavelengths already used for protection paths can be used for new protection paths as long as a single link failure does not entail the activation of more than one protection path on any wavelength on any link. This technique is based on the Shared Risk Link Group (SRLG) Constraint overviewed in [PHM02].

Path protection schemes previously reported in the literature have primarily addressed the computation of protection paths that are link disjoint with active paths under the assumption of a single link failure at a time. These path protection schemes use standard routing cost functions for the selection of active and protection paths. In this dissertation, we present a path protection approach that uses the alarms/alerts gathered by network surveillance modules in selecting the active and protection paths. Below, we briefly discuss the motivation of our alarm-based scheme.

Network service providers have made significant investments in building operational surveillance and trouble management tools. It is expected that next-generation network surveillance tools, alarm-analysis engines and network operations centers will have extensive capabilities not only for early problem detection and the prompt repair of failures but also for building up an overall picture of the operational condition and health of the various network components. The alarm-analysis engines of next-generation networks will have the capability to process unprecedented numbers of alarms, alerts, and warning messages from multitechnology/multivendor software and hardware components and precisely pinpoint the root-cause problems of failures (e.g., fiber cuts, laser failure, high levels of signal cross-talk).

Equally important, these alarm-analysis engines will also be able to proactively analyze impending network issues and identify network elements that can be the source of future problems. Existing network technology, for example, has already produced alarm interface controller modules (e.g., Cisco NM-AIC-64 card) that help in the remote monitoring of network elements & interfaces, thereby permitting the detection and reporting of alarms on building security (e.g., door and window open and close), fire and smoke indication, building environmental state (e.g., temperature and humidity) and utility power readings.

The alarm-based path protection approach presented in this dissertation is based on the idea of modifying the routing and path selection process by taking into consideration the alarms posted for the various links/nodes of the network in order to improve the reliability of the network and reduce service outage.

The remainder of this chapter is organized as follows: Section 6.2 presents our network model and the alarm-based cost function for path protection routing. In section 6.3, we introduce our alarm-based fault tolerant path protection method (FTPP). We use the US Long Haul and the NSFNET topologies to evaluate the performance of FTPP. Section 6.4 extends FTPP with a QoS enhanced path protection (QEFTPP) under different classes of service. Finally, we give concluding remarks in Section 6.5.

## 6.2 Network failure model and cost function

We model a network as a graph G(N,E) of N nodes (OXC's) and E links. Each link is bidirectional and carries W wavelengths (channels). We assume that there is a centralized network management system for detecting node and link failures, for reporting alarms according to the standard ITU X.721 defined in [ITA92, ITB92] and a technique for node recovery from faults. Unlike previous path protection schemes, we utilize the presence of alarms posted for the various links and nodes of the network in guiding the process of selecting active and backup (protection) routes.

We define the "tolerance to failure" function $T_P(t)$ of a path P as the probability that a failure does not occur along the path P before time t (i.e., this path has failure-free operation from time 0 to time t). The functions $T_V(t)$ and $T_L(t)$ are the corresponding "tolerance to failure" probabilities for a single node V and a single link L, respectively. If a path P is composed of M vertices ($V_1$, $V_2$… $V_M$) and M-1 links ($L_1$, $L_2$… $L_{M-1}$) for a connection request between source node $V_1$ and destination node $V_M$, the tolerance to failure function will be:

$$T_P(t) = \prod_{i=1}^{i=M} T_{V_i}(t) \times \prod_{i=1}^{i=M-1} T_{L_i}(t) \qquad (6.1)$$

If we assume that failure interarrival times are exponentially distributed and that the expected failure rate for node V and link L are $\mu_V$ and $\mu_L$, respectively, then we can easily establish that

$$T_P(t) = e^{-\beta t} \text{ and } \beta = \sum_{i=1}^{i=M} \mu_{V_i} + \sum_{i=1}^{i=M-1} \mu_{L_i} \qquad (6.2)$$

For simplicity of illustration and without loss of generality, source node $V_1$ (that initiates the connection establishment) is assumed to be functioning properly and we shall consider the first term $T_{V_1(t)}$ to be equal to 1. Since link $L_i$ connects nodes $V_i$ and $V_{i+1}$, we will denote the product $T_{V_{i+1}}(t) * T_{L_i}(t)$ as the combined node-link "tolerance to failure" function $TC_{L_i}(t)$. We will also combine the sum $\mu_{V_{i+1}} + \mu_{L_i}$ as the combined failure rate $\mu c_{L_i}$.

Equation (6.1) becomes: $$T_P(t) = \prod_{i=1}^{i=M-1} TC_{L_i}(t) \qquad (6.3)$$

And equation (6.2) becomes: $$T_P(t) = e^{-\beta t} \text{ and } \beta = \sum_{i=1}^{i=M-1} \mu c_{L_i} \qquad (6.4)$$

We have chosen the link-node failure rate $\mu c_{Li}$, which combines the expected failure rates of link $L_i$ [$V_i$, $V_{i+1}$] and node $V_{i+1}$, as a major component in the cost function for a given link Li. In our alarm-based scheme, the value of $\mu c_{Li}$ for a link Li will be higher when there are alarms posted against node $V_{i+1}$ and/or link $L_i$. In other words, the value of $\mu c_{Li}$ will increase when the severity and number of alarms posted for node $V_{i+1}$ and/or link $L_i$ increase.

When computing the shortest paths, the path protection schemes described in section 6.1 (DPP, JSPP and DSPP) use a routing cost of 1 for any given link and a cost of zero for any given node. Our FTPP scheme differs from the three path protection schemes in that it uses the alarming state of the links and nodes in computing the routing cost. A weighted routing cost function is used to estimate the cost of link Li as follows:

$$F_c(L_i) = w_1.\mu c_{Li} + w_2.U_W + w_3.U_P \qquad (6.5)$$

Equation 6.5 shows that the routing cost function is a weighted sum of the alarm-based node-link failure rate $\mu c_{Li}$, the number of wavelengths used by active and protection paths in link $L_i$ denoted as $U_W$ and the number of wavelengths reserved for protection in link $L_i$ denoted as $U_P$.

The first term in the right side of equation (6.5) is the most important term and represents the main mechanism to incorporate network alarms into the FTPP path protection scheme. The other two terms can be modified (e.g., the third term $w_3U_p$ can be entirely omitted) without

affecting the alarm-based nature of the scheme. Equation (6.5) is therefore intended to illustrate the basic approach of our scheme; finding an optimal formula of the cost function $F_c(L_i)$ is beyond the scope of this dissertation. In section 6.3, we describe the complete routing algorithm and the weight values $w_1$, $w_2$ and $w_3$.

## 6.3 Cost function Alarm based routing and path protection

Our approach combines the computation of active and backup paths. The protection capacity is shared but we make sure that if two working (active) paths have at least one common link, their protection paths should not use the same wavelength if these protection paths happen to share a common link.

### 6.3.1 Routing Algorithm

The routing cost of a link is computed using equation 6.5 based on the link load and on the alarms associated with that link. For the purpose of illustration in this dissertation, we use three alarm states: No alarm, Minor alarm, and Major alarm. Each link (node) has two counts $A_{MI}$ and $A_{MA}$ that keep track of the number of minor and major alarms that have been posted but not yet cleared for that link (node). The appendix provides the complete list of simulated alarm conditions and their associated probable causes. The alarms severities are defined in ITU X.721 and ITU X.722 standards [ITA92, ITB92].

Our routing and failure handling algorithm is as follow:

*I. Initialization:*

1. No failures in the network: $\mu c_{L_i} = 0$. All alarm counts $A_{MI}$, $A_{MA}$ set to 0.

2. All links have W wavelengths available: $U_W = 0$ and $U_P = 0$

*II. On new alarm event posted for link Li:*

Based on the type of the alarm (minor or major), increment the appropriate alarm counter ($A_{MI}$ or $A_{MA}$) for link $L_i$. In the basic scheme, the new alarms are only recorded in the counters and will therefore affect the routing and path protection of future requests. The new alarms do not cause re-computation of the protection paths of currently active connection. In section 6.4, we present an enhanced version of the scheme that adaptively changes the protection paths of high-priority active connections when new alarms arrive.

*III. On new alarm event posted for node Vi:*

Based on the type of the alarm, increment the appropriate alarm counter for this node.

*IV. On connection Request between source node s and destination d*:

1. Given the alarm counts for all nodes and links in the network, compute:

$$\mu_{V_i} = A_{MI}[V_i] + \alpha * A_{MA}[V_i] \quad (6.6)$$

$$\mu_{L_i} = A_{MI}[L_i] + \beta * A_{MA}[L_i] \quad (6.7)$$

where $\alpha$ and $\beta$ are weights representing the ratio of the loss typically incurred by a major alarm to the loss incurred by a minor alarm for a node and a link, respectively. In our simulation, 5 was the typical value used for $\beta$ while the value of $\alpha$ was made proportional to the degree of node $V_i$.

2. For a link $L_i$ ($V_i$, $V_{i+1}$), compute $\mu c_{Li} = \mu_{Vi+1} + \mu_{Li}$ as the alarm-based expected risk. Given the wavelength usage in all links $L_i$ denoted as $U_W$ (active and protection) and $U_P$ (for protection), compute the link cost function:

$$F_c(L_i) = w_1.\mu c_{Li} + w_2.U_W + w_3.U_P$$

In most of our simulation tests, we used $w_1=w_2=1$ and $w_3=0.2$.

3. Based on the link's cost function, determine a candidate active path (CAP) as the shortest path (i.e., a path that minimizes total cost) between source s and destination d. If there is no feasible shortest path, deny the request and block the connection.

4. Search for a wavelength that is free on all links of the candidate active path CAP (note: we assume wavelength conversion is not available, i.e., the wavelength continuity constraint applies). If there is no free common wavelength on all links of CAP, find the link $L_H$ in CAP with the highest cost, then set $F_c(L_H) = \infty$ to eliminate this link and go to step 3.

5. At this point, we have a viable active path AP (AP=CAP) between source s and destination d and a wavelength, say λa, that is free on all links of the active path AP. To compute the protection path, we first eliminate all links of AP as follows: for all links Li in AP, set $F_c(L_i) = \infty$.

6. Find the set $\Im$ of all active paths that share a link with the new active path AP.

7. Determine a candidate protection path (CPP) as the shortest path between source s and destination d. If there is no feasible shortest path, block the connection request (note: in the basic FTPP scheme, we block a connection if there is no protection path available. In contrast, the extended version of the scheme presented in section 4 allows low priority traffic to be served without having protection path).

8. Find a wavelength, say $\lambda_p$, to be used for CPP such that the following two conditions are satisfied: 1) $\lambda_p$ is not used by any active path that shares a link with CPP and 2) for each active path $P_i \in \Im$, if the protection path for $P_i$ uses wavelength $\lambda_{ip}$ and shares a link with CPP, then $\lambda_p \neq \lambda_{ip}$. If the two conditions are satisfied, we have found the protection path PP=CPP and the protection wavelength $\lambda_p$ for the new connection request. Otherwise, eliminate the link in CPP with the highest cost and go to step 7.

*V. On failure of link L or node V:*

1. Set $\mu_L=\infty$ or $\mu_V=\infty$ and re-compute the combined failure rates affected by $\mu_L$ or $\mu_V$.

2. Find the set $\Im$ of all active paths (connections) affected by the failed link or node.

3. For each active path $P_i \in \Im$, activate the protection path of $P_i$ and switch the connection to it. Compute a new protection path for the switched connection.

*VI. Heuristic for path elimination:*

To reduce the computational overhead of the search process, our simulation used a pruning heuristic to eliminate some paths due to congestion or to the crowdedness of protection paths. This was done by overriding the link cost computed by equation (6.5) and setting it to infinity in the following two cases: 1) when the value of $U_W$ is equal to the total number of wavelengths on the link, i.e., $U_W = W$ and 2) when the link suffers from crowdedness of protection paths as detected by the condition $U_P > 0.5.W$.

Unlike single failure models [TFP03, EMN02, JFL04, SYR04], our simulation model allows the occurrence of multiple failures (thus both the active and backup paths of a connection could be affected by failures, causing the connection to be disconnected). The alarm events are generated randomly. Each event, relevant to a node or a link in the network, increments the corresponding alarm counter of that link or node. This in turn increments the expected failure rates given by equation (6.6) and (6.7). An alarm of type Minor can escalate to a Major alarm as shown in Figure 44.

Note that a given link or node in the network can have multiple alarms. For example, two different Minor alarms could be posted for the same link (i.e., $A_{MI}$ =2 for that link) and each alarm could escalate independently or could get cleared based on the probabilistic model of Figure 44. When all existing alarms for a link are cleared ($A_{MI}$ =$A_{MA}$ =0), the transition from state "Cleared" to "No Alarm" takes place. If a Major alarm escalates to actual failure, all connections using this link should be switched to their protection paths and new protection paths are computed for the switched connections.

The probabilistic model we used in our tests was as follows: a Minor alarm could escalate to a Major alarm with probability 0.4 or could ultimately get cleared with probability 0.6. Similarly, a Major alarm could ultimately cause failure with probability 0.4 or could get cleared with probability 0.6. At the "No Alarm" state, 50% of the failures occur (suddenly) with no prior alarms and the other 50% occur after an alarm escalation process. Also 50% of the Major alarms occur (suddenly) without prior Minor alarms and the remaining 50% are escalations from Minor alarms.

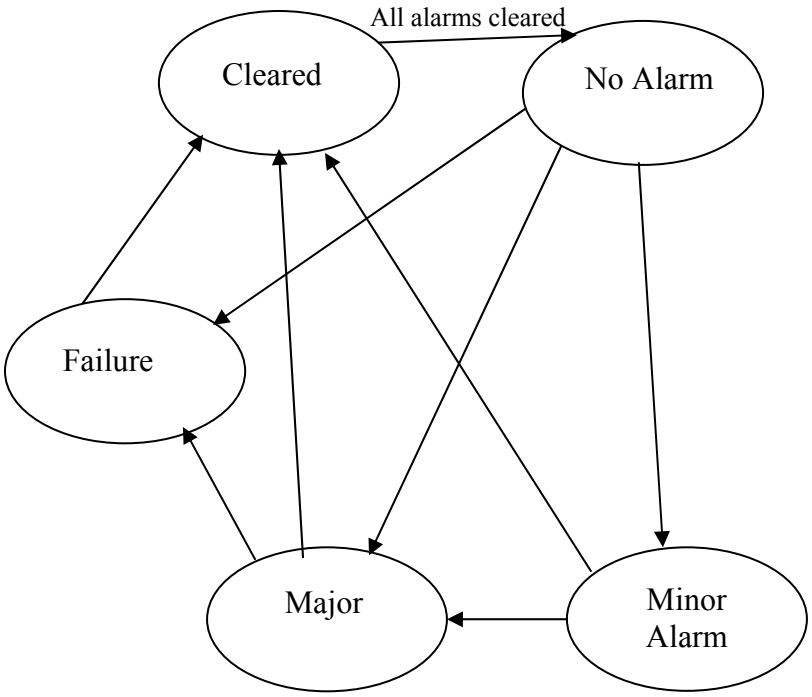


Figure 44: Alarm event generation and alarm escalation

### 6.3.2 Simulation and Results

We investigate the effectiveness of the four path protection schemes: Dedicated Path Protection (DPP), Disjoint Shared Path Protection (DSPP), Joint Shared Path Protection (JSPP) and our FTPP (alarm-based Fault Tolerant Path Protection). In this section, we assume that all connection requests are of the same type (no classes of traffic). Our results are based on two popular topologies: NSFNET topology for the NSF backbone of 16 nodes and 25 links [BLJ04] and USLH topology for the U.S Long Haul Network of 28 nodes and 45 links [BLJ03]. All simulation results in this dissertation are given with 95% confidence intervals using the batch means method with 50 batches.

We use the following notations:

1. $N_T$: The total number of connection requests. $N_T$ is $10^6$ throughout our simulation tests.

2. $N_A$: The number of accepted requests (successfully established paths).

3. $N_F$: The number of working paths that experienced failures.

4. $N_P$: The number of working paths that switched successfully to their protection paths.

We focus on the following performance metrics:

1. Loss of Service Ratio (LSR) defined as the percentage of connections that got disconnected out of all established connections. $LSR = \frac{N_F - N_P}{N_A}$.

2. Connection Blocking-Disconnection Percentage (CBDP) defined as the percentage of all blocked connection requests or disconnected connections out of all connection requests arriving to the network. $CBDP = \frac{(N_T - N_A) + (N_F - N_P)}{N_T}$.

3. Connection Blocking Percentage (CBP) defined as the percentage of all blocked connection requests out of all connection requests arriving to the network. $CBP = 1 - \frac{N_A}{N_T}$. This metric is considered in section 4 for our QoS enhancements.

We compare all four Path Protection schemes (DPP, DSPP, JSPP and FTPP) via extensive simulation tests using the NSFNET and US Long Haul topologies. We assume that the traffic is uniformly distributed between all node pairs. The connection requests arrive as a Poisson process with an arrival rate $\lambda_c$. The connection duration is exponentially distributed with a mean of $1/\mu_c$.

We explore each performance metric based on the following parameters:

1. Load intensity defined as: $\frac{\lambda_c / \mu_c \times P_a}{2 \times L \times W}$, Pa is the average path length in the network, L is the total number of links and W is the number of wavelengths per link (W=16).

   This metric is a normalized value of the offered load intensity based on the network capacity 2.L.W. Within a unit of time, there will be on the average λc connection requests, each has a duration of $1/\mu_c$ and uses $P_a$ links.

2. Connection and Failure Arrival Rate Ratio (CFARR) defined as: $\frac{\lambda_c}{\lambda_F}$, where $\lambda_c$ is the connections arrival rate and $\lambda_F$ is the link failure arrival rate.

3. Failure and Connection Holding Time Ratio (FCHTR) defined as: $\frac{\mu_c}{\mu_F}$, where $1/\mu_c$ is the mean holding time of a connection request and $1/\mu_F$ is the mean duration of a failure (until it is repaired).

In Figure 45 and Figure 46, we present LSR as a function of the load intensity for the US Long Haul and the NSFNET topologies. We fixed the value of CFARR and FCHTR to 0.8. We can see that FTPP outperforms all three path protection schemes (DPP, JSPP and DSPP) especially when the load intensity is high. Under low loads (less than 0.3 for US Long Haul and 0.2 for NSFNET), DSPP experienced the highest Loss of Service ratio. Otherwise, DPP has the worst performance of all schemes.

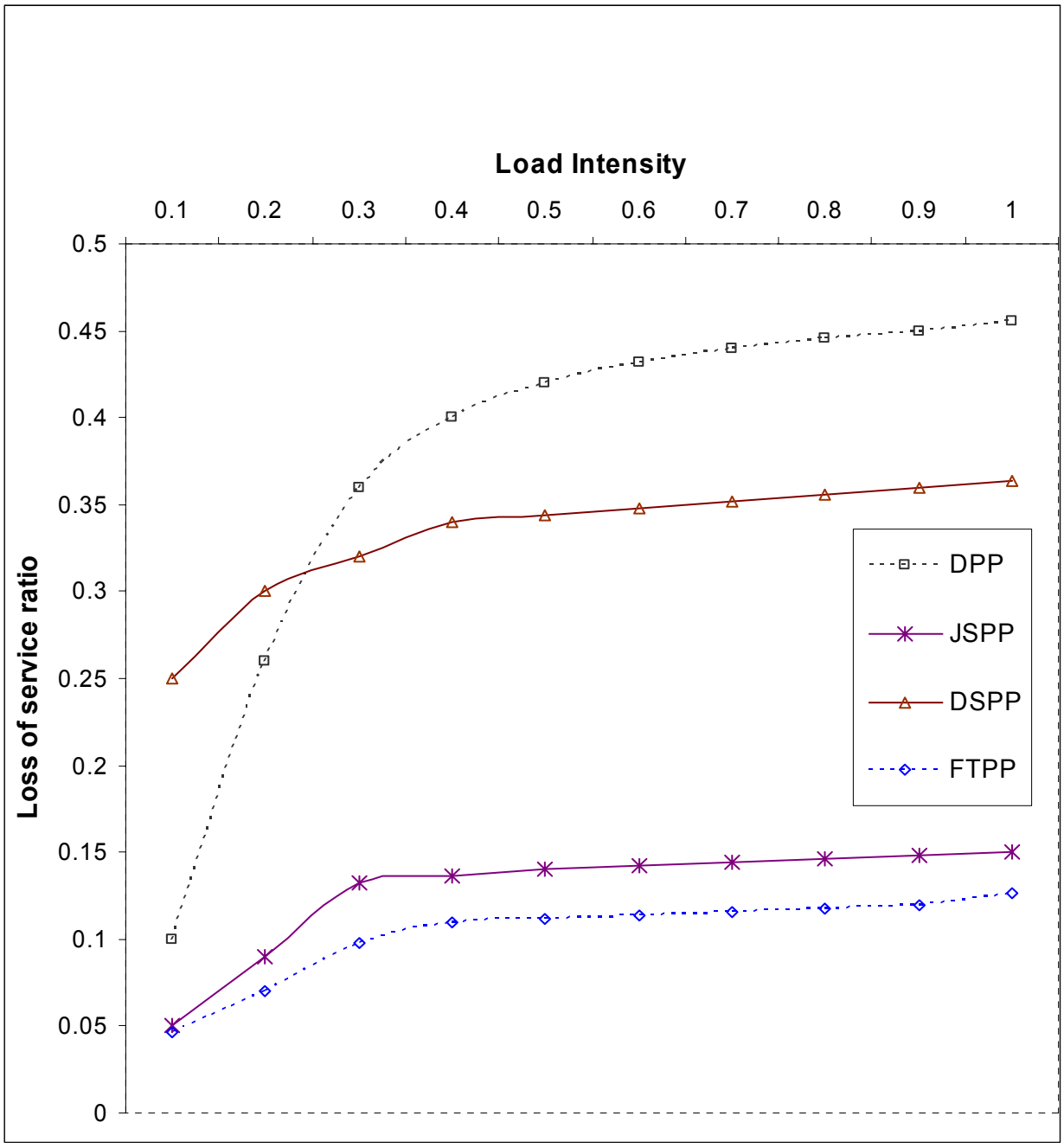


Figure 45: LSR versus Load for USLH

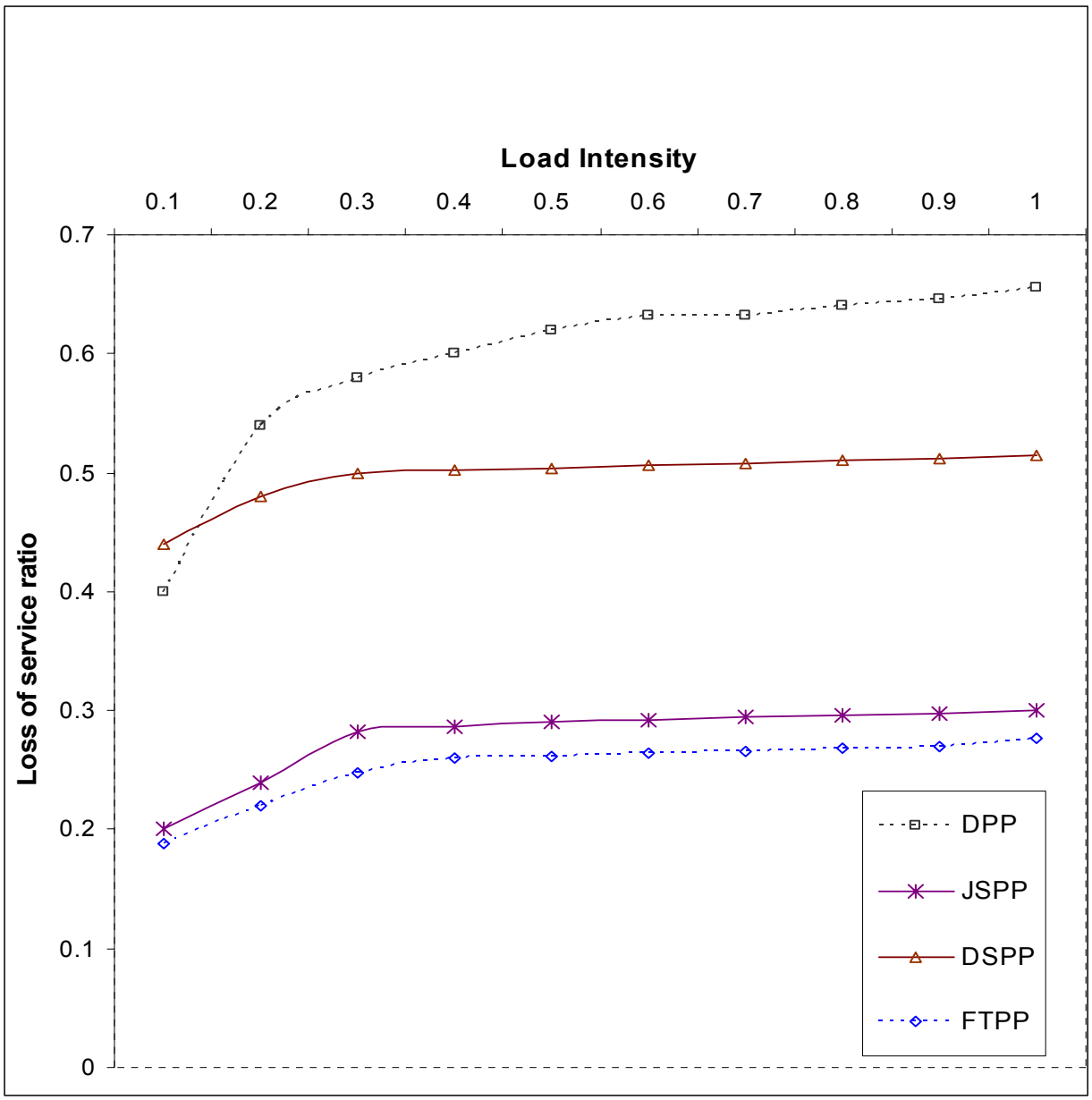


Figure 46: LSR versus load for NSFNET

It should be noted that because the US Long Haul topology has higher node degree and more links than the NSFNET topology, it has more working and protection paths available. This explains why NSFNET has higher LSR values than US Long Haul.

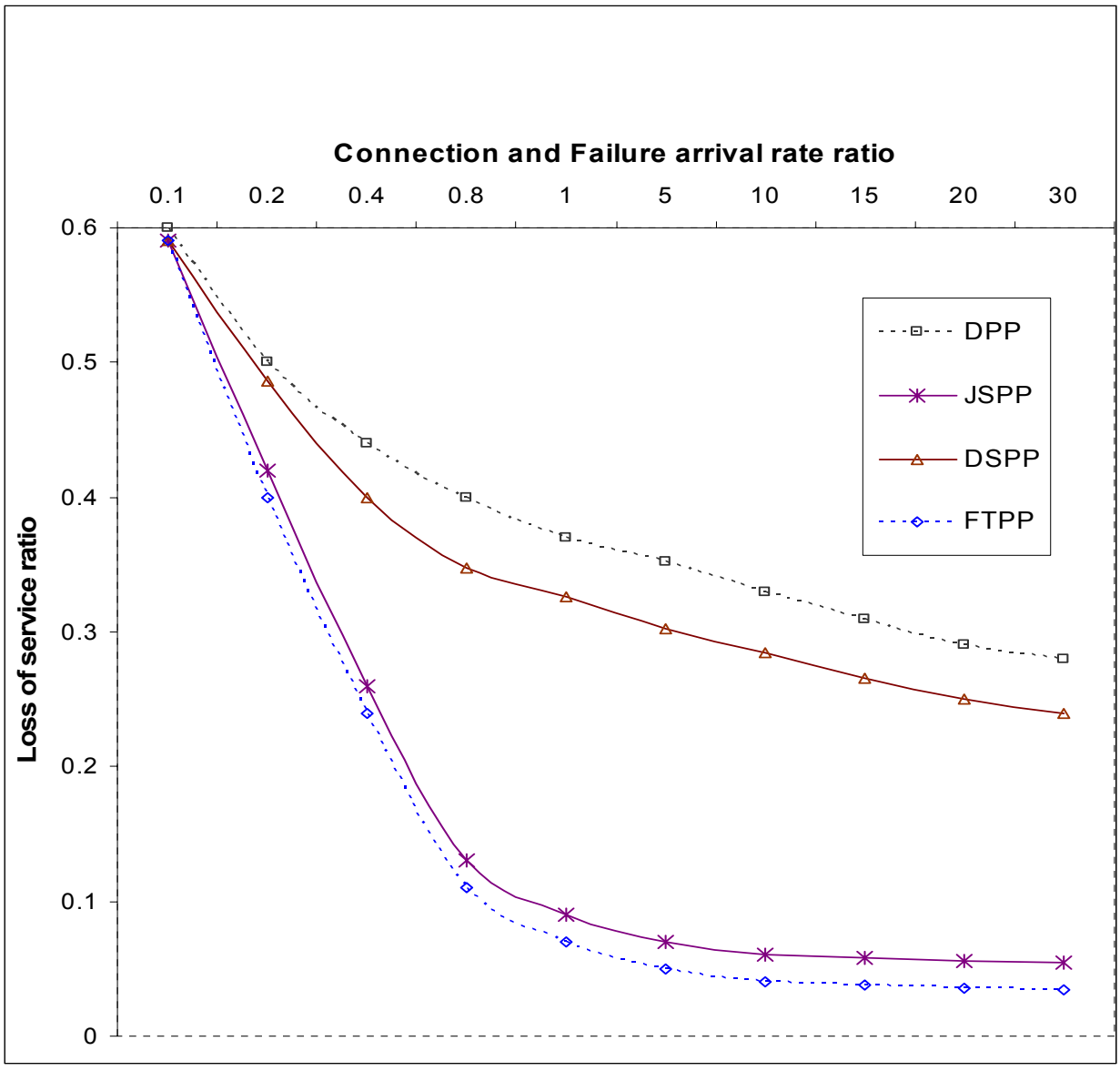


Figure 47: LSR versus CFARR for US Long Haul

In Figure 47 and Figure 48, we present LSR as a function of CFARR for the US Long Haul and the NSFNET topologies. We fixed the load intensity to 0.4 and FCHTR to 0.8. We can see that FTPP outperforms all other path protection schemes. Under high failure arrival rates (i.e. small

CFARR values), FTPP and JSPP have comparable performance. When the failure arrival rate decreases, DSPP improves faster than DPP (but much slower than FTPP and JSPP). DPP is the least capacity efficient scheme which is more evident in the NSFNET topology. FTPP achieves the lowest loss of service under moderate and low failure arrival rates especially compared to DPP and DSPP.

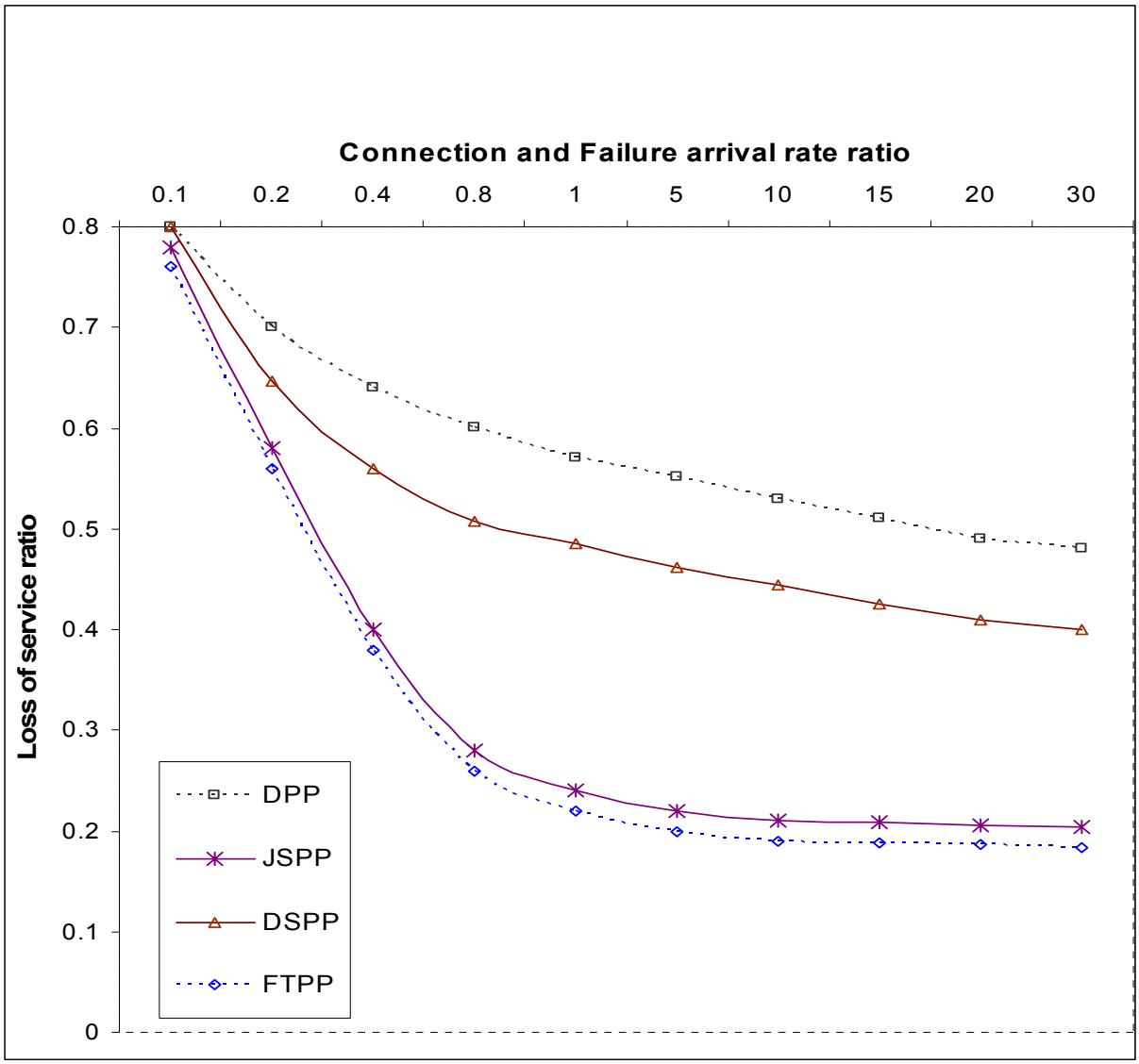


Figure 48: LSR versus CFARR for NSFNET

In Figure 49 and Figure 50, we plot LSR as a function of FCHTR for the US Long Haul and the NSFNET topologies. We fixed the value of the load intensity to 0.4 and CFARR to 0.8. Again, FTPP outperforms all other three path protection schemes. FTPP is better able to handle multiple failures and maintains the best protection efficiency. Under high failure holding time (large FCHTR values), FTPP and JSPP achieve a low loss of service compared to DPP and DSPP. The loss of service ratio decreases for all four schemes when the value of FCHTR decreases: LSR decreases slowly under both DPP due its capacity inefficient nature and DSPP due to the full sharing of protection wavelengths that makes DSPP less tolerant to multiple failures.

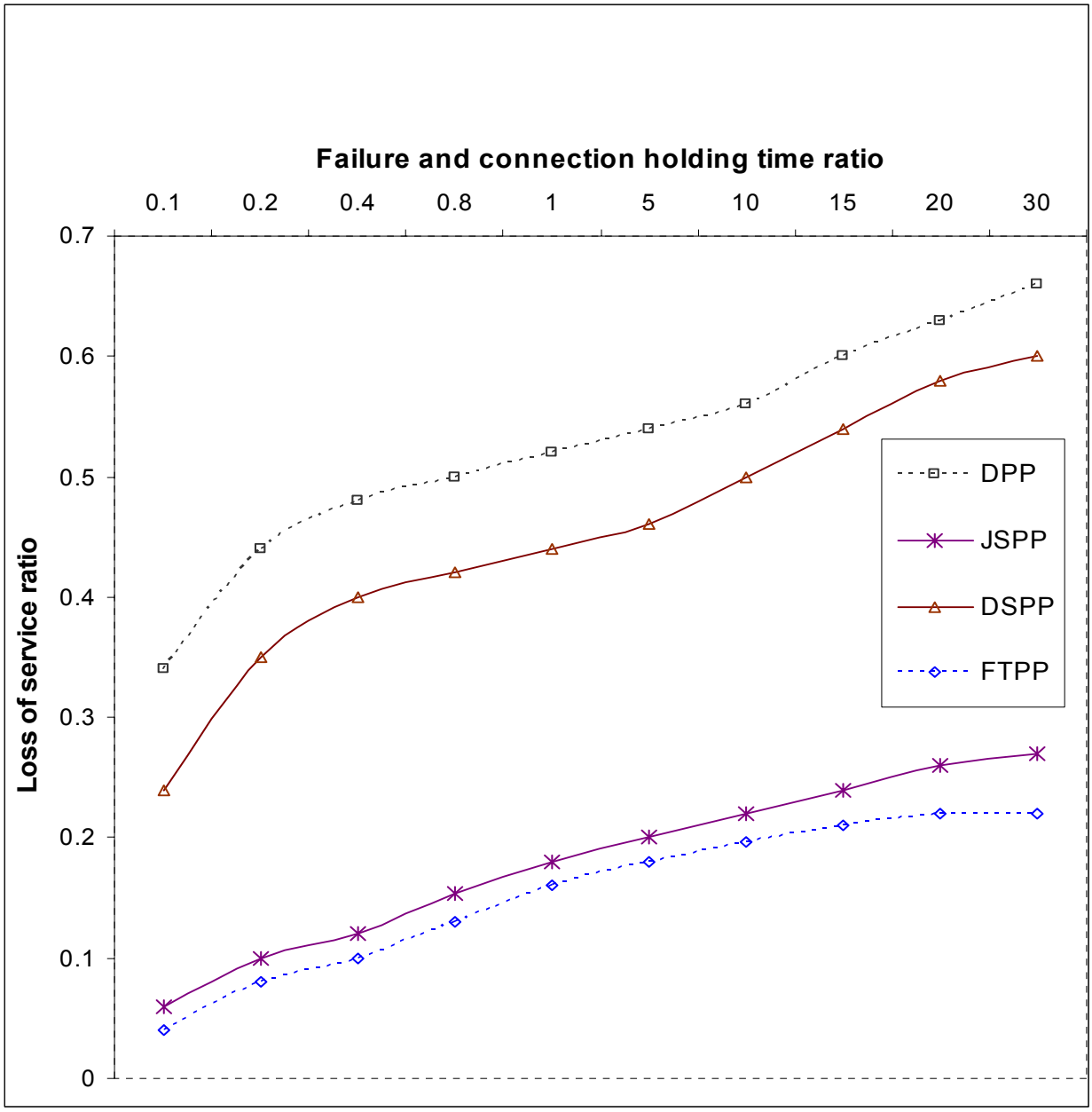


Figure 49: LSR versus FCHTR for USLH

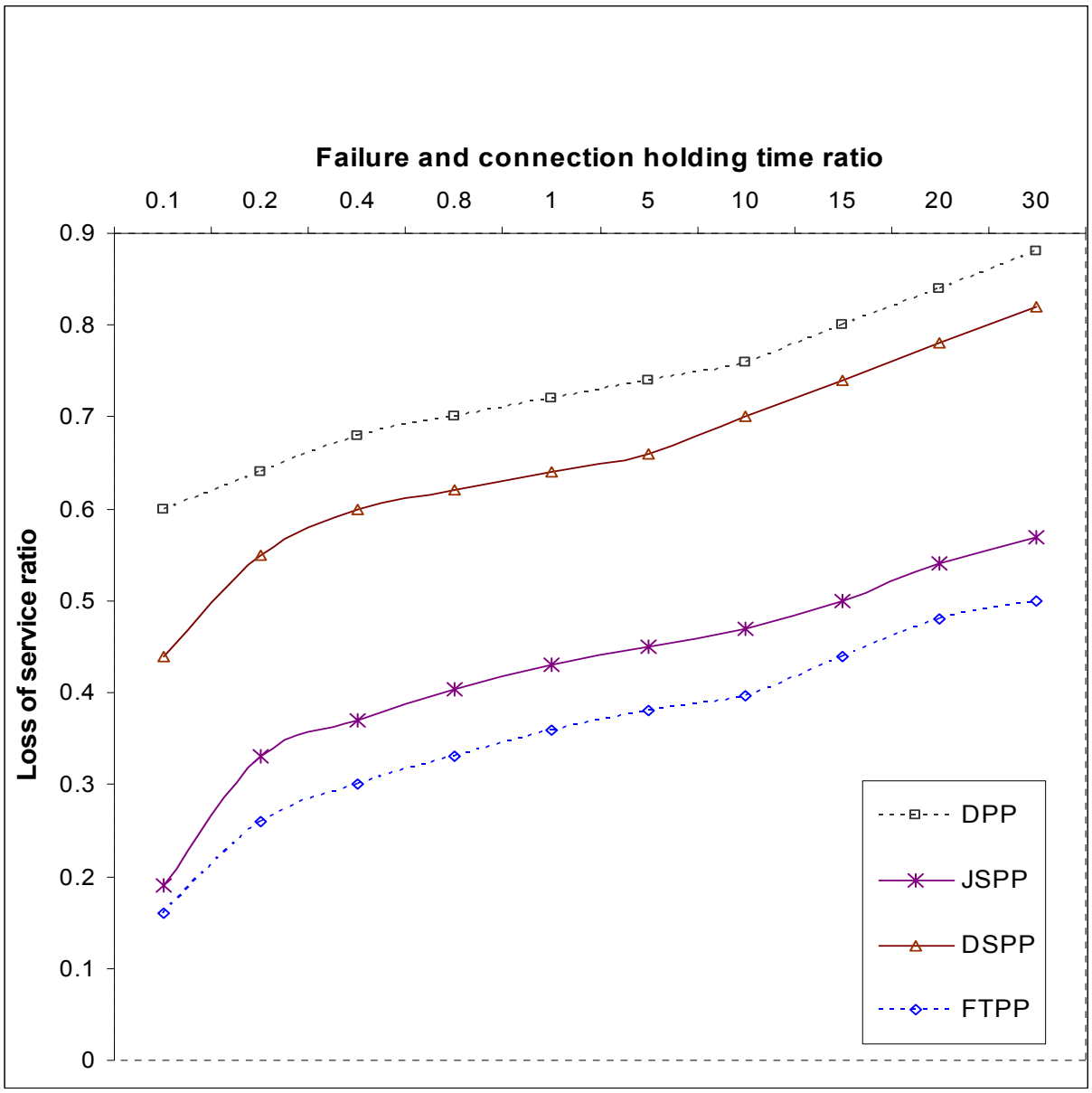


Figure 50: LSR versus FCHTR for NSFNET

Next, we investigate the connection blocking and disconnection percentage (CBDP). In Figure 51 and Figure 52 we plot CBDP as a function of the load intensity for the US Long Haul and the NSFNET topologies. We fixed CFARR and FCHTR to 0.8. We see that FTPP achieves the

lowest CBDP (corresponding to highest network throughput) for both topologies and under both low and high loads.

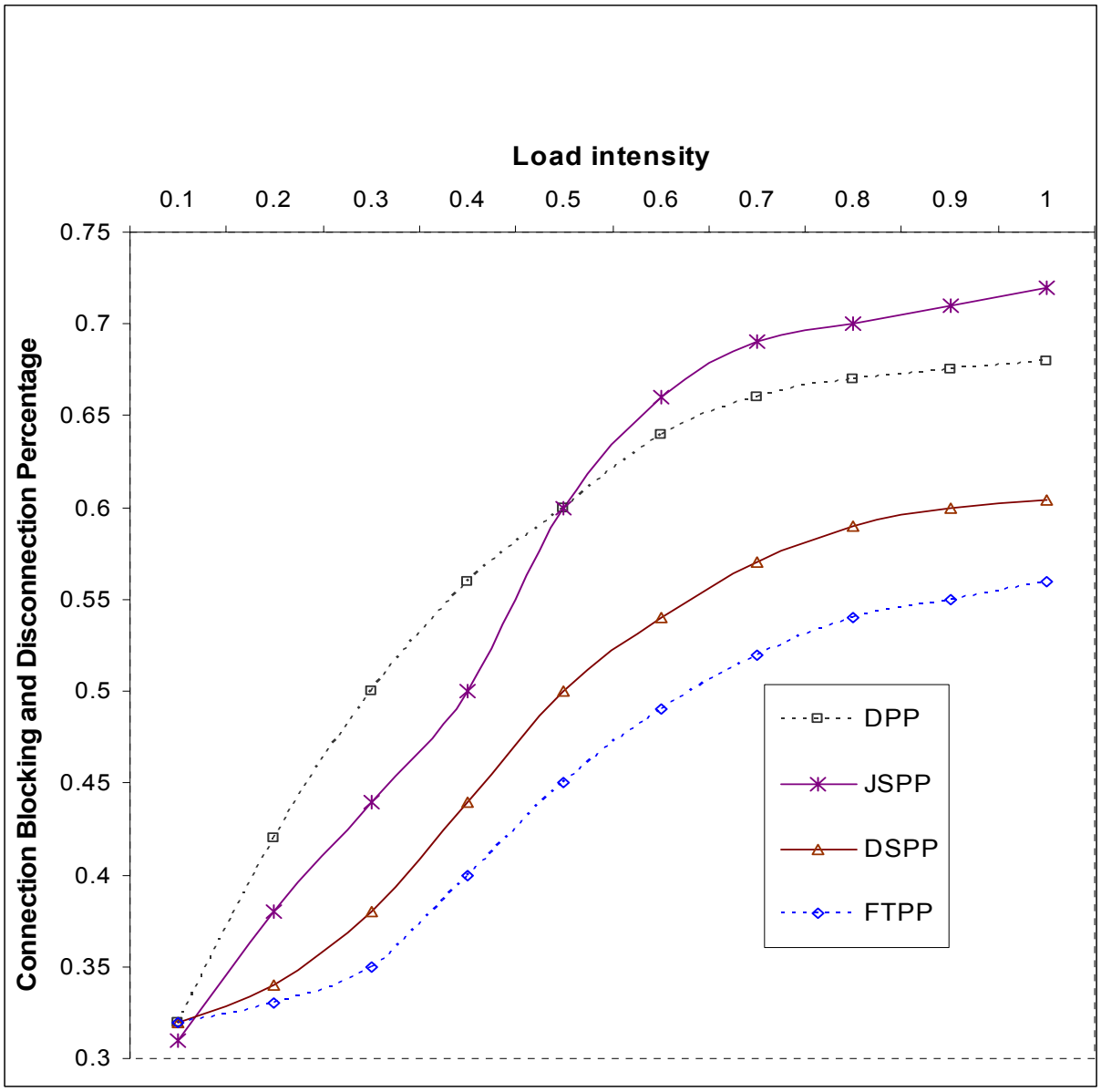


Figure 51: CBDP versus load for USLH

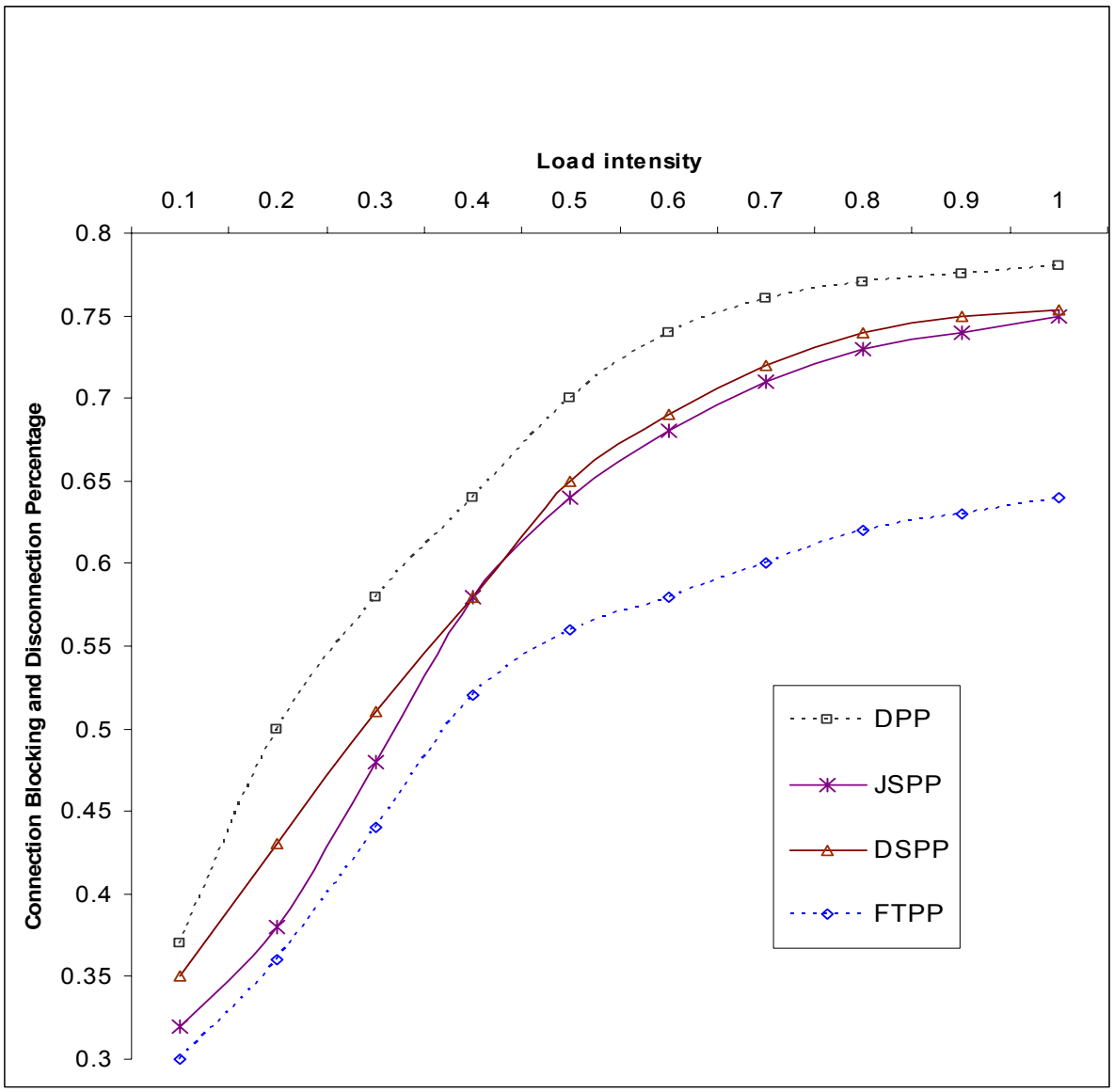


Figure 52: CBDP versus load for NSFNET

In Figure 53 and Figure 54, we present CBDP as a function of CFARR for the US Long Haul and the NSFNET topologies. We fixed the load intensity to 0.4 and FCHTR to 0.8. We can see that under both low and high failure arrival rates, FTPP outperforms all of the considered path protection schemes.

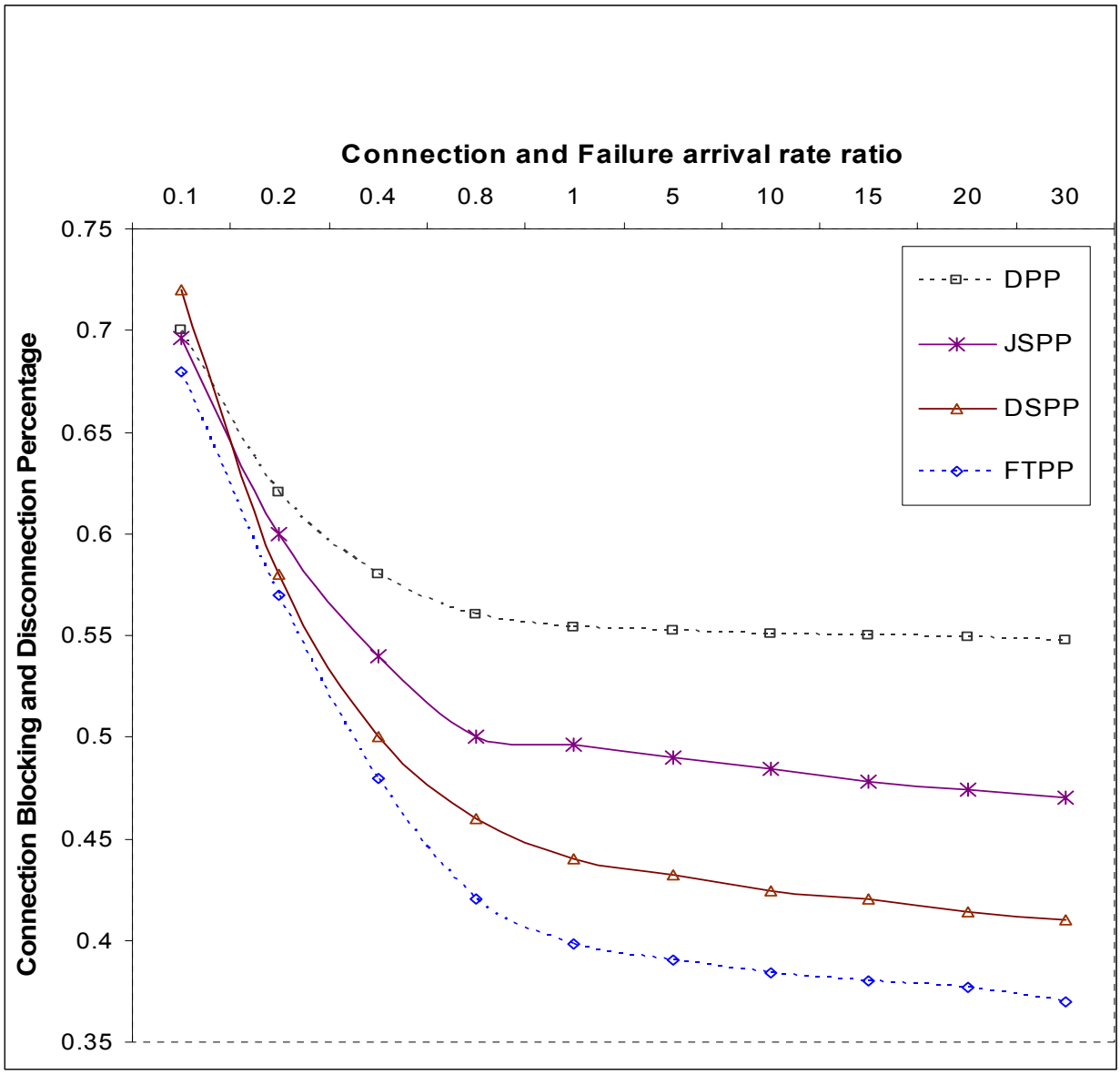


Figure 53: CBDP versus CFARR for USLH

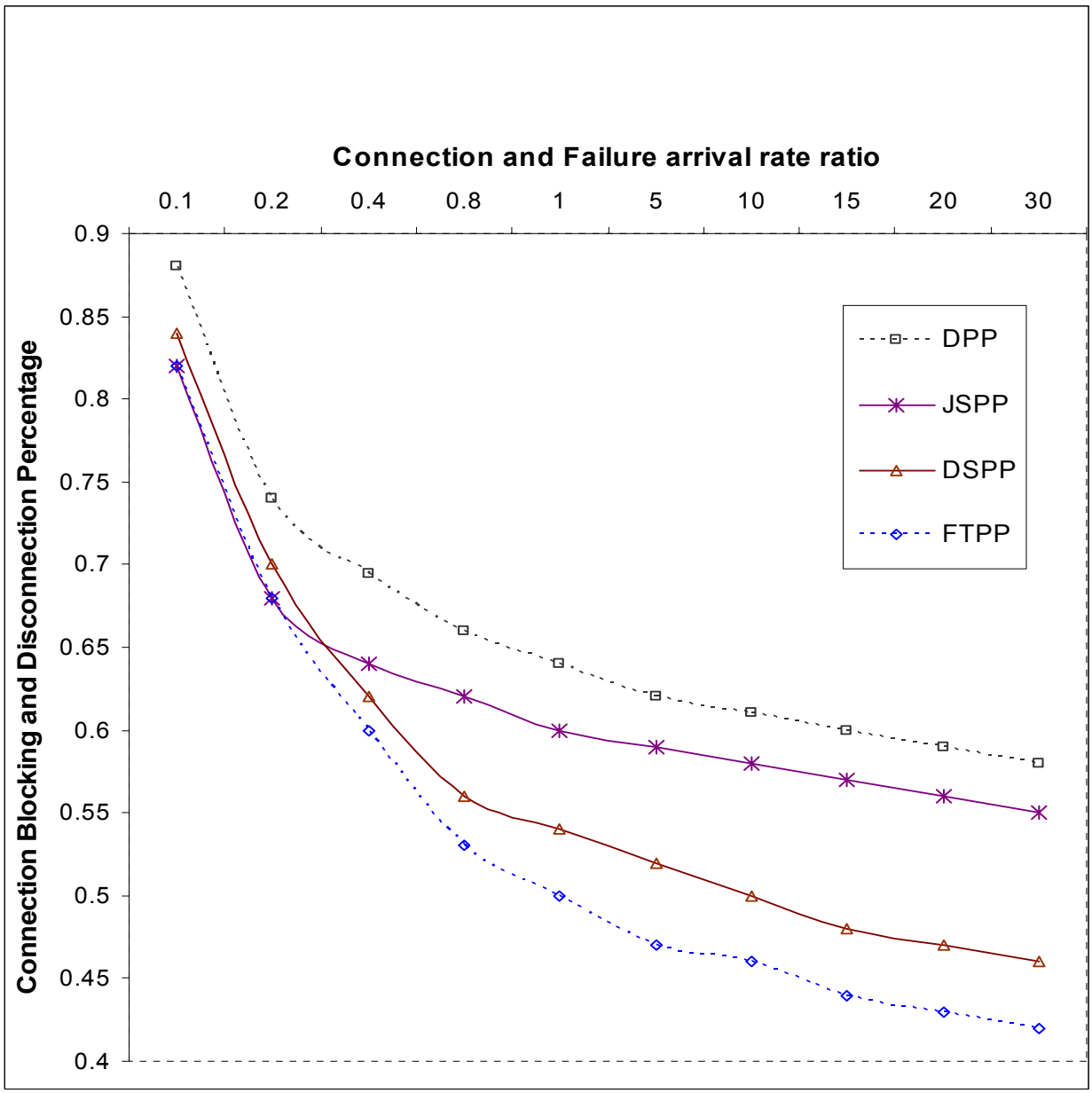


Figure 54: CBDP versus CFARR for NSFNET

In Figure 55 and Figure 56, we plot CBDP as a function of FCHTR for the US Long Haul and the NSFNET topologies. We fixed the load intensity to 0.4 and CFARR to 0.8. Again, FTPP outperforms all of the other schemes under low and high failure holding times.

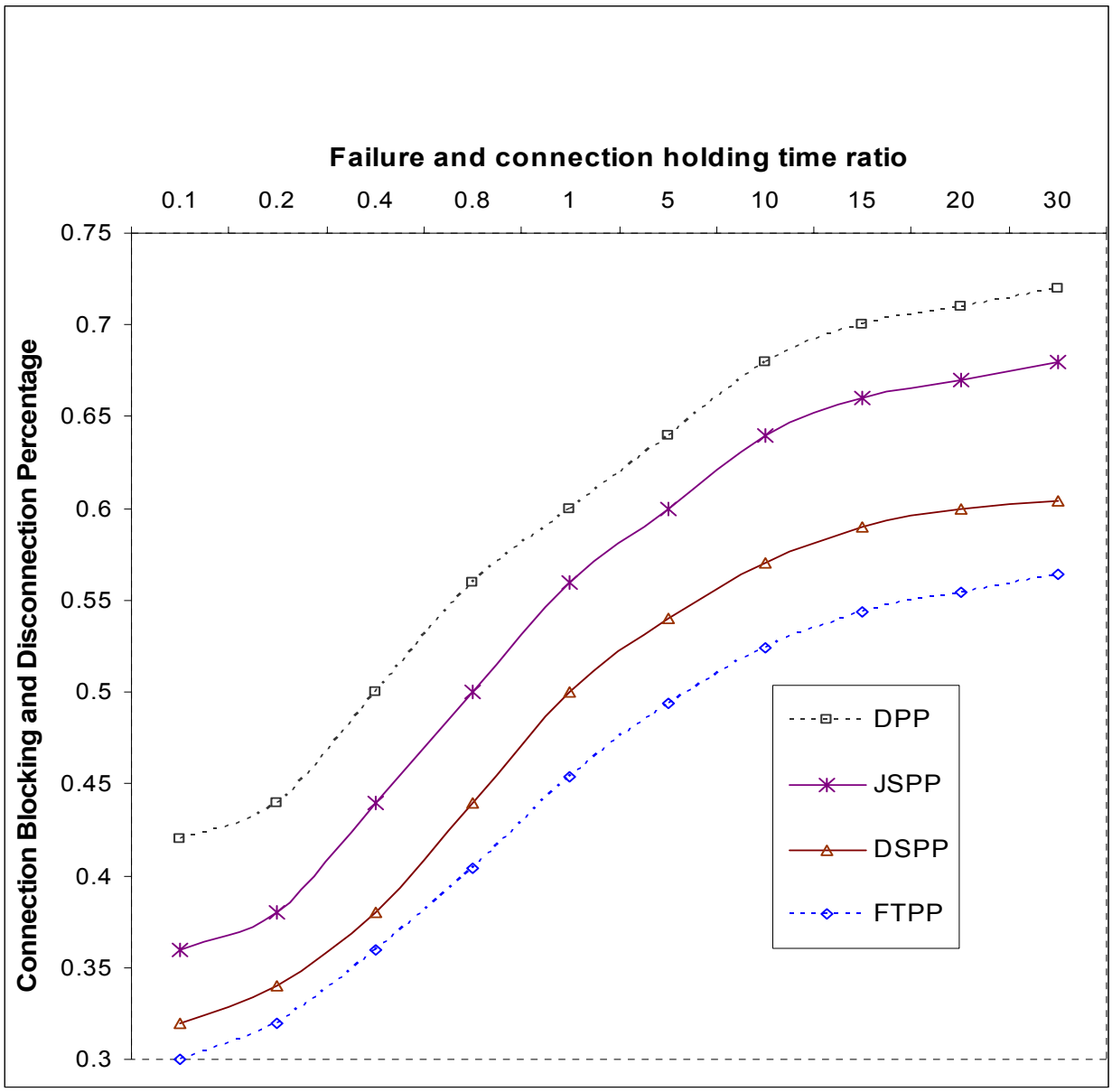


Figure 55: CBP versus FCHTR for USLH

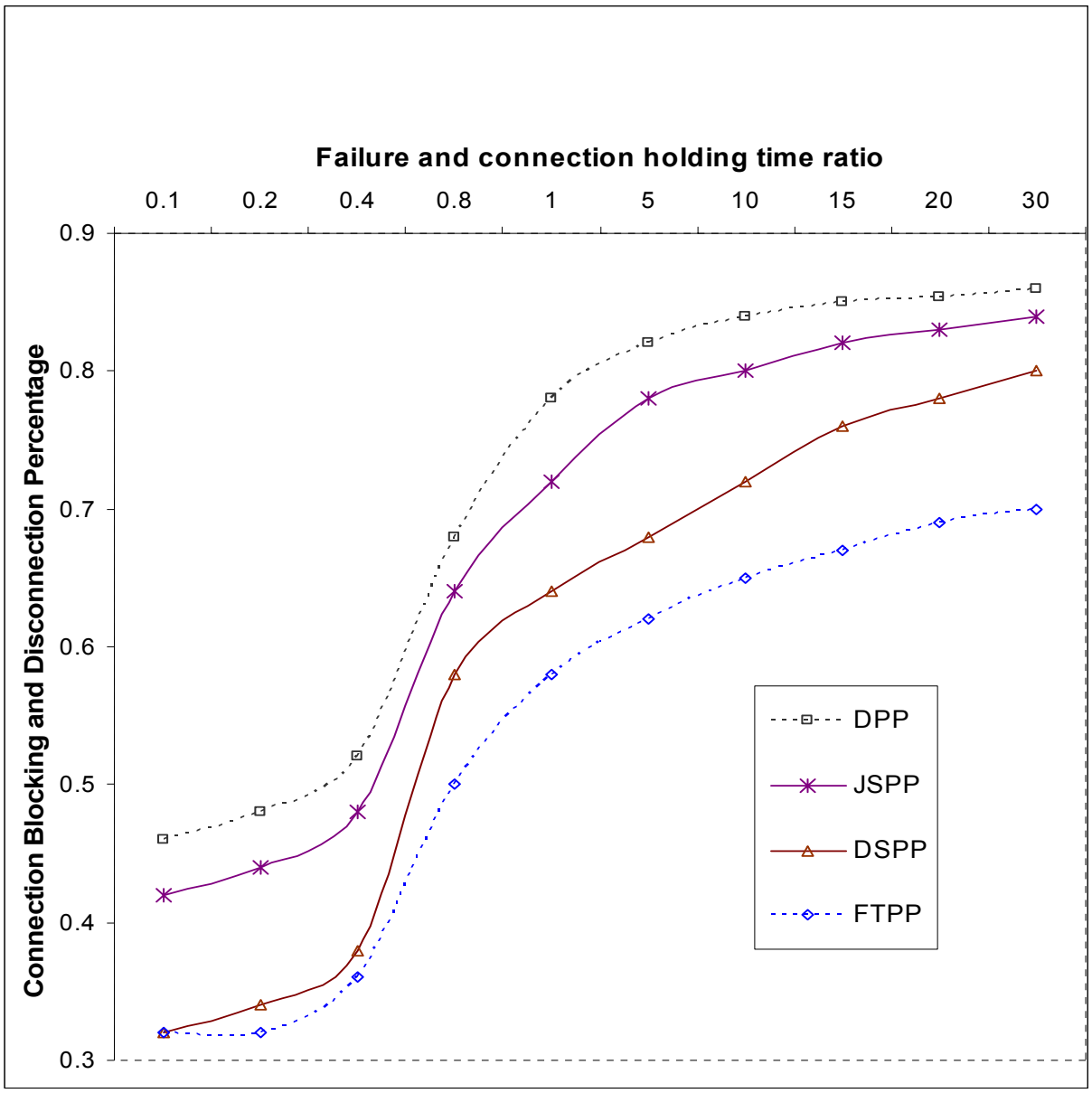


Figure 56: CBP versus FCHTR for NSFNET

## 6.4 Enhanced FTTP for QoS alarm based routing and path protection

In this section, we present Our QoS enhanced FTPP (QEFTPP) scheme that uses a class based connection admission policy and path protection with priority. We define four classes of connections in ascending order of priority:

1. Preempted with no protection (PNP): at any time even after a successful setup, this type of connections can be pre-empted by higher priority connections for their active and backup paths. There is no path protection available for PNP connections and any failure will cause the connection to be lost.

2. Preempted with shared protection (PSP): This type of connections can be pre-empted by higher priority connections but it has a protection path fully shared with other protection paths.

3. Non-preempted with shared protection (NPSP): These connections are never pre-empted and after a successful setup they can get disconnected only in the case of failures that affect both the active and protection paths.

4. Non-preempted with guaranteed protection (NPGP). These connections have the highest priority. The protection path of NPGP connection can change as a result of newly posted link/node alarms.

For example, we may allow a given connection $C_1$ of class PNP to use some or all the backup links of an active connection $C_2$. The connection $C_1$ can be preempted and disconnected when:

(1) A failure occurs in the active path of $C_2$ that requires switching it to the backup links used by $C_1$.

or

(2) No active path can be found for a new connection $C_3$ of class NPGP or NPSP.

In the following section, we will evaluate the admission control policy of QEFTPP compared to FTPP and DSPP via simulation using the US Long Haul and NSFNET topologies.

Next, we show the benefits of QEFTPP supporting all 4 classes of traffic. The considered performance metric is the Connection Blocking Percentage (CBP) as a function of the load intensity and the number of wavelengths W.

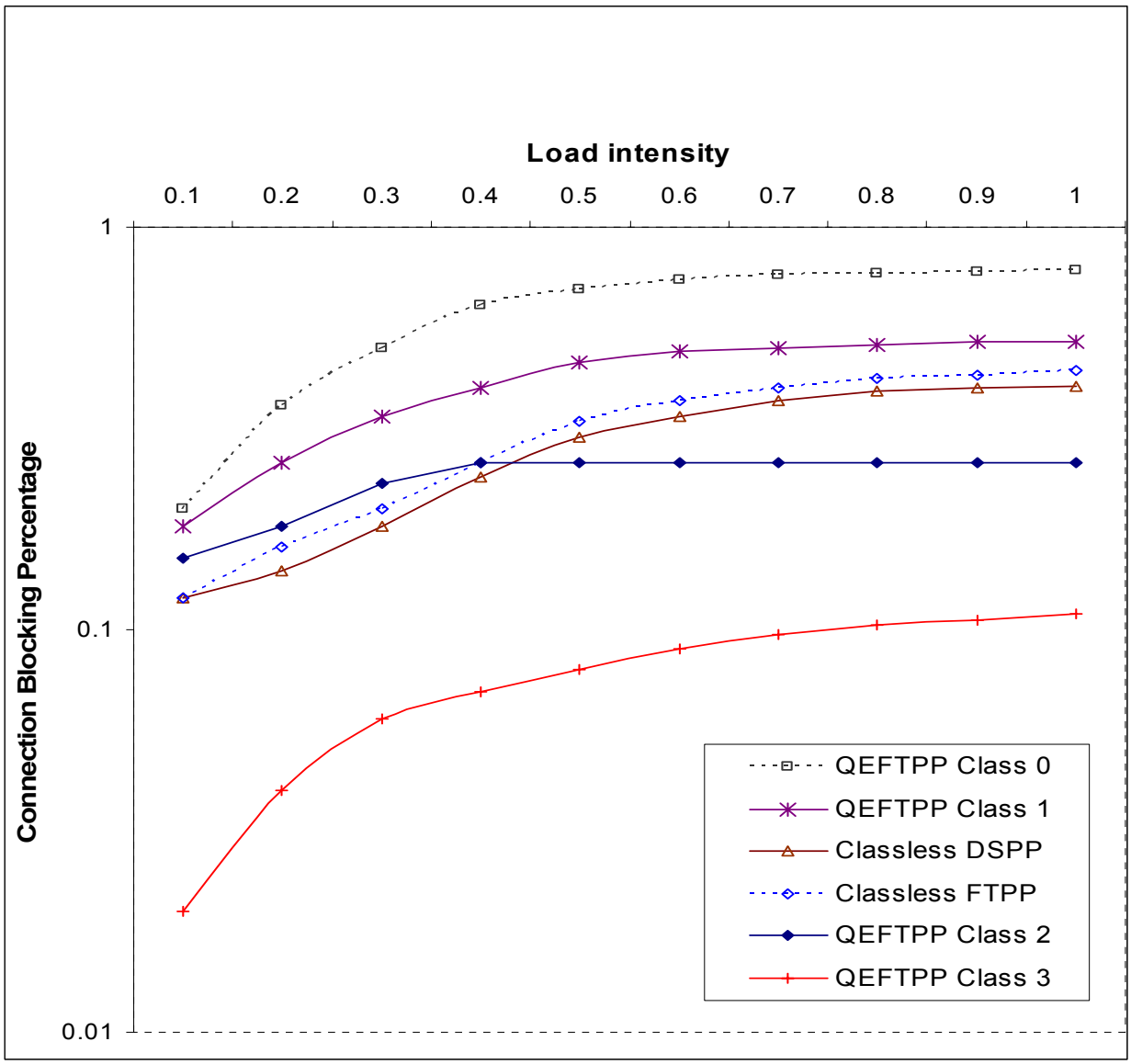


Figure 57: CBP versus load (USLH W=16)

In Figure 57 and Figure 58, we show the relationship between CBP and the load intensity ranging from 0.1 to 1 for the US Long Haul topology. We measured the experienced CBP for classless FTPP and DSPP and also when QEFTPP is supporting 4 classes of traffic (class 0 has the lowest priority and class 3 has the highest).

The performance tests are done using W=16 in Figure 57 and W=64 in Figure 58. All classes of traffic have equal mean connection length and generate an equal amount of traffic. Our results show that QEFTPP achieves a class differentiation in terms of incurred CBP: class 3 experienced a reduction of CBP as compared to the classless JEFTPP and DSPP when W=16 and 64, respectively. For the case of 16 wavelengths per fiber, we observe that class 3 under QEFTPP has lower CBP than the classless FTPP and DSPP for all values of the load intensity and class 2 achieves CBP less than the classless FTPP and DSPP only when the load intensity is higher than 0.4. We also note that class 0 and 1 experience higher CBP than the classless FTPP and DSPP schemes for all considered loads.

When we use 64 wavelengths per fiber, we notice that the QoS performance can be significantly improved by increasing the number of wavelengths: Only classes 0 and 1 incurred higher CBP than the classless FTPP and DSPP. Class 2 and 3 incurred less connection blocking for all loads. The overall average CBP for QEFTPP is slightly higher than FTPP and DSPP for low loads but for loads higher than .4 for W=16 and than .7 for W=64, the classless FTPP and DSPP experience higher overall average CBP. Results for the case of the NSFNET topology are similar and are not given in this dissertation.

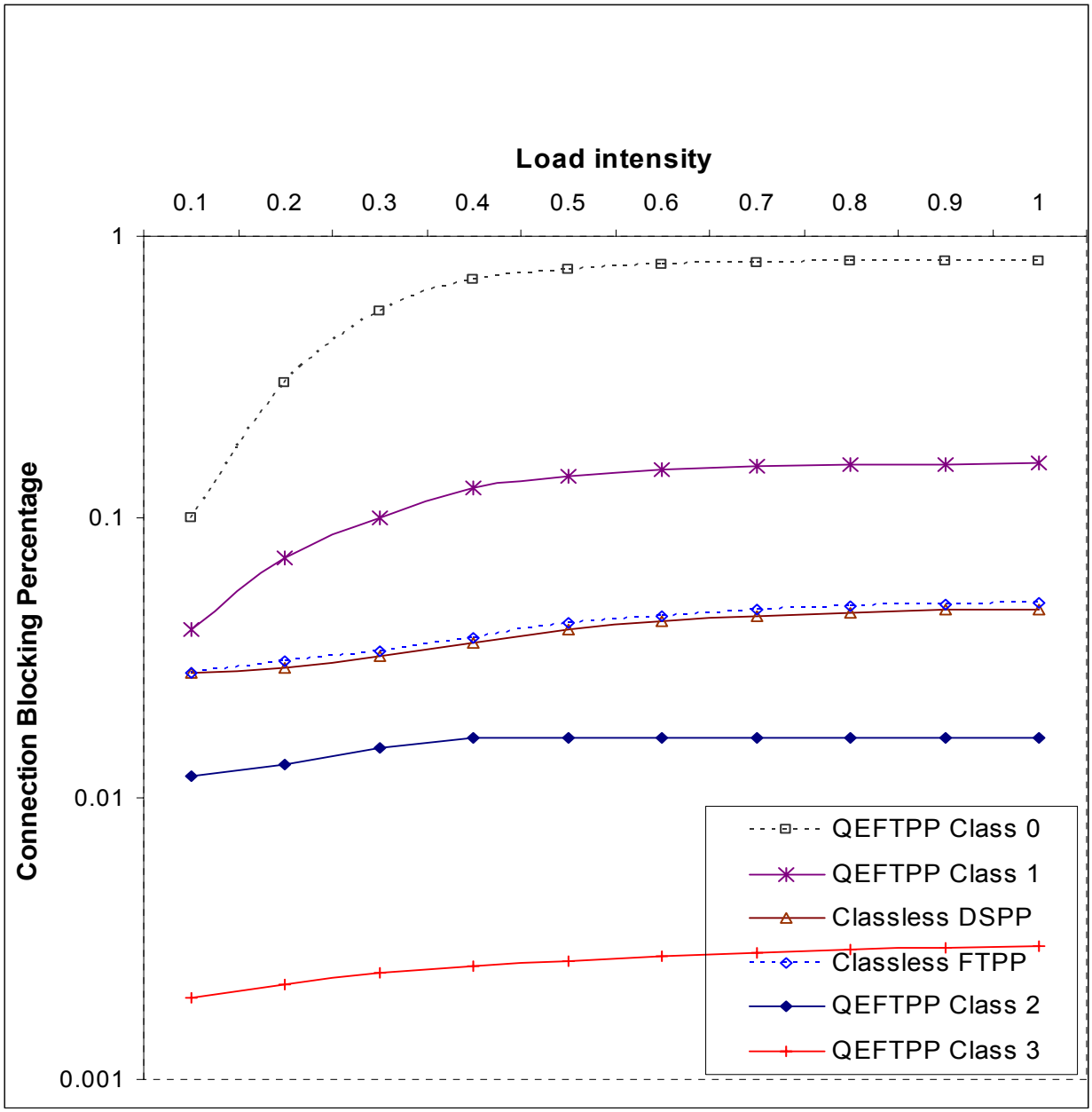


Figure 58: CBP versus load (USLH W=64)

Notice that Figure 57 and Figure 58 present the evaluation of the admission control policy of the three algorithms since the metric CBP measures the blocking when the connections are submitted. This is the reason we selected DSPP for comparison against QEFTPP since DSPP

allows full sharing of the protection capacity and is more aggressive than DPP and JSPP in admitting new connections.

When we consider the throughput-oriented metric CBDP, the benefit of EQTFPP and its QoS differentiation compared to DSPP are more significant as shown in Figure 59 and Figure 60 where we present the network throughput or CBDP as a function of the load.

In conclusion, our simulation results show that classes of traffic can be differentiated based on our QoS enhanced FTPP (QEFTPP). With low wavelengths (W=16), QEFTPP is unfair to low priority traffic: Higher priority classes experience less CBP compared to lower priority classes.

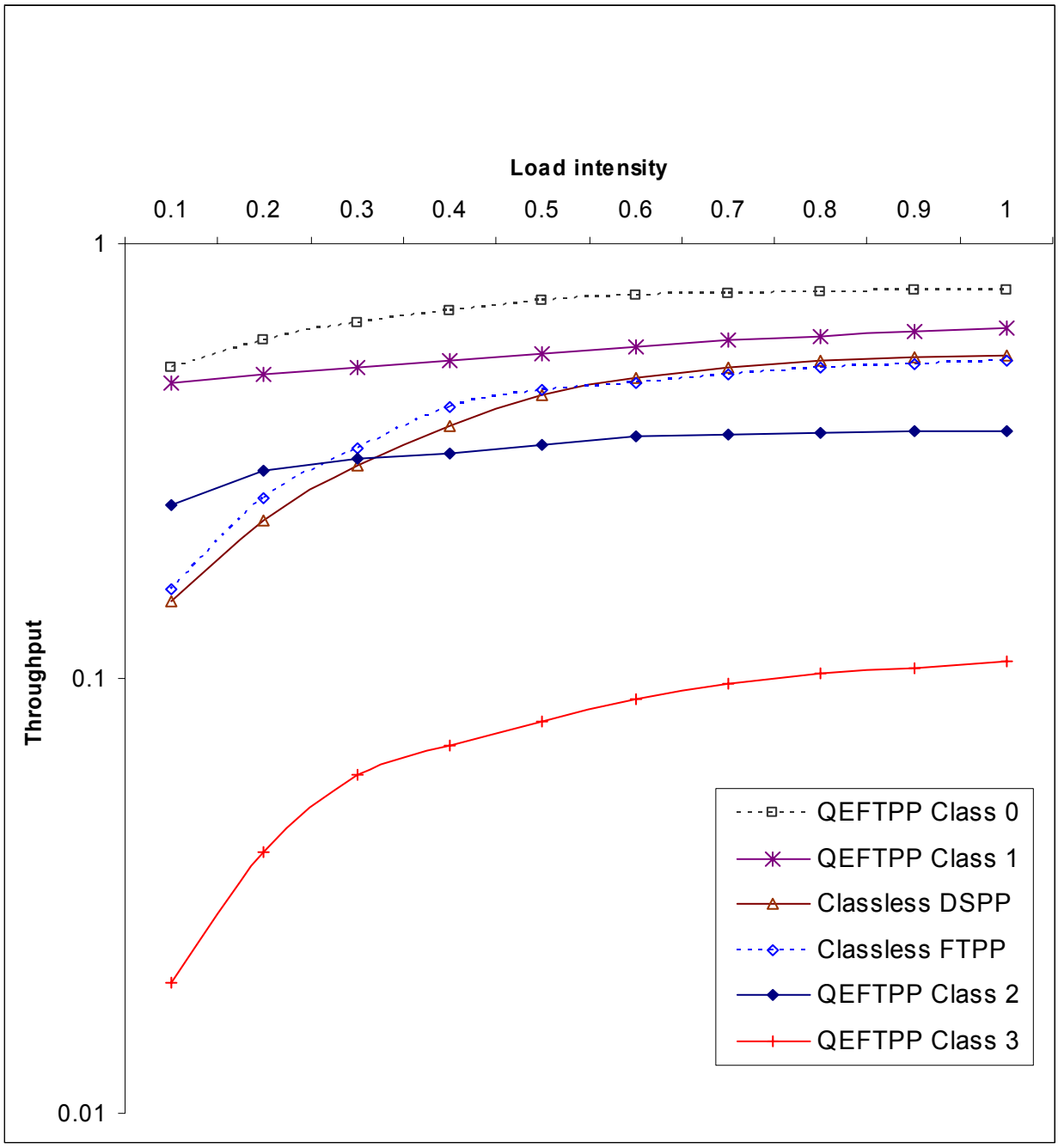


Figure 59: QEFTPP: Throughput versus load (USLH W=16)

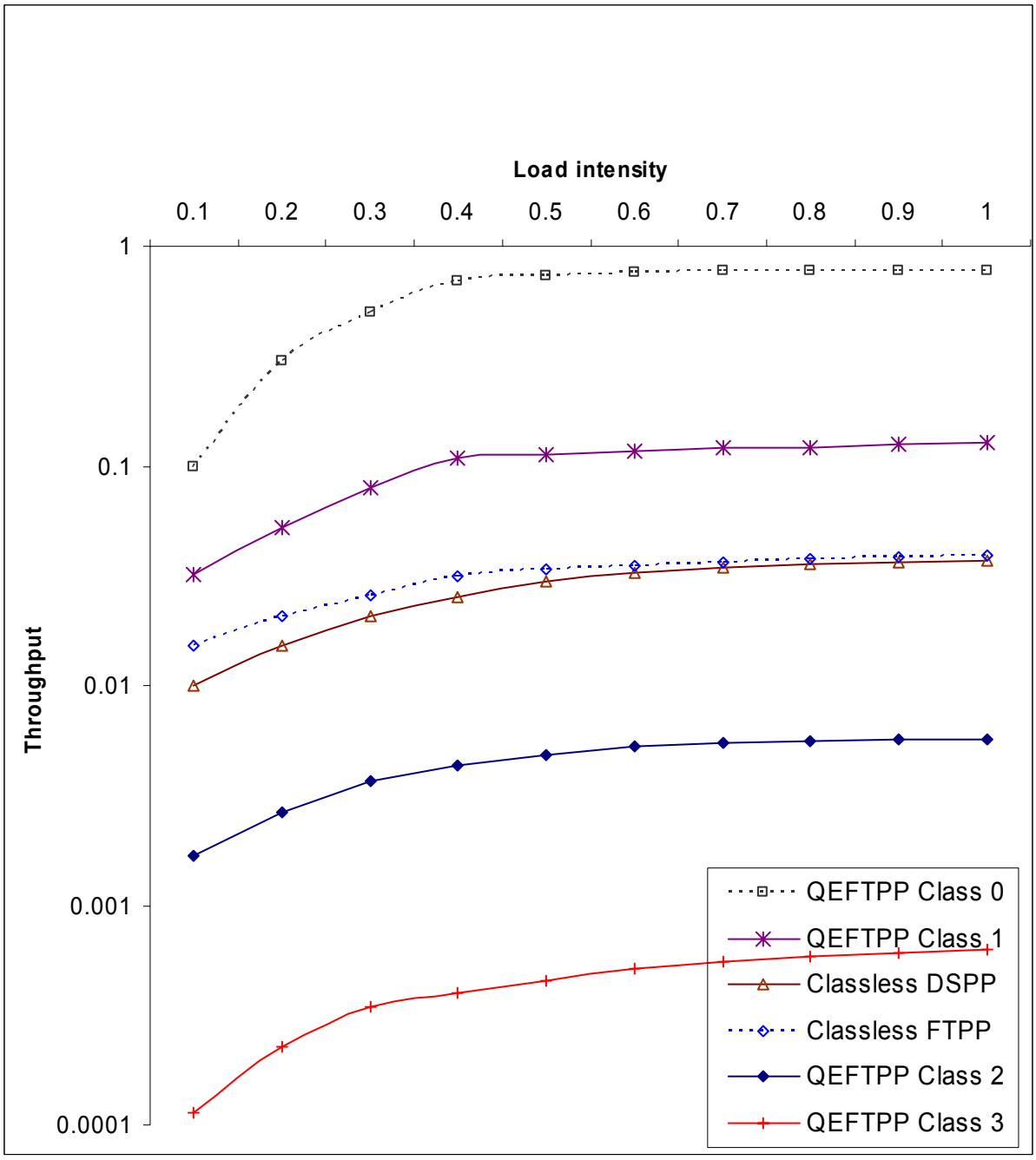


Figure 60: QEFTPP: Throughput versus load NSFNET (W=64)

We also showed that by using more wavelengths (W=64), more classes are less affected by the unfairness of QEFTPP to low priority classes of traffic.

## 6.4 Conclusions

The work presented in this chapter dealt with the path protection problem in WDM mesh networks. We presented FTPP for multiple failures path protection based on the alarming state of the nodes and links in the network. We used the following metrics: the Loss of Service Ratio (LSR), Connection Blocking Percentage (CBP) and Connection Blocking and Disconnection Percentage (CBDP) as the performance metrics for evaluating the FTPP path protection scheme and comparing it with three other schemes: DPP, DSPP and JSPP.

The simulation tests used a wide range of values for the network load intensity, the failure arrival rate and the mean failure holding time. Our simulation results showed that our scheme outperforms all three path protection schemes. The effectiveness of our scheme has been demonstrated by extensive performance tests using the US Long Haul and the NSFNET topologies.

We presented a QoS-enhanced FTPP (QEFTPP) routing and path protection in WDM networks. QEFTPP allows pre-emption of low priority classes while minimizing the connection blocking percentage for high priority traffic. The simulation results showed that QEFTPP can achieve a clear QoS-based separation between the different classes of service and at the same time provide a good overall performance. The work presented in this dissertation can be extended in several ways: introducing more alarm types, investigating other formulas for the cost function and fine tuning the search pruning heuristics to further improve performance.

# 7. CONCLUSION

Below, we present a summary of the contributions of the work presented in this dissertation and discuss future research ideas to extend this work.

## 7.1 Placement of wavelength converters in optical networks

We presented three algorithms (k-DS, HYBRID and LIMITED) for sparse placement of full and limited wavelength conversion in optical networks. The proposed algorithms are based on finding the k-dominating sets of the topology graph.

With randomly generated graphs, the k-DS algorithm provides an optimal placement of full wavelength conversion. k-DS provides a sub-optimal placement of full wavelength conversion under the uniform traffic assumption using the topology of the network as input and independently of the number of wavelength per link. With the U.S Long haul topology, almost 50% improvement is achieved with only 17% of the nodes having full wavelength conversion. The time complexity of k-DS is of order O (N. Δ. k) which is better than k-BLK whose complexity is of order O(N. C. NUMCONV) + O($N^3$). Where C is the total number of connection request simulated. NUMCONV is the number of converters to be placed.

k-DS alone cannot handle the case of arbitrary number of nodes for full conversion placement. The HYBRID algorithm is introduced to take advantage of k-DS and k-BLK for any desired arbitrary number of full wavelength converters. HYBRID has a time complexity comparable to

k-BLK but it achieves better performance as has been shown by the simulation results for the U.S Long Haul topology.

Finally, our proposed optical switch designs take advantage of limited wavelength conversion including the reduced cost, the improved fault tolerance and the ability to provide nearly similar improvement as full wavelength conversion in selected nodes of the network. Our results also show that the limited conversion capability can achieve performance very close to that of the full conversion capability, while not only decreasing the optical switch cost but also enhancing its fault tolerance.

The decision, about the switch design to use, depends on the number of wavelength converters to be placed and the traffic load in the network. When 25% or less wavelength conversion units are available in the network, the flexible node-sharing is recommended as the optical switch design of choice. When more than half of the maximum wavelength converter is to be placed, all three designs seem to have comparable performances. On the other hand, the static mapping switch design is recommended when more than 50% of the maximum possible is placed in the network. This is due to the cost and simplicity of the static mapping switch design.

Initially, the network traffic was assumed to be uniformly distributed on the node pairs. We investigated an extension of k-DS for non uniform traffic, referred to as k-WDS, for realistic networks exploitation. Our model assigns weights to each node based on the generated traffic and we use a Weighted Dominating Set scheme (k-WDS) for the placement of wavelength conversion under non-uniform traffic.

Our assumption in this dissertation is that all nodes have the same optical switch design. In future work, we plan to investigate the combination of the three designs in the network where certain nodes can have a flexible node-sharing switch design and other might have static mapping or strict node-sharing switch designs.

Our LIMITED algorithm for limited conversion is faster and more stable than the F-SEARCH heuristic reported in [JIM99]. It avoids the local minimum problem and gives better blocking performance than F-SEARCH. We also proposed a cost-effective optical switch designs, based on non-tunable optical multiplexers, for limited wavelength conversion: Flexible node-sharing, Strict node-sharing, and static mapping optical switch designs [BLS03].

## 7.2 Contention resolution in optical burst switched networks

We extensively investigated the sparse FDLs placement problem. We modeled non-uniform traffic between node pairs by assigning weights to the nodes. Our simulation results showed that our placement algorithm, k-WDS, captures the non-uniformity nature of the traffic in OBS. With the NSFNET topology, the k-WDS algorithm achieves almost 60% improvement in burst blocking over the no-FDL case with only four nodes selected for FDLs deployment. An extended version of the algorithm, called A-WDS, is presented to handle the placement of an arbitrary number of FDLs and full converters. The effectiveness of this algorithm has been demonstrated by extensive performance tests using the NSFNET network topology and randomly generated graphs. We focused on the burst loss rate and relative end-to-end delay as the key metrics for

evaluating network performance, and we presented comparison results for the tradeoffs of combining fiber delay lines and wavelength converters in solving the contention problem.

We finally presented a cost-effective optical switch and FDL designs along with a QoS-enhanced JET (QEJET) protocol suitable for optical burst switched WDM networks. QEJET allows classes of traffic to benefit from FDLs and OWCs while minimizing the end-to-end delay for high priority bursts. Extensive simulation results were presented showing that QEJET can achieve a clear QoS-based separation between the different classes of service and at the same time provide a good overall performance.

The work presented in this dissertation can be extended in several ways. Two of the issues that we plan to investigate in the near future are:

1. Applying QEJET to other OBS architectures with a limited number of OWCs and FDLs [BLJ04, BLS03].

2. Developing an analytical model that take into consideration the dependency and correlation of FDLs usage in order to improve the speed and blocking performance of our algorithms for FDLs placement.

## 7.3 Dependency based analytical model for blocking rates computation

We presented an analytical model to capture link dependencies and compute the blocking probabilities in all-optical WDM networks. We validated the analytical model via simulation tests using several topologies. The model is generally accurate in capturing link dependencies and estimating the blocking probabilities with and without wavelength converters available in the network. The A-Block algorithm presented in section 5.3 is reasonably fast; it divides longer paths into smaller ones and computes the results iteratively. The algorithm has provided accurate results and reduced the computational overhead of the simulation-based algorithm. Further research is needed to enhance the robustness of the link dependency formula by adapting/extending it to handle special topologies, very low loads, non-uniform traffic [BLO03] or non-random wavelength assignment.

One aspect of our proposed future work will be to enhance our analytical model taking into consideration the dependency and correlation of wavelength usage between adjacent links in order to avoid the simulation step and improve the speed and blocking performance of our HYBRID and LIMITED algorithms for wavelength conversion placement.

Another future enhancement to our analytical model applies to the case of non-uniform traffic. We are currently exploring a weighted approach and combining our Weighted Dominating Set algorithm (WDS) with our proposed analytical model for wavelength converters placement under different traffic patterns.

## 7.4 Path protection in survivable wavelength routed all-optical

We presented a Failure tolerant Path protection scheme for multiple failures path protection based on the alarming state of the nodes and links in the network. We used the following metrics: the Loss of Service Ratio (LSR), Connection Blocking Percentage (CBP) and Connection Blocking and Disconnection Percentage (CBDP) as the performance metrics for evaluating the FTPP path protection scheme and comparing it with three other schemes: DPP, DSPP and JSPP.

The simulation tests used a wide range of values for the network load intensity, the failure arrival rate and the mean failure holding time. Our simulation results showed that our scheme outperforms all three path protection schemes. The effectiveness of our scheme has been demonstrated by extensive performance tests using the US Long Haul and the NSFNET topologies.

We presented a QoS-enhanced FTPP (QEFTPP) routing and path protection in WDM networks. QEFTPP allows pre-emption of low priority classes while minimizing the connection blocking percentage for high priority traffic. The simulation results showed that QEFTPP can achieve a clear QoS-based separation between the different classes of service and at the same time provide a good overall performance. The work presented in this dissertation can be extended in several ways: introducing more alarm types, investigating other formulas for the cost function and fine tuning the search pruning heuristics to further improve performance.

# APPENDIX: ALARM PROBABLE CAUSE AND SEVERITY ASSIGNMENT

ITU X.721 ISO/IEC 10165-2 [ITA92, ITB92] defines a standard for alarm reporting including alarm severities, security alarm causes and general alarm probable causes.

1. Perceived Severity

   Critical, major, minor, warning and cleared.

2. General Alarm Probable Cause and severity assignment

Table 3 lists the general alarm causes and shows our assigned severity to each alarm condition.

Table 3: Severity Assignment

| | |
|---|---|
| performanceDegraded (Minor) | applicationSubsystemFailure (Minor) |
| powerProblem (Major) | bandwidthReduced (Minor) |
| queueSizeExceeded (Minor) | callEstablishmentError (Major) |
| receiveFailure (Major) | communicationsProtocolError (Major) |
| receiverFailure (Major) | communicationsSubsystemFailure (Major) |
| remoteNodeTransmissionError (Major) | configurationOrCustomizationError (Minor) |
| resourceAtOrNearingCapacity (Minor) | congestion (Minor) |
| responseTimeExcessive (Minor) | corruptData (Minor) |
| retransmissionRateExcessive (Minor) | cpuCyclesLimitExceeded (Minor) |
| softwareError (Minor) | degradedSignal (Major) |
| softwareProgramAbnormalTerminated (Minor) | enclosureDoorOpen (Critical) |
| softwareProgramError (Minor) | equipmentMalfunction (Major) |

| | |
|---|---|
| storageCapacityProblem (Minor) | excessiveVibration (Critical) |
| temperatureUnacceptable (Major) | fileError (Minor) |
| thresholdCrossed (Minor) | fireDetected (Critical) |
| timingProblem (Minor) | floodDetected (critical) |
| transmitFailure (Major) | framingError (Major) |
| transmitterFailure (Major) | heatingOrCoolingProblem (Critical) |
| underlyingResourceUnavailable (Minor) | humidityUnacceptable (Critical) |
| versionMismatch (Minor) | inputOutputDeviceError (Minor) |
| lossOfFrame (Major) | inputDeviceError (Minor) |
| lossOfSignal (Major) | lANError (Minor) |
| multiplexerProblem (Major) | leakDetected (Critical) |
| outOfMemory (Major) | localNodeTransmissionError (Major) |

3. Security Alarm Cause

All Security Alarms were assigned a severity type of critical.

Table 4: Security Alarms

| | | |
|---|---|---|
| informationMissing | outOfHoursActivity | authenticationFailure |
| informationModificationDetected | outOfService | breachOfConfidentiality |
| informationOutOfSequence | proceduralError | cableTamper |
| intrusionDetection | unauthorizedAccessAttempt | delayedInformation |
| keyExpired | unexpectedInformation | denialOfService |
| nonRepudiationFailure | unspecifiedReason | duplicateInformation |

# LIST OF REFERENCES


[ABR96] A. Birman, "Computing approximate blocking probabilities for a class of all optical networks", IEEE Selected Areas Com., vol. 14: 5, pp. 852-857, June 1996.

[AKM03] S. Arakawa, J. Katou and M. Murata, "Design method of logical topologies with quality of reliability in WDM networks", J. Photo. Net. Comm., vol. 5:2, pp. 107-221, March 2003 (Kluwer).

[ASS00] A. Sridharan and K. N. Sivarajan, "Blocking in all-optical networks," in Proc. IEEE INFO-COM, vol. 2, Tel Aviv, Israel, Mar. 2000, pp. 990–999.

[ASS02 ] A. S. Arora, S. Subramaniam, "Wavelength conversion placement in WDM Mesh Optical Networks", Photonic Network Communications, 4:2, 167-177, 2002.

[ASS04] A. Sridharan and K. N. Sivarajan, "Blocking in all-optical networks," IEEE/ACM Trans. Networking, vol. 12, no. 2, pp. 384–397, April. 2004.

[BLJ03] M. El Houmaidi, M. Bassiouni and G. Li "Dominating set algorithms for sparse placement of full and limited wavelength converters in WDM optical networks", Journal of Optical Networking, Optical Society of America, Vol. 2, No. 6, pp. 162- 177, June 2003.

[BLJ04] M. El Houmaidi, M. Bassiouni and G. Li, "Architecture and Sparse Placement of Limited Wavelength Converter for Optical Networks", Journal of Optical Engineering, SPIE, Vol. 43, No. 1, pp. 137-147, January, 2004.

[BLJ05] M. El Houmaidi, M. Bassiouni and G. Li "Alarm based Routing and Path Protection in Survivable Wavelength Routed All-Optical Mesh Networks",

Journal of Optical Networking, Optical Society of America, Vol. 4, No. 4, pp. 176-190, April 2005.

[BLJ06] M. El Houmaidi, M. Bassiouni "Dependency Based Analytical Model for Computing Connection Blocking Rates and its Application in the Sparse Placement of Optical Converters", revised under final review by IEEE Journal: Transactions on Communications, (Paper code 04-0135R2), 2006.

[BLX04] M. El Houmaidi, O. Kachirski and R. Guha, "FANS Simulation of Optical Burst Switching for NSFNET", WSEAS Journal: Transactions on computers (World Scientific and Engineering Academy and Society, Vol. 3, No. 5, pp. 1232-1237, ISSN 1109-2750 Paris Athens, November 2004.

[BLA04] M. El Houmaidi, O. Kachirski and R. Guha, "FANS Simulation of Optical Burst Switching for NSFNET", Proceedings of ISA 04 (International Conference on Information Science and application), April 21-23, 2004.

[BLD03] M. El Houmaidi, M. Bassiouni and G. Li, "Architectures and Algorithms for Resource Allocation", IEEE Globecom'03, Invited to The Second International Workshop on Optical Burst Switching in IEEE Globecom'03. December 1-5, 2003.

[BLF04] M. El Houmaidi, M. Bassiouni and G. Li,"Optimal traffic grooming in WDM mesh networks under dynamic traffic", IEEE/OSA OFC 04 (Optical Fiber communications conference), No. ThG3, pp. 43-45, February 22-27, 2004.

[BLO03] M. El Houmaidi and M. Bassiouni, "k-Weighted Minimum Dominating Sets for Sparse Wavelength Converters Placement under Non-uniform Traffic", in the proceedings of MASCOTS 03, the 11th IEEE/ACM international symposium on

modeling, analysis and simulation of computer and telecommunication systems. (IEEE, October 2003).

[BLN03] M. El Houmaidi, M. Bassiouni and G. Li, ”Limited range wavelength conversion in WDM optical networks”, Invited at OSA/SPIE OISE 03 (Optics in the Southeast conference), No. SE 03-D4, November 12-13, 2003.

[BLS03] M. El Houmaidi, M. Bassiouni, G. Li; “Algorithm for placement of limited wavelength conversion in WDM optical networks”. ITCom03 proceedings for Optical Transmission Systems and Equipment for WDM Networking, Vol. 5247, pp. 185-195, September 2003.

[BRP02] I. Baldine, G.N. Rouskas, H.G. Perros and D. Stevenson “JumpStart: a just-in-time signaling architecture for burst-switched networks“, IEEE Comm. Mag., Vol. 40:2, pp. 82-89, Feb. 2002.

[BSR02] S. Bose, Y. N. Singh, A. N. Raju and B. Popat, “Sparse converter placement in WDM networks and their dynamic operation using path-metric based algorithms”, in the proceedings of ICC 02, IEEE International Conference on Communications, vol. 5, pp. 2855-2859, (IEEE, 2002).

[CCB96] C. Chen and S. Banerjee “A new model for optimal routing in all-optical networks with scalable number of wavelength converters” available at http://home.att.net/~sbanerjee/dissertations/ChBa96.pdf.

[CLC03] X.-W. Chu, B. Li, and I. Chlamtac, .Wavelength Converter Placement under Different RWA Algorithms in Wavelength-Routed All-Optical Networks,. IEEE Trans. on Comm., Vol. 51, No. 4, April 2003.

[CLY94] C. Lund and M. Yannakakis, “On the Hardness of approximating Minimization Problems”, Journal of the Association for Computing Machinery, vol. 41, N. 5, pp.960-981, 1994.

[CLS02] G. Conte, M. Listanti, M. Settembre, and R. Sabella, ”Strategy for protection and restoration of optical paths in WDM backbone networks for next-generation Internet infrastructures”, IEEE J. of Lightwave Technology, vol. 20:8, pp. 1264 – 1276, August 2002.

[CQY99] C. Qiao and M. Yoo, “Optical burst switching (OBS) – a new paradigm for optical internet”, Journal of high speed networks, vol. 8:1, pp. 69 -84, 1999.

[DLG04] D. Leung and W. D. Grover, “Restorable mesh network design under demand uncertainty: Toward future proofed transport investments”, IEEE Proc. of Optical Fiber Comm. Conf.. ThO2, pp. 35-37, OFC 04, February 2004.

[DLJ02] D. Li, X. Jia, “Allocating wavelength converters in shared-per-link structure in WDM networks”, IEE Proc. Commun., vol. 149, No. 3, pp. 185-188, 2002.

[DLL02] Liu, D.Q.; Liu, M.T., “Differentiated services and scheduling scheme in optical burst-switched WDM networks”, 10th IEEE Int. Conference on Networks, pp. 23 -27. ICON02. Aug. 2002.

[DMB02] M. Duser, I. D. Miguel, P. Bayvel and D. Wischik, “Timescale analysis for wavelength-routed optical burst-switched (WR-OBS) networks”, OFC, pp. 222 - 224, OFC02 , March 2002.

[DSS03] D. A. Schupke and M. C. Scheffel, “Configuration of p-Cycles in WDM networks with partial wavelength conversion”, J. Photo. Net. Comm., vol. 6:3, pp. 239-252, November 2003 (Kluwer).

[EMN02] E. Modiano and A. Narula-Tam, "Survivable lightpath routing: a new approach to the design of WDM-based networks" IEEE J. of Selected Areas in Comm., vol. 20:4 , pp. 800 – 809, May 2002.

[GCM03] A. Groebbens, D. Colle, S. D. Maesschalck, I. Lievens, M. Pickavet and P. Demeester, "Efficient Protection in MPλS networks using backup trees: Part one-Concepts and Heuristics, ", J. Photonic Network Communications, vol. 6:3, pp. 191-206, November 2003 (Kluwer).

[GCS03] A. Groebbens, D. Colle, S. D. Maesschalck, I. Lievens, M. Pickavet and P. Demeester, "Efficient Protection in MPλS networks using backup trees: Part two-Simulations, ", J. Photonic Network Communications, vol. 6:3, pp. 207-222, November 2003 (Kluwer).

[GKS04] G. Raghu Kiran and C. Siva Ram Murthy, "QoS based survivable logical topology design in WDM optical networks", J. Photo. Net. Communications, vol. 7:2, pp. 193-206, March 2004 (Kluwer).

[GWW98] G. Wilfong and P. Winkler, "Ring routing and wavelength translation", in the proceedings of 9th annual ACM-SIAM Symposium on Discrete Algorithms, pp. 333-341, (SODA, 1998).

[HES04] A. G. Hailemariam, G. Ellinas and T. Stern, "Localized failure restoration in Mesh optical networks", IEEE Proc. of Optical Fiber Comm. Conf. TuP1, pp. 16-18, OFC 04, February 2004.

[HLH02] C. Hsu, T. Liu and N. Huang, "Performance of adaptive routing in wavelength-routed networks with consideration of delay-sensitivity", INFOCOM proc., vol. 1, pp. 66 -73, June 2002.

[HMH97] H. Harai, M. Murata and H. Miyahara, "Performance of alternate routing methods in all-optical switching networks," in Proc. IEEE INFOCOM'97, Apr. 1997, pp. 516–524.

[HMH99] H. Harai, M. Murata, H. Miyahara, "Heuristic algorithm for allocation of wavelength convertible node and routing coordination in all-optical network", Journal of lightpath technology, vol. 17, no. 4, pp. 535-545, April 1999.

[IAM03] S. Ishida, S. Arakawa and M. Murata, "Reconfiguration of logical topologies with minimum traffic disruptions in reliable WDM-based mesh networks" Photonic Network Communications, Vol. 6, pp. 265-277, November 2003.

[ITA92] ITU X.721 ISO/IEC 10165-2, Information Technology - Open Systems Interconnection - Part 2: Definition of Management Information www.itu.int/ITU-T/asn1/database/itu-t/x/x721/1992/Attribute-ASN1Module.asn

[ITB92] ITU-T X.722 | ISO/IEC 10165-4 Draft Ammendment 4 - Guidelines for the Definition of Managed Objects (GDMO). http://www.itu.int/ITU-T/asn1/database/itu-t/x/x722/1992/

[JCP02] J.B Chang and C.S. Park, "Efficient channel-scheduling algorithm in optical burst switching architecture" IEEE Workshop Optical and IP Tech. and High Perf. Switching, pp. 194 -198, May 2002.

[JFL04] J. F. Labourdette, "Shared Mesh Restoration in Optical Networks", IEEE Proc. of Optical Fiber Communication Conference. TuP3, pp. 22-24, OFC 04, February 2004.

[JIM99] J. Iness, B. Mukherjee; “Sparse Wavelength Conversion in Wavelength-Routed WDM Optical Networks”, Photonic Network Communication, vol. 1:3, pp. 183-205, 1999.

[JLA02] J. Liu and N.Ansari,”Class-based dynamic buffer allocation for optical burst switching networks”, IEEE Workshop on Merging Optical and IP Tech. and High Perf. Switching, pp. 295 -299, May 2002.

[JPX01] J. P. Pue, G. Xiao, “Analysis of Blocking probabilities for connection Management Schemes in Optical networks”, Global Telecommunication Conference, GLOBECOM ‘2001, pp. 1546-1550, 2001.

[JRT02] J. Ramamirtham and J. Turner “Design of wavelength converting switches for optical burst switching”, INFOCOM proc., vol. 1, pp. 362-370, June 2002.

[JWM00] J.Y. Wei and R.I. McFarland,” Just-in-time signaling for WDM optical burst switching networks”, Journal of Lightwave Technology, Vol. 18:12, pp. 2019-2037, December 2000.

[KDZ02] E. Kozlovski, M. Duser, A. Zapata and P. Bayvel, “Service differentiation in wavelength-routed optical burst-switched networks”, Optical Fiber Communication Conference. pp.774-776, March 2002.

[KKK02] S. Kim, N. Kim and M. Kang, “Contention resolution for optical burst switching networks using alternative routing”, IEEE Int.Conf. Comm., vol. 5, pp. 2678 - 2681, ICC02, May 2002.

[KLJ 93] K. Lee and V. Li "A Wavelength-Convertible Optical Network," IEEE Journal of Light wave Technology, Vol. 11, May/June 1993, pp. 962-970.

[KLM93] K. Lee and V. Li "Routing and switching in a wavelength convertible optical network" Proc. IEEE INFOCOM, March 1993, pp. 578-585.

[LLS00] L. Li and A. Somani, "A new analytical model for multifiber WDM networks", IEEE Journal on Selected Areas in Communications, vol. 18, no. 10, pp. 2138-2145, October 2000.

[LXC03] K. Lu, G. Xiao, and I. Chlamtac, "Behavior of distributed wavelength provisioning in wavelength-routed networks with partial wavelength conversion," in Proc. IEEE INFO-COM, vol. 3, San Francisco, CA, Apr. 2003, pp. 1816–1825.

[MDB02] M. Duser, P. Bayvel, "Analysis of a dynamically wavelength-routed optical burst switched network architecture", Journal of Lightwave Technology, Vol. 20:4, pp. 574-585, April 2002.

[MKA96] M. Kovacevic and A. Acampora, "Benefits of wavelength translation in all-optical clear-channel networks", IEEE Journal on Selected Areas in Communications, vol. 14, no. 5, pp. 868-880, June 1996.

[MLZ01] R. Melhem, S. Li and T. Znati, "Minimizing wavelength conversions in WDM path establishment", Journal of Photonic Network Communications, vol. 3:3, pp. 197-211, (Kluwer, 2001).

[MMB00] A. Medina, I. Matta, and J. Byers, "BRITE: A Flexible Generator of Internet Topologies", Tech. Rep. BU-CS-TR-2000-005, Boston University, January, 2000.

[MSS02] M. Sivakumar, S. Subramaniam; "On the Performance impact of wavelength assignment and wavelength conversion architecture and placement algorithms", SPIE, Optical Networks Magazine, pp. 44-53, March/April 2002.

[NLR03] C. Nuzman, J. Leuthold, R. Ryf, S. Chandrasekhar, C.R. Giles, "Design and implementation of wavelength-flexible network nodes", J. Lightwave Tech., Vol. 21: 3, pp. 648 -663, March 2003.

[OAM01] I. Ogushi, S.Arakawa, M. Murata, and K. Kitayama, "Parallel reservation protocols for achieving fairness in optical burst switching", IEEE Workshop on High Perf. Switching, pp. 213 -217, May 2001.

[OCB98] O. Crochat and J. L. Boudec, "Design protection for WDM optical networks", IEEE J. Select. Areas of Commun., vol. 16:7, pp. 1158-1165, (IEEE, 1998).

[OZZ03] C. Ou, J. Zhang, H. Zang and B. Mukherjee, "Near-optimal approaches for shared-path protection in WDM mesh networks," IEEE Int. Conf. on Comm., pp. 1320–1324, May 2003.

[PHM02] P. Ho and H. T. Mouftah, "A framework for service-guaranteed shared protection in WDM mesh networks", IEEE Communications Magazine, vol. 40:2, pp. 97 – 103, February 2002.

[PPP03] G.I Papadimitriou, C. Papazoglou and A.S. Pomportsis, "Optical switching: switch fabrics, techniques, and architectures", J. Light. Technology, Vol. 21:2, pp. 384-405, February 2003.

[QMJ03] Y. Qin; L. Mason, Ke Jia, "Study on a joint multiple layer restoration scheme for IP over WDM networks" IEEE Network, vol. 17:2 , pp. 43 – 48, April 2003.

[QZM03] Q. Zhen and G. Mohan, "Protection approaches for dynamic traffic in IP/MPLS-over-WDM networks", IEEE Communications Magazine, vol. 41:5, pp. S24-S29, May 2003.

[RBM95] R. Barry and D. Marquis, “Evaluation of a model of blocking probability in all-optical mesh networks without wavelength changers”, Proc. SPIE, All optical communication systems, Vol. 2614, pp. 154-167, December 1995.

[RDH01] L. Ruan, D. Du, X. Hu, X. Jia, D. Li and Z. Sun, “Converter placement supporting broadcast in WDM optical networks ”, IEEE trans. on computers, vol. 50:7, pp.750-758, (IEEE, 2001).

[RKR72] R. Karp, “Reducibility among combinatorial problems” in R. Miller and J. Thatcher editors, Complexity of computer computations pp. 85-103. Plenum Press, New York, 1972.

[RRM02] R. Ramamurthy and B. Mukherjee, “Fixed-alternate routing and wavelength conversion in wavelength-routed optical networks”, IEEE/ACM Trans. Networking, vol. 10, no. 3, pp. 351-367, June 2002.

[RRS00] R. Ramaswami and A. Segall, “Distributed Network Control of Optical networks”, IEEE/ACM Trans. Net., vol. 5, no. 6, pp. 936-43, Dec. 2000.

[RSM03] S. Ramamurthy, L. Sahasrabuddhe and B. Mukherkee, “Survavible WDM Mesh Networks”, IEEE J. of Lightwave Technology, vol. 21:4, pp. 870-882, April 2003.

[SAS96] S. Subramaniam, M. Azizoglu and A. K. Somani, “All-optical networks with sparse wavelength conversion”, IEEE/ACM Trans. Networking, vol.4, pp. 544-557, Aug. 1996.

[SAS99] S. Subramaniam, M. Azizoglu and A. K. Somani, “On optimal placement in wavelength-routed networks”, IEEE/ACM Trans. Networking, vol. 7, no. 5, pp. 754-766, October 1999.

[SGK96] S. Guha and S. Khuller, "Approximation algorithms for connected dominating sets", Proc. of 4th Annual European Symposium on algorithms, pp. 179-193, 1996.

[SOK02] S.Y. Oh and M. Kan, "A burst assembly algorithm in optical burst switching networks", Optical Fiber Communication Conference and Exhibit. pp. 771 -773, OFC02 , March 2002.

[SRM02] L. Sahasrabuddhe, S. Ramamurthy, B. Mukherjee, "Fault management in IP-over-WDM networks: WDM protection versus IP restoration" IEEE J. SAC., vol. 20:1 , pp. 21-33, January 2002.

[SSY04] S. Shah-Heydri and O. Yang, "Hierarchical protection tree scheme for failure recovery in mesh networks", J. Photonic Network Communications, vol. 7:2, pp. 145-159, March 2004 (Kluwer).

[SSZ02] I. Stojmenovic, M. Seddigh and J. Zunic, "Dominating Sets and Neighbor Elimination Based Broadcasting Algorithms in Wireless Networks", IEEE Trans. On Parallel and Distributed systems, vol. 13, pp.14-25, January 2002.

[SYR04] L. Shen, X.Yang and B. Ramamurthy, "A load-balancing shared-protection-path reconfiguration approach in WDM wavelength-routed networks", IEEE Proc. of Optical Fiber Communication Conference. ThO3, pp. 38-40, OFC 04, February 2004.

[TFP03] M. Tacca, A. Fumagalli, A. Paradisi, F. Unghvary,K. Gadhiraju, S. Lakshmanan, S. M. Rossi, A. de Campos Sachs, and D. S. Shah, "Differentiated reliability in optical networks: theoretical and practical results" IEEE J. of Lightwave Technology, vol. 21:11, pp. 2576 – 2586 , November 2003.

[TTM97] T. Tsai and P. K. McKinley, “An Extended Dominating Node Approach to Broadcast and Global Combine in Multiport Wormhole-Routed Mesh Networks”, IEEE Trans. On Parallel and Distributed systems, vol. 8, pp.41-58, January 1997.

[VJS02] V. A. Vokkarane, J. P. Jue and S. Sitaraman, ”Burst segmentation: an approach for reducing packet loss in optical burst switched networks”, IEEE Int. Conf. on Communications, vol. 5, pp. 2673 -2677, ICC02, May 2002.

[VRK98] Venugopal, K.R.; Rajan, E.E.; Kumar, P.S. Kumar, ”Performance Analysis of Wavelength Converters in WDM Wavelength Routed Optical Networks” Proc. of 5th International Conference On High Performance Computing, pp. 239–246, 1998.

[VSK99] K. R. Venugopal, M. Shivakumar and P. S. Kumar, “A heuristic for placement of limited range wavelength converters in all-optical networks”, in the proceedings of IEEE INFOCOM, vol. 2, pp. 908-915, (IEEE, 1999).

[VWS03] V. W. S. Chan, “Some thoughts on optical networks”, MIT, DOD-N presentation, http://www.darpa.mil/mto/solicitations/BAA03-19/S/presentations/mit_chan.pdf (2003).

[WGD02] W. D. Grover and J. Doucette, “Design of a meta-mesh of chain subnetworks: enhancing the attractiveness of mesh-restorable WDM networking on low connectivity graphs” IEEE J. of Selected Areas in Communications, vol. 20:1, pp. 47 – 61, January 2002.

[WLW01] Y. Wang, L. Li and S. Wang, “A new algorithm of design protection for wavelength-routed networks and efficient wavelength converter placement”, in

the proceedings of ICC 01, IEEE International Conference on Communications, vol. 6, pp. 1807-1811, (IEEE, 2001).

[WLY04] D. Wang, G. Li, J. Yates and C. Kalmanek,"Efficient Segment-by-Segment Restoration" IEEE Proc. of Optical Fiber Communication Conference. TuP2, pp. 19-21, OFC 04, February 2004.

[WMC04] G. Weichenberg, M. Medard and V. Chan, "Multiple Failure Restoration in Mesh Optical Networks", IEEE Proc. of Optical Fiber Comm. Conf. ThO1, pp. 31-34, OFC 04, February 2004.

[XCQ04] D. Xu, Y. Chen and C. Qiao, "A new heuristic for finding the shortest path with disjoint counterpart", IEEE Proc. of Optical Fiber Comm. Conf. ThG2, pp. 40-42, OFC 04, February 2004.

[XJD02] X. Jia, D. Du, X. Hu, H. Huang and D. Li, "Placement of Wavelength Converters for minimal Wavelength Usage in WDM Networks", in the proceedings of IEEE INFOCOM, vol. 3, pp.1425-1431, (IEEE, 2002).

[XPR01] L. Xu, H.G. Perros and G. Rouskas, "Techniques for optical packet switching and optical burst switching", IEEE Communications Magazine, Vol. 39:1, pp. 136 - 142, January 2001.

[YLE96] J. Yates, J. Lacey, D. Everitt and M. Summerfield, "Limited wavelength translation in all-optical networks", in the proceeding of INFOCOM, vol. 3, pp. 954-961, (IEEE, 1996).

[YQD00] M. Yoo, C. Qiao and S. Dixit, "QoS performance of optical burst switching in IP-over-WDM networks", J. on Selected Areas in Communications, vol. 18:10, pp. 2062 -2071, October 2000.

[YQD01] M. Yoo, C. Qiao and S. Dixit, "Optical Burst Switching for service Differentiation in the Next-Generation Optical Internet", IEEE Comm. Mag., pp. 98-104, Feb. 2001.

[YST02] M. C. Yuang, J Shih and P. L. Tien, "QoS burstification for optical burst switched WDM networks", Optical Fiber Communication Conference. pp. 781 -783, OFC02 , March 2002.

[ZJM00] H. Zang, J. P. Jue, and B. Mukherjee, " A review of Routing and Wavelength Assignment Approaches for Wavelength-Routed Optical WDM Networks", Opt. Net. Mag., vol. 1, no. 1, pp. 47-60, Jan 2000.

[ZJS01] H. Zang, J. P. Jue, L. Sahasrabuddhe, R. Ramamurthy, B. Mukherjee, "Dynamic Lightpath establishment in wavelength-routed WDM Networks", IEEE Comm. Mag, pp. 100-108, Sept. 2001.

[ZOM03] H. Zang, C. Ou and B. Mukherjee, "Path-Protection Routing and Wavelength Assignment (RWA) in WDM Mesh Networks under Duct-Layer constraints", IEEE/ACM J. Transactions on Networking, vol. 11:2, pp. 248 -258, April 2003.

[ZRP00] Y. Zhu, G. N. Rouskas, and H. G. Perros, "A path decomposition approach for computing blocking probabilities in wavelength-routing networks," IEEE/ACM Trans. Networking, vol. 8, no. 6, pp. 747–762, Dec. 2000.